Selective oxidation processes of organic substances in water by means of photocatalytic systems

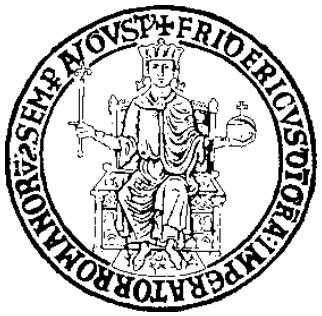

PhD thesis
March 2013

Ph.D student: Danilo Spasiano

Scientific Committee:

R. Andreozzi[a] , V. Augugliaro[b], I. Di Somma[c], R. Marotta[a]

[a] Dipartimento di Ingegneria Chimica, dei Materiali e della Produzione Industriale, Università di Napoli "Federico II", Naples, Italy

[b] Dipartimento di Ingegneria Chimica, Università di Palermo, Palermo, Italy

[c] Istituto Nazionale Ricerche (CNR), Naples, Italy

"On the arid lands there will spring up industrial colonies without smoke and without smokestacks; forests of glass tubes will extend over the plains and glass buildings will rise everywhere; inside of these will take place the photochemical processes that hitherto have been the guarded secret of the plants, but that will have been mastered by human industry which will know how to make them bear even more abundant fruit than nature, for nature is not in a hurry and mankind is."

Giacomo Luigi Ciamician
Science 36, 385-394 (1912)

INDEX

ABSTRACT

Selective oxidation of benzyl alcohol into benzaldehyde in anoxic acidic aqueous solution, through a TiO_2/Cu(II)/solar UV photocatalytic system, has been investigated both in a laboratory scaled reactor equipped with a high-pressure mercury lamp as well as in a solar pilot plant.

During the laboratory experiments, benzaldehyde gave best results, in terms of yield, equal to 35% with respect to the initial benzyl alcohol concentration. A partial conversion of benzaldehyde to benzoic acid has also been observed. Traces of hydroxylated by-products have also been detected. On the basis of the formation of these species, a production of HO radicals has been thus inferred.

The study has suggested that different operative parameters, such as the composition and amount of TiO_2 photocatalyst, pH, ionic inorganic components in water, and the initial concentration of Cu(II) ions, play an important role in the photocatalytic selective oxidation of benzyl alcohol.

The mechanism of photocatalytic selective oxidation of benzyl alcohol into benzaldehyde and benzaldehyde into benzoic acid has been investigated in the presence of TiO_2 catalyst and cupric ions, as electron acceptor, in water at a pH = 2.0 and under deaerated conditions.

A competitive adsorption has been proposed in which the aromatic substrates are adsorbed on the TiO_2 surface and react with the positive holes. Whereas Cu(II) ions are reduced to Cu(0) by the photogenerated electrons.

A new kinetic model has been developed by writing a set of mass balance equations for the main species involved in the photocatalytic oxidation process. The resulting mathematical model has been used for the analysis of the data collected at different starting substrates' concentrations. During each of the selective photoxidation runs, it satisfactorily predicts the concentrations of Cu(II) species, organic substrates, and intermediates. The effect of ionic components, which compete with benzyl alcohol and benzaldehyde for the reaction with positive holes on the catalyst surface and behave as scavengers towards HO radicals, has been taken into account in the model.

The values of some rate constants of the reactions of the holes with benzyl alcohol, benzaldehyde, Cu(II) species, and inorganic anions (SO_4^{2-} and $H_2PO_4^-$), not available in the literature, have been estimated by a proper optimizing procedure.

The conversion of hydroxybenzyl alcohols, methoxybenzyl alcohols and nitrobenzyl alcohol into the corresponding aldehydes has been attempted by using the same process.

The presence and position of substituent groups in the aromatic alcohols structure change the photocatalytic oxidation rates and product selectivities with respect to that previously observed for unsubstituted benzyl alcohol. In particular, the presence of both electron donating (hydroxy, methoxy groups) and electron withdrawing (nitro group) on the aromatic ring of the substrate causes a detrimental effect on the selectivity of the process with respect to that of benzyl alcohol.

The technical feasibility of selective photocatalytic oxidation of benzyl alcohol to benzaldehyde, in aqueous solutions and in presence of cupric ions, has been then investigated in a solar pilot plant with Compound Parabolic Collectors.

Under deaerated conditions, the presence of reduced copper species has been proved by XPS analysis. The results indicated that, at the end of the process, cupric species can be easily regenerated and reused, through a re-oxidation of reduced copper that is produced during the photolytic run, with air or oxygen in dark conditions.

A figure-of-merit (A_{CM}), proposed by the International Union of Pure and Applied Chemistry (IUPAC) and based on the collector area, has been estimated, under the proposed conditions, with the aim to provide a direct link to the solar-energy efficiency independently of the nature of the system. Generally speaking, it can be considered that the lower A_{CM} values are, the higher is the system efficiency.

1 STATE OF THE ART

1.1 Aldehydes

Aldehydes are represented by the general formula RCHO (figure 1), where R can be hydrogen or an aliphatic, aromatic, or heterocyclic group.

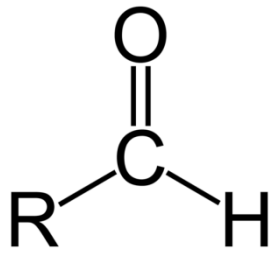

Fig. 1 Aldehydes general formula.

Aldehydes, particularly the aryl ones, due to their high reactivity, represent an important chemical intermediate class for the production of useful fine chemicals in many industrial sectors: pharmaceutical, food, fragrance, etc.[1]

Knowing that they can be easily found in nature[2-4], such as in the oils of some plant species (figure 2), aldehydes are produced through suitable industrial processes to meet the global demand.

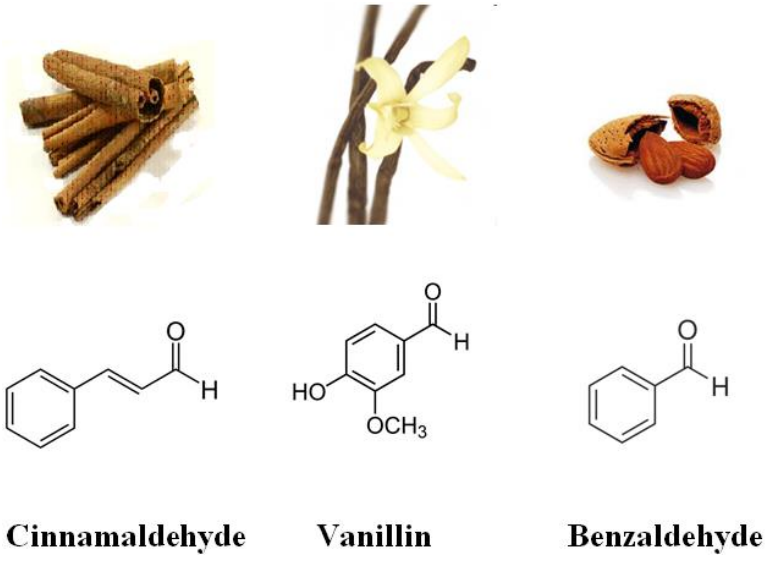

Fig. 2 Some aldehydes present in nature.

Usually, their industrial production relies on the selective catalytic oxidation of the corresponding alcohols. In general, the oxidation processes are carried out in harmful organic solvents at high temperature and pressure, in presence of expensive and environmental toxic oxidant agents (such as permanganate and dichromate salts), and lead to the formation of dangerous side products[5,6].

1.2 Industrial production of aldehydes

Although many processes are known for the synthesis of aldehydes, but only some of them are used on an industrial scale[7]. The most important ones on the industrial scale are the following:

- Hydroformylation of olefins (oxo synthesis) [7]:

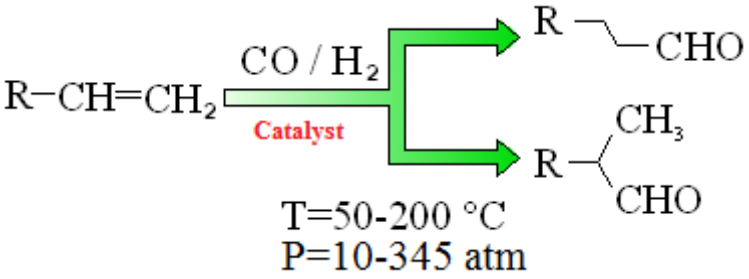

Fig. 3 Oxo synthesis.

In this process, olefins react with synthesis gas (CO, H_2) to form aldehydes at a temperature and pressure respectively ranging from 50-200 °C and 10-345 atm in presence of Ru, Rh, and Co based catalysts;

- Dehydrogenation of primary alcohols[7]:

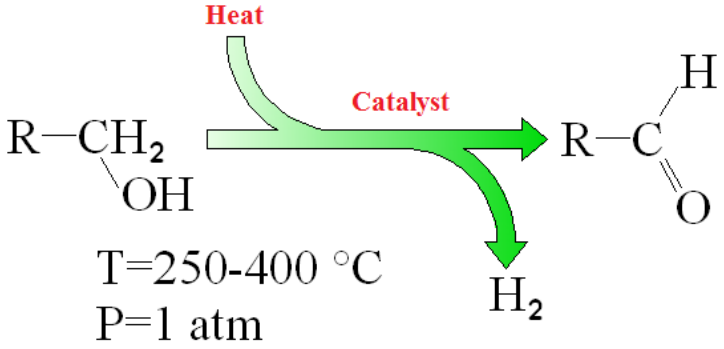

Fig. 4 Dehydrogenation of primary alcohols.

The endothermic dehydrogenation reaction is carried out at room pressure and temperature ranging from 250-400°C in presence of Ag and Cu catalysts activated by the addiction of Zn, Co or Cr;

- Partial oxidation of primary alcohols[7]:

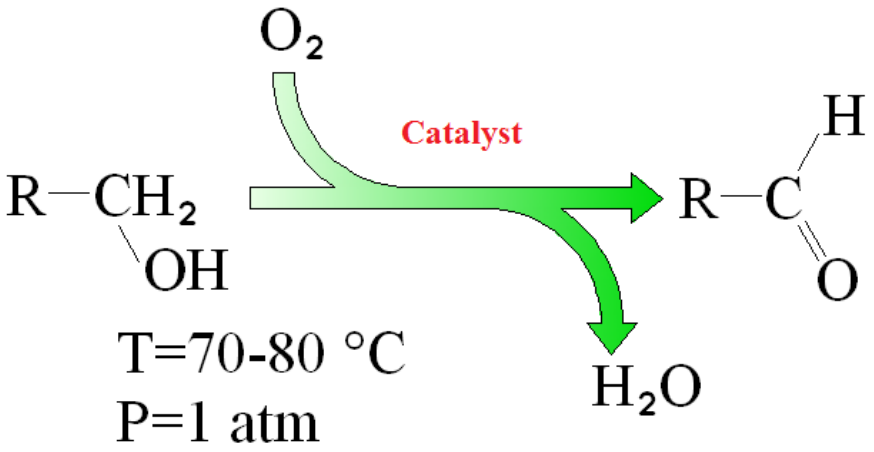

Fig. 5 Partial oxidation of primary alcohols.

The oxidation reaction is carried out in the liquid phase with a stoichiometric excess of air or oxygen, at temperature ranging between 70-80°C, and in presence of catalysts consisting of Mn(II) and Co(II) acetate. In traditional processes, Cr(VI) compounds, as potassium chromate or bichromate, were used instead of oxygen.

Other processes, less utilized, for aldehyde production are the oxidative dehydrogenation, the hydrocarbons oxidation, and the olefin oxidation.

The main concerns about the listed processes are:

- use of rather expensive and often harmful to the environment catalysts;
- severe operating conditions (high temperatures and pressures);
- recovery costs of catalysts for environmental and economic reasons;
- system costs to ensure a good safety level (highly flammable mixtures, ignition phenomena, etc...).

During the last decades, with the aim to overcome these difficulties, numerous studies devoted for the development of catalytic processes that use, for environmental and safety reasons, less dangerous solvents, as water, have been performed[8-10].

New processes essentially differ from the previous one in:

- use of chemical reagents with lower environmental impact;
- use of solvents that are less toxic, less flammable, and cheaper;
- use of cheaper catalysts with lower environmental impact;
- use of less severe operating conditions;
- possible use of solar radiation.

1.3 Solar radiation in chemical processes

Chemical industry has already investigated, partially at least, the possibility of exploiting solar energy for the conduction of chemical processes.

In this regard, a very interesting case is the Japanese company Toyo Rayon Ltd. In 1991, Toyo Rayon has reached the production of 160,000 t/yr of ε-caprolactam (5% of global demand) by using the photonitrosation of cyclohexane process (fig. 6), reducing production costs by 17%[11].

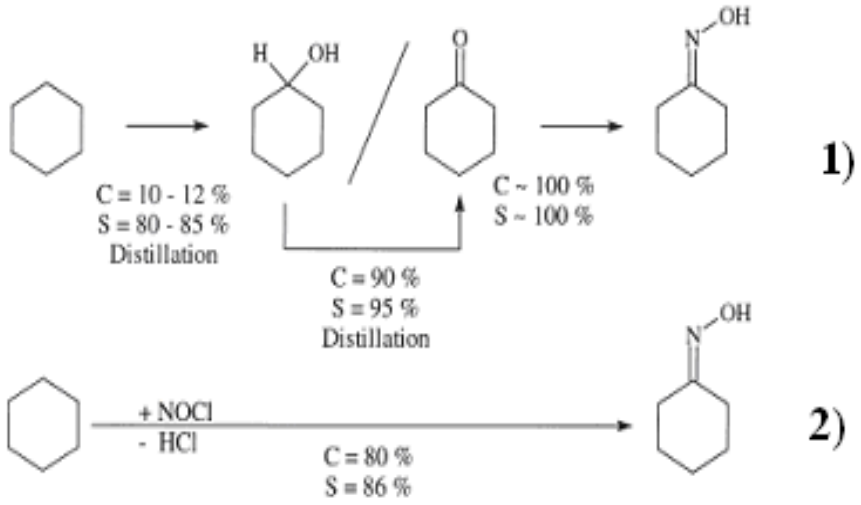

Fig. 6 Comparison of selectivity (S) and conversion (C) between thermochemical (1) and photochemical (2) synthesis process of cyclohexanone oxime.

According to Funken *et al.*[11], it is reported that the process is carried out using industrial lamps that could be replaced, when possible, with solar radiation, adequately concentrated, by using a reactor such as the one in figure 7.

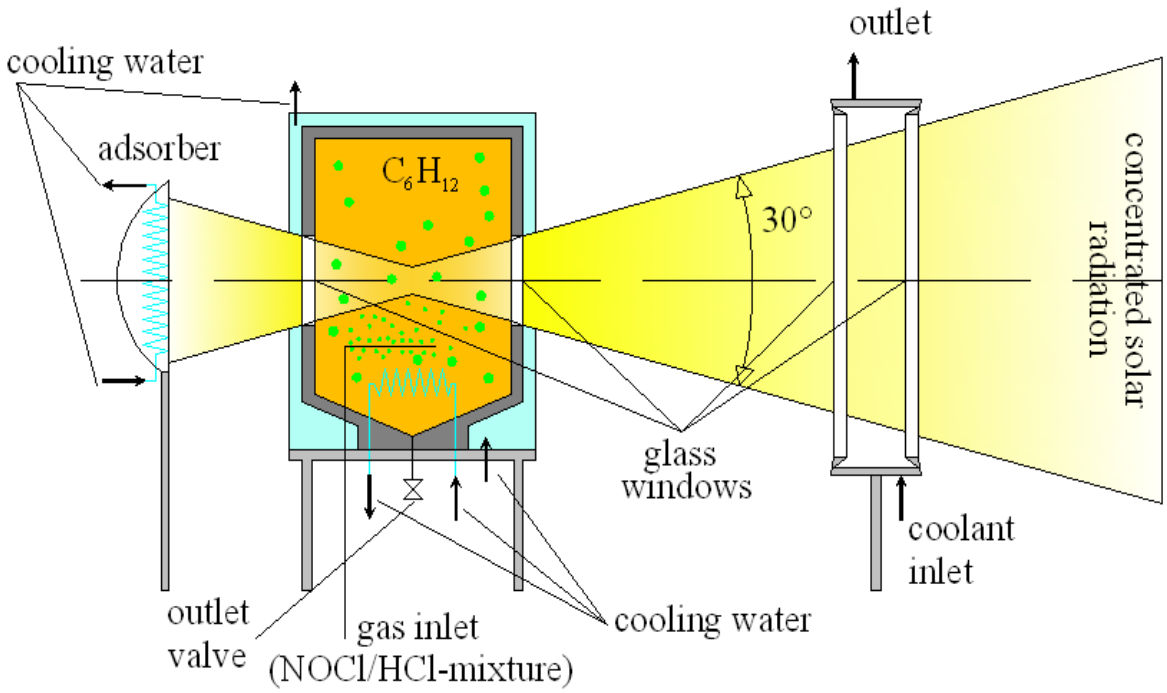

Fig. 7 Example of a reactor for solar photonitrosation of cyclohexane process.

The Authors have shown that, by including solar reactors into a ε-caprolactam production plant like that reported in figure 8, it's possible to further reduce production costs of ε-caprolactam due to the fact that the consumed electricity by the industrial lamps is greatly limited[12]. Moreover, considering that electrical energy is mainly derived from the combustion of fossil fuels, it was estimated that, for a production of 160,000 t/yr of ε-caprolactam, the use of solar reactors could reduce CO_2 emissions of about 280,000-400,000 t/yr.

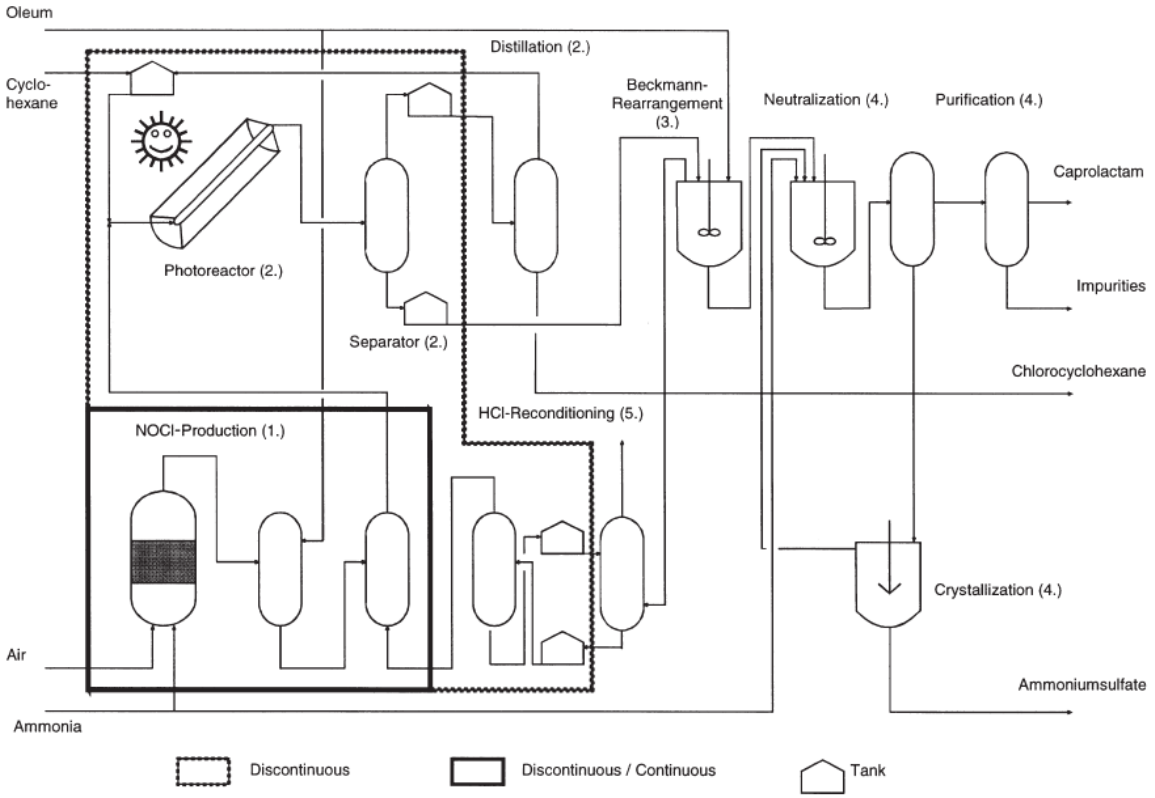

Fig. 8 Block diagram for a solar a ε-caprolactam production plant.

Another interesting application of solar radiation is represented by the synthesis of juglone (5-hydroxy-1,4-naphthoquinone), a coloring agent for foods and cosmetics, from 1,5-dihydroxynaphthalene (figure 9)[13-14]. Most of the corresponding thermal pathways are characterized by severe disadvantages concerning yield, selectivity, sustainability, or reproductivity[15-16]. In contrast, the photosensitized oxygenation of 1,5-dihydroxynaphthalene with artificial light sources furnishes juglone in yields ranging between 70–88%, even on multigram scales[17].

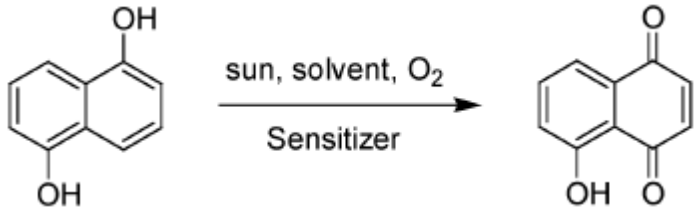

Fig. 9 Photooxygenation of 1,5-dihydroxynaphthalene.

On this basis, in August 2003, M. Oelgemoller *et al.*[18] tried to use a specific reactor for the solar production of juglone from 1,5-dihydroxynaphthalene by using rose bengal as sensitizer and isopropanol as solvent. The reactor was made of a glass tube equipped with holographic

mirrors (figure 10), designed to reduce warm-up effects (and thus the costs for process cooling) caused by infrared radiation. The given holographic concentrators (2 elements; 20 × 100 cm total) were made of dichromated gelatin which show a reflectivity range of 550 ± 140 nm, optimal for the usage of rose bengal[19].

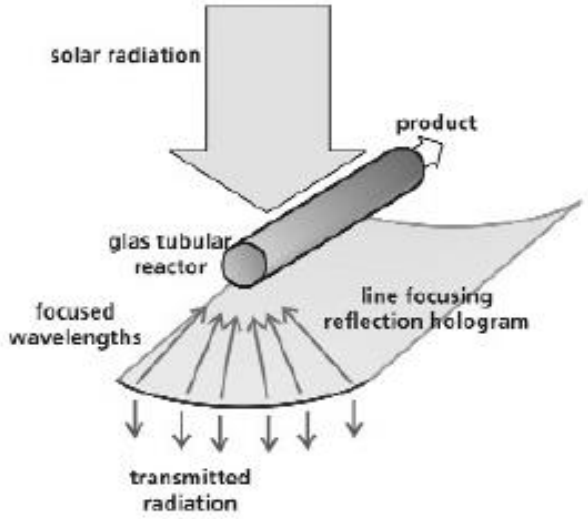

Fig.10 concept of holographic mirrors.

On the 12th August 2003, a test run was conducted with 1.0 g (6.2 mmol) of 1,5-dihydroxynaphthalene and 0.1 g of rose bengal in 200 mL of solvent. After less than 3 hours (figure 11), GC analysis revealed that most of the initial dihydroxynaphthalen had been consumed. At this stage, the collector has received 2.3 mol of photons and juglone was isolated in a yield of 79 %, which is an improvement on laboratory experiments carried out under identical conditions.

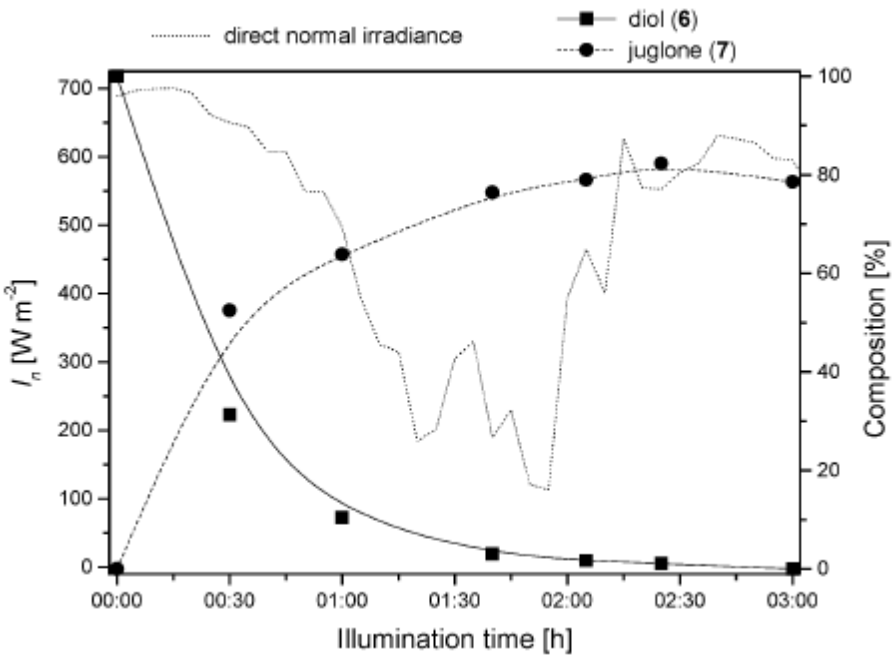

Fig. 11 Direct normal irradiance and product composition vs. illumination time for the rose bengal-mediated photooxygenation of 1,5-dihydroxynaphthalene (August 2003).

1.3.1 Solar photo-reactors

Solar photo-reactors have been generally used for the treatment of wastewater, for biological applications and, only in recent years, for the selective oxidation of organic substances. In literature, different kinds of solar powered photo-reactors are reported[20-25] and are discussed briefly in this section.

Particularly, all the used solar photoreactors can be divided in three families:

1. Parabolic Trough Collectors (PTCs);
2. Non-Concentrating Collectors (NCCs);
3. Compound Parabolic Collectors (CPCs).

The engineering concept for the PTCs comes from the solar thermal applications. The system supports turbulent flow with good homogenization. It is a closed system, preventing vaporization of volatile compounds. Its main disadvantage though, is that, through their geometry, the collectors can only use direct beam radiation, making them practically useless during cloudy days (figure 12).

Fig. 12 PTCs reactors during the photooxygenation of citronellol[14].

On the other hand, Non-Concentrating Collectors (NCCs), generally used for biological applications, are much cheaper than the PTCs. They have no tracking system, and harvest both direct beam and diffuse radiation. The disadvantages are the problems caused by mass transfer through laminar flow, possible vaporization of contaminants, and difficult scale up properties (figure 13).

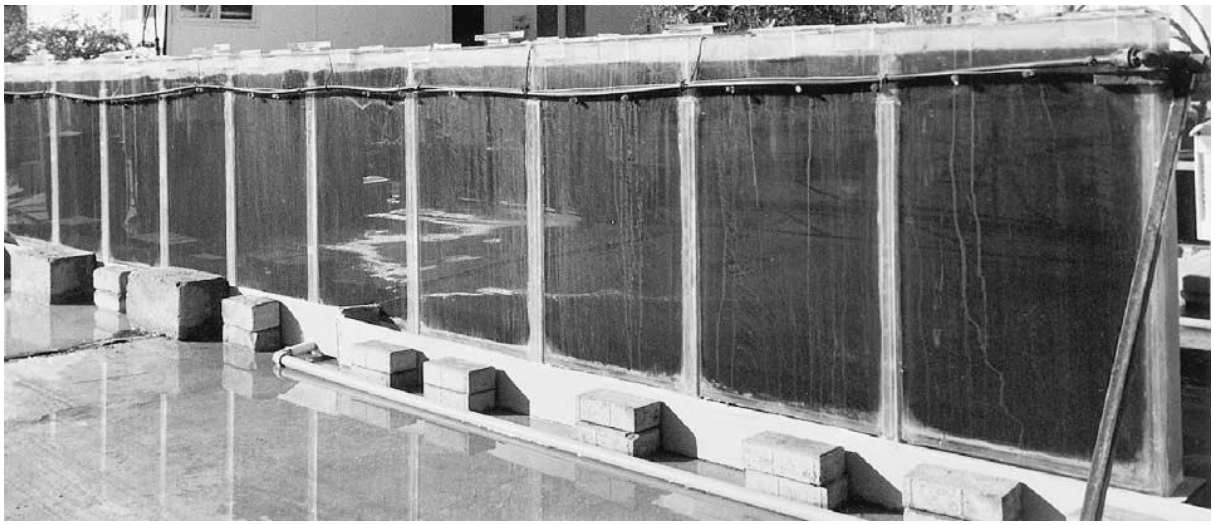

Fig. 13 NCCs glass photobioreactor, with a 10 cm light-path for mass production of *Nannochloropsis* sp.[23]

The Compound Parabolic Collectors (CPCs) combine the advantages of the two abovementioned reactor types eliminating their disadvantages. They are static reactors

without tracking system and have been found to be the most efficient harvesting optics for non-concentrating systems[26]. They support turbulent flow, have a closed system, are cheap, and easy to maintain. Since the temperature does not play any significant role, there is no need of insulation. For these reasons, in the last years, the CPCs are the solar reactors most commonly used, in particular for the treatment of wastewater (figure 14).

Fig. 14 CPC-solar reactors for the treatment of contaminated waters in southern Spain in El Ejido in the province of Almeria (Albaida S.A).

The photochemical CPCs reactor consists of various parts:

- tanks where mixing of the solutions with various chemicals take place;
- resistant pipes, to bring the reactive mixture to the CPC reactor;
- pumps used to provide a steady mass flow with minimal pressure drops.

The pipes can be made of high density polyethylene (HDPE) or polypropylene (PP), avoiding the use of metallic or composite material which could be degraded by possible oxidation during the process. All materials used must be inert to UV degradation in order to be compatible with the minimum lifetime requirements of the system (usually 10 years). The piping, valves, and reactor must be strong enough to resist the necessary water flow pressure, which has typical values of 2-4 atm (nominal system pressure drop) and a maximum of 5-7 atm.

The reflective material should be cheap, weather resistant, and should have a high reflectivity in the desired range. For example, if the process carried out in the reactor needs UV radiation (photo-Fenton or application with TiO_2), the reflectivity of traditional silver-coated mirrors, ranging between 300 and 400 nm, is very low (25.2% at 280 nm to 92.8% at 385 nm). Aluminum is the only metal surface which is highly reflective throughout the UV spectrum, with a reflectivity ranging from 92.3% at 280 nm to 92.5% at 385 nm. However, the aluminum surface has to be treated, due to the fact that when it is freshly deposited, its surface

tends to be fragile. Using a conventional glass cover, the reflectivity is lowered and UV light is filtered. The thin oxide layer that forms naturally on aluminum is insufficient to protect the surface under outdoor conditions. Since the oxide layer continues to grow, a dramatic UV reflectance drop is observed. For applications that need UV radiation, the best materials available nowadays are electropolished aluminum or organic plastic films with aluminum coating[20].

For this type of applications, the tubes are required to be:

- UV and visible light transparent;
- resistant to UV, low or high pH and chemicals present in the reactor (oxidant, pollutants and their degradation products);
- resistant to high temperatures during summer (60ºC).

The materials for these reactors, therefore, are limited to fluoropolymers, quartz glass, and borosilicate glass. Quartz has excellent properties (chemical and thermal stability, mechanical resistance and excellent UV transmission), but its high production cost makes it not completely feasible for photocatalytic applications. Fluoropolymers have a good thermal stability, good UV transmittance, excellent UV stability, and chemical inertness. One disadvantage is that the wall thickness of flouroploymer tubes has to be increased to achieve the desired minimum pressure rating, which in its turn will lower its UV transmittance. Borosilicate glass has a good transmittance with a UV cut-off of about 285 nm. It is chemically, mechanically, and UV stable, as well as cheaper than quartz glass.

A uniform flow distribution inside the reactor must be assured, as non-uniform flow distribution leads to non-uniform residence times, resulting in decreased performance compared to ideal flow situations. The flow inside the reactor should be turbulent to ensure good mixing and to ensure that there is no settlement of suspended solids (even more important when using catalyst like TiO_2, in suspension).

The system is composed of a tube positioned above a reflector consisting of two truncated parables with a concentration factor (R_C) (ratio of tube perimeter to aperture) of almoste one (figure 15). The concentration factor (R_C) of a two dimensional CPC is given by:

$$R_{C,CPC} = \frac{1}{sin\theta_a} = \frac{1}{2r\pi}$$

The normal values for the semi-angle of acceptance (θ_a), for photocatalytic applications are between 60º and 90º. This wide angle allows the receiver to collect both direct and a large part

of the diffuse light ($1/R_C$ of it). A special case is when the acceptance angle is θ_a=90º and $1/R_C$=1 (non-concentrating system). When this happens, all the UV radiation (direct and diffuse) can be collected and redirected to the reactor.

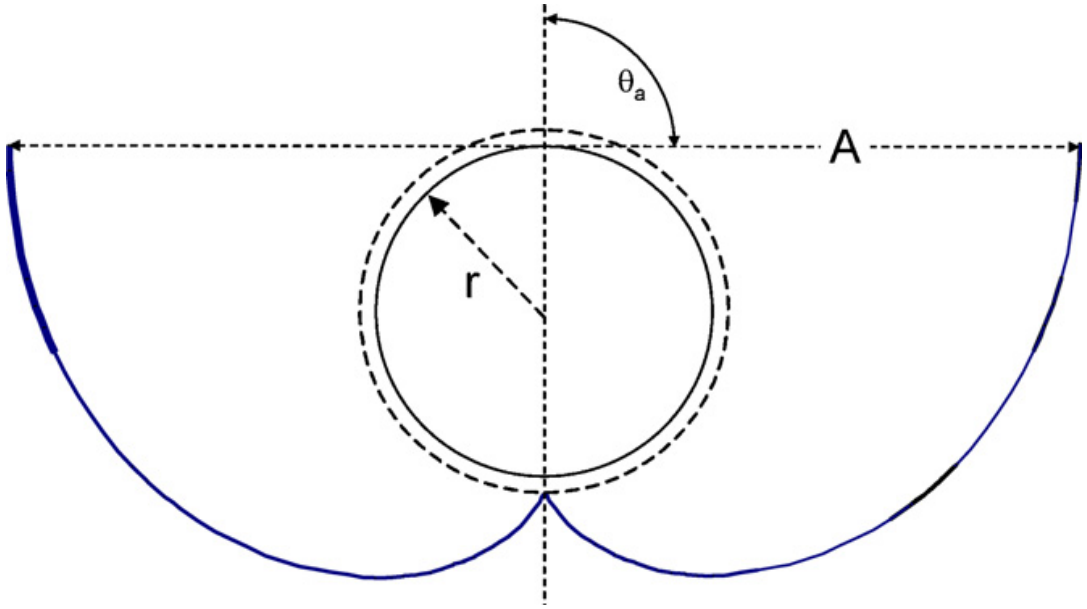

Fig. 15 Section of a CPC reactor.

If the CPC is designed for an acceptance angle of +90º to -90º, all incident diffuse radiation can be collected. Moreover the reflected light is distributed all around the tubular receiver, so that almost the entire circumference of the receiver tube is illuminated (figure 16).

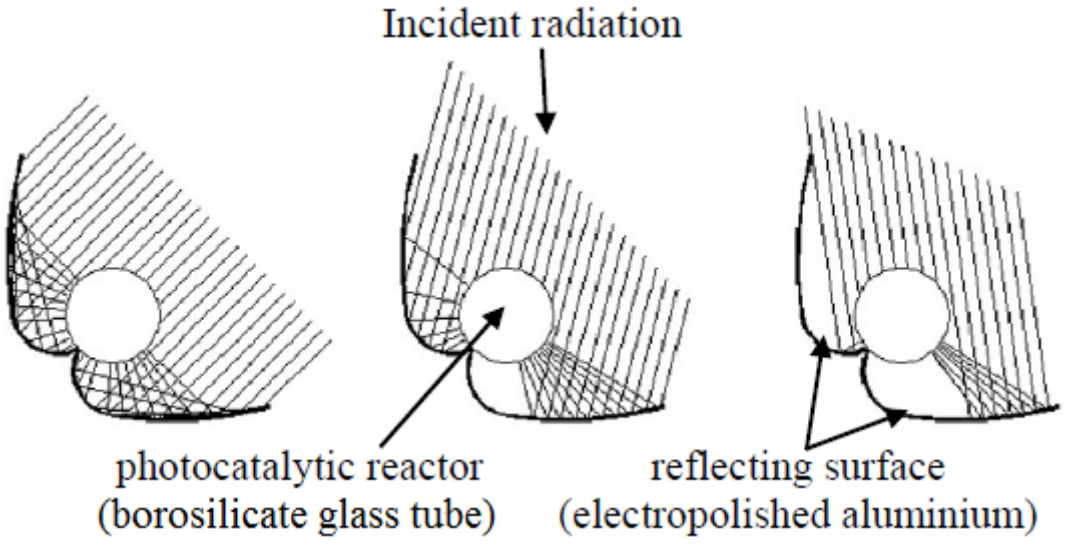

Fig. 16 Behavior of incident solar radiation on a CPC reactor

1.4 Selective photocatalytic systems for aryl aldehydes production

Most of the recent studies, focused on development of industrial alternative processes for the production of aldehydes, are aimed at the elaboration of selective photocatalytic systems that make use of solar radiation.

These processes would offer significant advantages over the classical ones such as:

- use of renewable energy source;
- optimal operating conditions: room pressure and temperature;
- use of readily available and environmental friendly catalysts.

Generally, photocatalytic systems uses oxides of semiconductor metal (SC) as catalysts and oxygen as oxidant[27]. It has been shown that titanium dioxide (TiO_2) is one of the best photocatalysts because it is characterized by high stability, good performance, and low cost[28]. For these reasons, during the last three decades, it has been extensively studied as a tool to oxidize organic pollutants in aqueous solution by means of a UV source and oxygen (or air)[20, 29-30].

The photocatalytic process can be represented as in the diagram of figure 17, where A is an electron acceptor (oxidant species) and D is the electron donor (species to be oxidized).

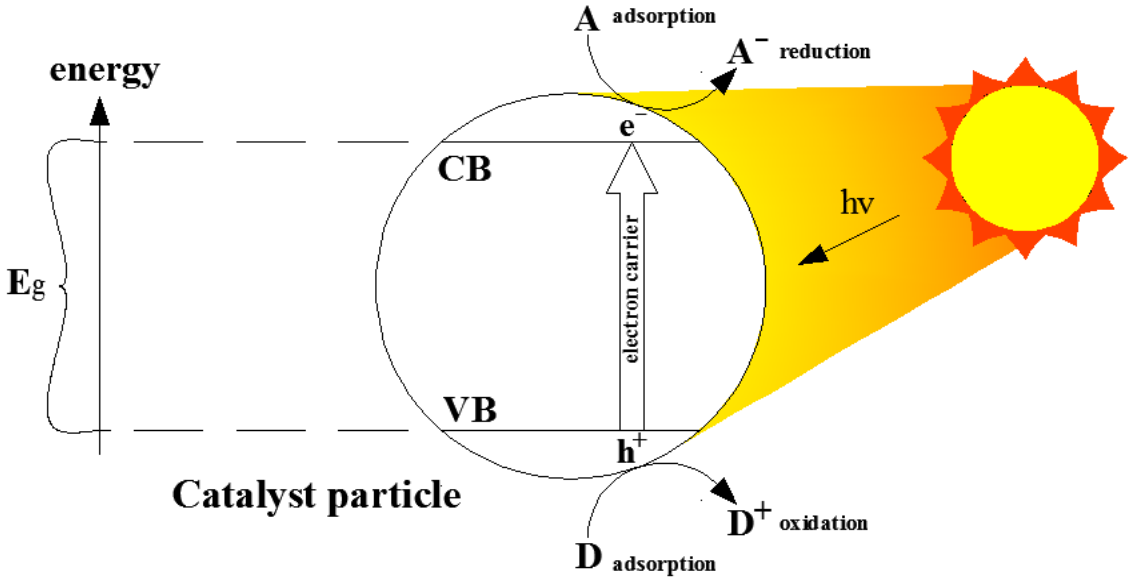

Fig. 17 Diagram of a general photocatalytic process.

The process begins with the absorption of UV radiation by the catalyst and with the formation of an "electron-hole" pair:

$$TiO_2 \xrightarrow{hv} h^+_{VB} + e^-_{CB}$$

While the high reducing capability of photogenerated electrons allows the reduction of the electron acceptor, that traditionally is represented by dissolved oxygen. In the latter case, the reaction leads to the formation of $O_2^{\bullet-}$ radicals[20, 29-30]:

$$O_2 + e^-_{CB} \rightarrow O_2^{\bullet-}$$

The positive hole can directly react with dissolved organic substances, water molecules, or OH^- ions adsorbed on the catalyst surface. In particular, the last two reactions generate $HO^\bullet$ radicals.

$$S + h^+_{VB} \rightarrow P$$
$$H_2O + h^+_{VB} \rightarrow HO^\bullet + H^+$$
$$HO^- + h^+_{VB} \rightarrow HO^\bullet$$

In recent years, titanium dioxide photocatalysis has been used for the functionalization of light n-alkanes[31-32] and the selective photo-oxidation of aromatic alcohols[33-34] or phenols[35]. In particular, in 2009 Zhang *et al.*[36] have studied the mechanism of the photocatalytic oxidative transformation of alcohols performed in benzotrifluoride by using bare TiO_2 anatase. The mechanism proposed by the Authors (figure 18) begins with the alcohol adsorption on the surface of TiO_2 by a deprotonation process. Hence, the adsorbed alcohol reacts with the photogenerated hole on the TiO_2 surface forming a carbon radical whereas the electron transforms Ti(IV) in Ti(III). Both the carbon radical and Ti(III) easily react with O_2 and a Ti peroxide intermediate is formed. The cleavage of this species gives rise to carbonylic species, produced from the partial oxidation of the alcohol, and hydrogen peroxide molecules, coming from the reaction between Ti peroxide intermediate and two H^+ ions.

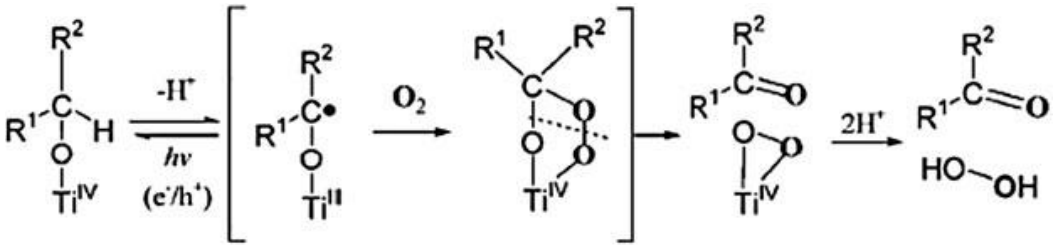

Fig. 18 Reaction scheme between TiO_2 and alcohol molecule.

In the same year, Higashimoto *et al.*[37] have proposed a photocatalytic process by which benzyl alcohol and some of its derivates, dissolved in acetonitrile, under light radiation, in presence of TiO_2 and O_2, were converted into the corresponding aldehydes with a conversion and selectivity of *ca.* 99%. The only exception to this behaviour was represented by the 4-hydroxybenzyl alcohol that was oxidized to 4-hydroxy benzaldehyde (selectivity of *ca.* 23% with a conversion of *ca.* 85%) along with some unidentified products. Remarkably, the reactions proceed not only under UV, but also under solar radiation. It means that the process proceeds without the use of industrial lamps.

Besides TiO_2, other solid semiconductors or substances have been tested[40-41]. Heteropoly acid solids (HPAs), also called polyoxometallates (POM), are ionic crystals made up of oxygen with certain metals (such as tungsten, molybdenum or vanadium), non-metals (such as sylicon, phosphourous or arsenic), hydrogen, and crystallization water. An example of POM is reported in figure 19.

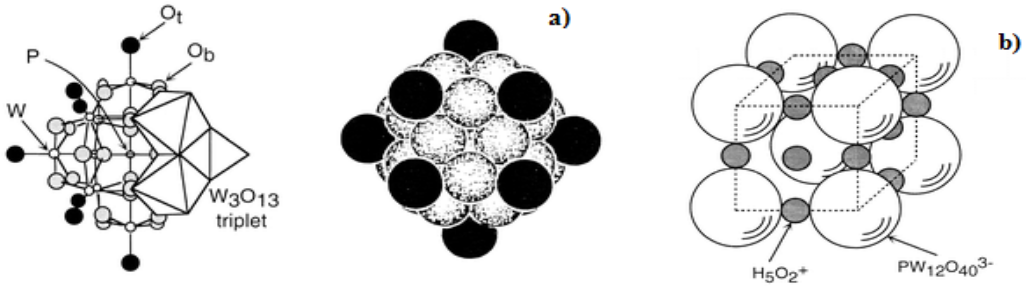

Fig. 19 a) primary structure (Keggins structure, $PW_{12}O_{40}^{3-}$); b) secondary structure ($H_3PW_{12}O_{40}\cdot 6H_2O$).

POMs are used in solution as well as in the solid state as acid and oxidation catalysts[40]. As semiconductor photocatalysts, also the POMs have photochemical characteristics. In fact, both classes of materials are constituted by d^0 transition metal and oxide ions and exhibit

similar electronic characteristics (HOMO–LUMO transition for the POMs and band-gap transition for semiconductors). The irradiation in the UV-Vis region results in an excited state, consisting in a charge transfer from the oxygen to the metal, which is able to draw oxidation reactions[42-43]. The photoexcited POM is then reduced but its regeneration is easily obtained by oxidation with the O_2 present in the reacting medium.

In this regard, in 2005 Farhadi et al.[38] reported the partial oxidation of benzyl alcohols using sol–gel silica-encapsulated $H_3PW_{12}O_{40}$ as a heterogeneous photocatalyst and acetonitrile as solvent, under O_2 flux at room temperature (r.t.). They optimized the reaction conditions for the partial oxidation of 1-phenyl ethanol to acetophenone with yield of 84% (figure 20).

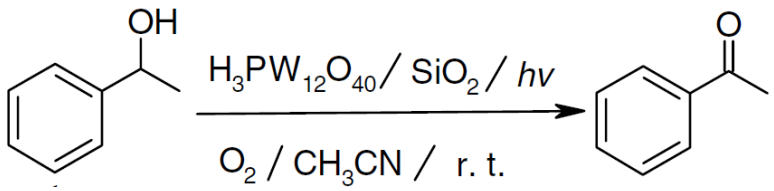

Fig. 20 Selective oxidation of benzyl alcohol by means of sol–gel silica-encapsulated $H_3PW_{12}O_{40}$.

In a very similar process, primary and secondary benzyl alcohols have been oxidized to the corresponding aldehydes and ketones in high selectivity (*ca.* 90% after 3 hours of reaction) when $H_3PW_{12}O_{40}$ entrapped into a ZrO_2 matrix is used[39]. The photocatalytic cycle for the partial oxidation of alcohols with this catalyst is shown in figure 21.

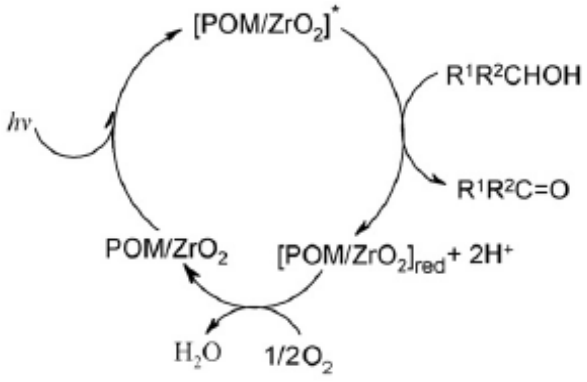

Fig. 21 Selective oxidation of benzyl alcohol by means of $H_3PW_{12}O_{40}$ entrapped into a ZrO_2 matrix.

With this typology of catalyst, it was also found a dependence of selectivity on the nature of solvent. In fact, the highest yield values in aldehydes are achieved using acetonitrile as solvent (table 1).

Entry	Solvent	Irradiation time (h)	Yield[b] (%)
1	*n*-Hexane	5	67
2	**CH_3CN**	**3**	**93**
3	$CHCl_3$	5.5	48
4	CH_2Cl_2	6	52
5	Et_2O	5	55
6	Acetone	5.5	60
7	Toluene	4.5	58
8	CH_2ClCH_2Cl	6	56
9	C_6H_6	4.25	60
10	Cyclohexane	5	53
11	AcOEt	5	60
12	PhCl	4.5	57

Tab. 1 Experimental procedure: 4-chlorobenzyl alcohol (10 mmoles); POM/ZrO_2 (0.25g); solvent (10mL).

Although these processes are characterized by considerable advantages already mentioned, such as high selectivity and the use of renewable resources, they also have some disadvantages, such as:

- possibility of generating flammable mixtures;
- use of organic solvents.

During the last decade, aiming to minimize the environmental impact of industrial processes, a new approach, known as "Green Chemistry", has been increasingly making inroads into the world of research. Accordingly, reducing the use of organic solvents is being attempted knowing that these solvents are not only often flammable and toxic for operators but can be also a source of environmental pollution[43], is being done.

In this perspective, Palmisano group[44-47] proposed a very interesting study about a photocatalytic process by which 4-methoxybenzyl alcohol (MBA) is partially converted in p-anisaldehyde (PAA) in presence of oxygen and a home prepared TiO_2, by using water as solvent. In these works, it is shown that MBA oxidation proceeds through two parallel pathways[48]: partial oxidation of MBA to the corresponding aldehyde and complete oxidation of MBA to CO_2 and H_2O (figure 22).

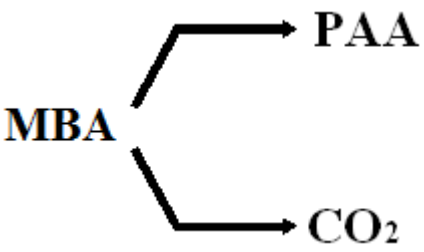

Fig. 22 Two parallel pathways of MBA photoxidation in presence of TiO_2 and O_2.

Particularly, by using different TiO_2 samples, prepared with low treatment temperature[49], a selectivity over 74%, with a conversion over 80%, was achieved (figure 23).

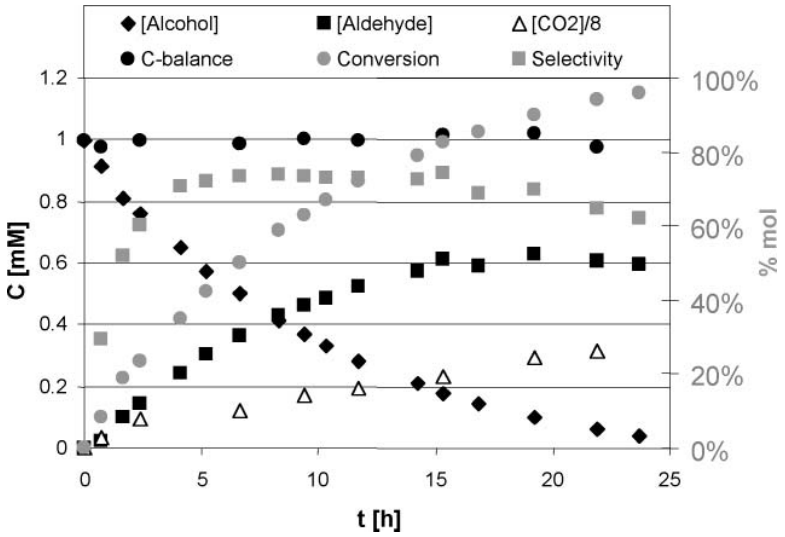

Fig. 23 Experimental results of MBA photocatalytic oxidation obtained with a TiO_2 load equal to 0.2 g/L.

The proposed process does not require the use of organic solvents, but needs the presence of oxygen which, in contact with solution of alcohols or other organic substances, could generate explosive mixtures.

1.5 Photodeposition of metals

Substituting oxygen with reducing agents that trap electrons in the conducting band still enables the oxidation of the organic species. An interesting case is in which oxygen as a reducing agent is replaced by a metal ion (M^{n+}) present in the solution. As reported by D.

Chen *at al.*[50], the process begins with the absorption of UV radiation by the catalyst with the "electron-hole" pair formation:

$$TiO_2 + hv \longrightarrow h^+_{VB} + e^-_{CB}$$

The metal ion M^{n+}, reacting with the conduction band electron (e^-_{CB}), reduces to a lower oxidation state:

$$M^{n+} + e^-_{CB} \longrightarrow M^{(n-1)+}$$

Whereas the organic species (RH) are oxidized through a direct reaction with the positive holes h^+_{VB}:

$$RH + h^+_{VB} \longrightarrow R^{\bullet} + H^+$$

or mineralized by HO radicals:

$$HO^{\bullet} + RH \longrightarrow R^{\bullet} + H_2O \longrightarrow \ldots\ldots \longrightarrow H_2O + CO_2 + \text{inorganic acids}$$

In absence of oxygen, the hydroxyl radicals are produced only by the reaction with the positive holes:

$$HO^- + h^+_{VB} \longrightarrow HO^{\bullet}$$

In some cases, the reduction of the metal results into its precipitation from the solution, thus enabling its separation and recovery. The reduction of many metals such as Cu(II), Ni(II), Pb(II) and Zn(II) has already been investigated [51-54]. Among others, some papers have been devoted to the photoreduction of Cu(II) ions in the presence of simple organic species such as

formic acid[55], sodium acetate, ethanol, tert-butyl alcohol, acetone, sodium oxalate, EDTA, citric acid and other substances[56] in the absence of oxygen, as reported in table 2.

	illum., N_2 purge		no illum., air oxidation	
compounds	% init. $[Cu^{2+}]^a$	TiO_2 Color	% init. $[Cu^{2+}]^b$	TiO_2 color
water	98	White	99	white
sodium acetate	99	White	100	white
sodium propionate	98	White	99	white
ethanol	97	off-white	100	white
ethanol (3.9 M)	1	Purple	100	white
tert-butyl alcohol	96	White	96	white
tert-butyl alcohol (1.9 M)	100	White	100	white
Acetone	87	White	93	white
acetone (3.1 M)	100	White	100	white
sodium oxalate	1	Pink	87	white
sodium formate	1	Purple	100	white
citric acid	1	gray-purple	55	pale pink
EDTA	1	Purple	8	purple
methanol	40	dark purple	100	white
methanol (5.7 M)	1	dark purple	100	white
2-propanol	54	Purple	99	white
2-propanol (3.0 M)	1	Purple	100	white

Tab.2 Cu(II) photodeposition in presence of TiO_2 and various organic compounds.
a) The experimental runs were carried out with a solution of 130mL containing $CuSO_4$ at the concentration of 50μg/mL, 1M (except when indicated) of organic substances and 0.26g of TiO_2. The solution was buffered to a pH range 3.5-3.6 whit HCl and NaOH and was exposed to UV radiation for 45min.
b) The solution was poured in a 400mL beaker and stirred in contact with air for 40min.

It has been reported (Table 2) that, at the end of the process, the simple addition of air into the system allows the re-oxidation of precipitated copper, which completely dissolves. As its photodeposition, also the copper re-oxidation depends on the organic substance present in the solution[57] as reported in figure 24:

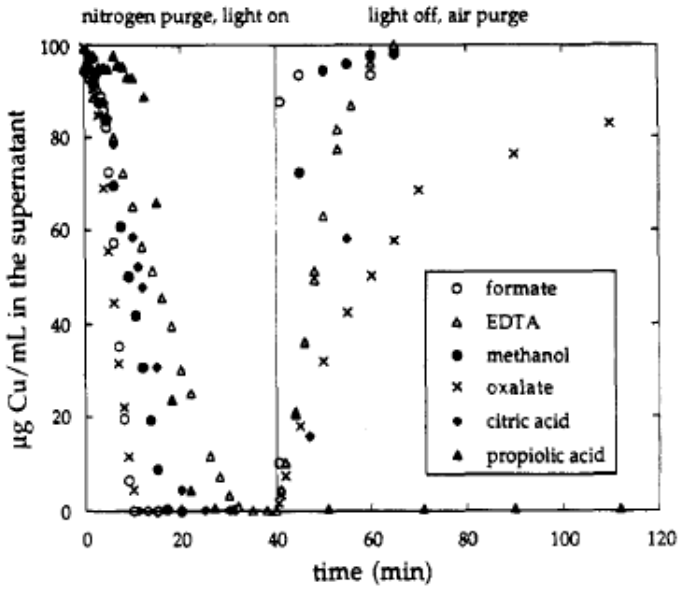

Fig. 24 Concentration profiles of dissolved copper into a solution buffered to a pH range of 3.5-3.6 containing 100mM of organic substance, 2g/L of TiO_2 and 100μg/ml of Cu.

After the photocatalytic run, chemical state of solid copper was also intensively investigated, but controversial results were reported. Most of the researchers reported that the solid is composed of a mixture of zero valent copper and cupric oxide (and, in some case, cuprous oxide)[57-60]. In some studies it was concluded that the reduced Cu species was zero valent copper[55, 61]. However, the possibility of the presence of both Cu(I)/Cu(II) species, due to a reoxidation of metal copper during the preparation of the analytical samples, was not completely ruled out[62].

2 THE AIM OF THE RESEARCH

The study evolves around an innovative and environmentally friendly process capable of selectively oxidize alcohols into their respective aldehydes: the TiO_2/Cu(II)/hv photocatalytic system. In fact, it's possible to assume, as shown in figure 25, that alcohols diluted in an aqueous solution can be selectively oxidized into aldehydes with the simultaneous reduction of Cu(II) to Cu(0).

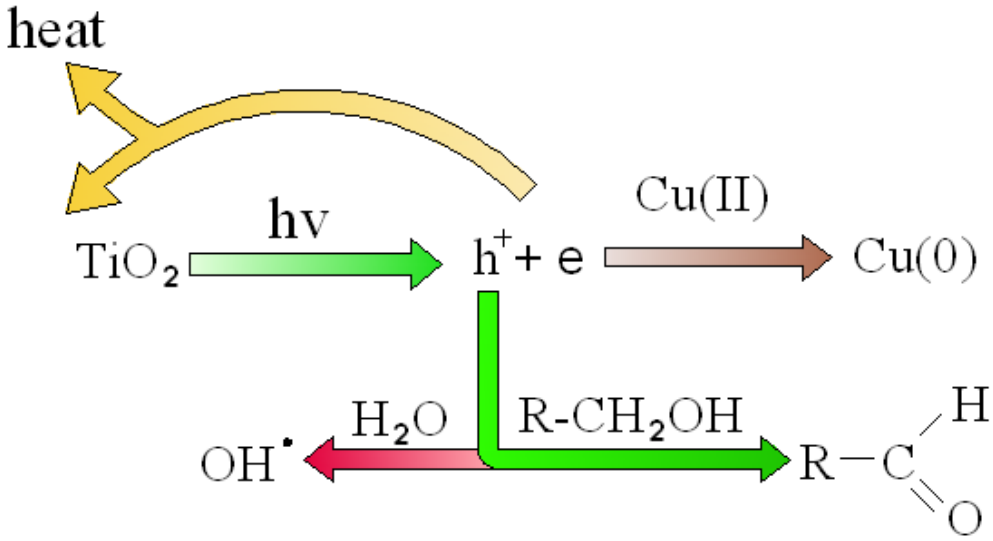

Fig. 25 Diagram of TiO_2/Cu(II)/hv photocatalytic system for the selective oxidation of alcohols.

In particular, titanium dioxide, under the effect of UV/VIS radiation, is energized and, successively, generates electron-hole pairs. The Cu(II), present in solution, captures the photogenerated electrons of the valence band reducing itself first to Cu(I) and then to Cu(0). At the same time, the holes can react with molecules of alcohol, which oxidise to respective aldehydes and water, generating $HO^{\bullet}$ radicals. The described process occurs in absence of oxygen to prevent competition with Cu(II) or Cu(I) in capturing photogenerated electrons. Once the aldehyde is produced and separated from the solution, it is possible to reoxidize the copper using an airflow, as reported in figure 26. Consequently, it is possible to consider copper as a catalyst.

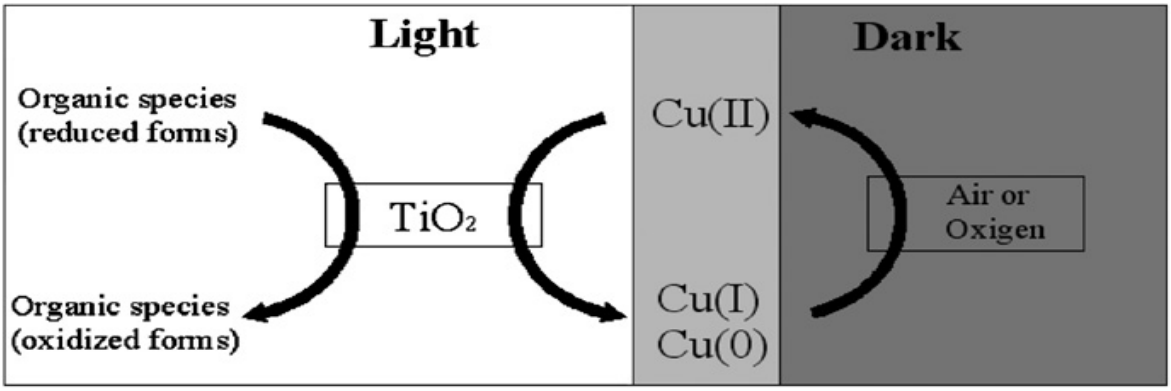

Fig. 26 Diagram representing the possibility to reuse the copper.

The described process is studied, by using laboratory scale reactors, and modelled at varying operating conditions such as:

- type of TiO_2;
- TiO_2 load;
- Cu(II) concentration;
- pH;
- effect of anions concentration
- UV irradiation;

The Cu(II)/TiO_2/hv process is very interesting and innovative not only because it could use a renewable energy source (solar energy), but also because it solves problems related to aldehydes production. In fact the proposed process is characterized by:

- the use of chemical reagents, alcohols, with low environmental impact;
- the use of water as solvent;
- the use of a cheap and environmental friendly catalyst, as TiO_2;
- optimal operating conditions: room pressure and temperature;
- the difficulty to create flammable mixtures due to the absence of oxygen.

Moreover, the development of the TiO_2/Cu(II)/solar radiation system for the selective oxidation of benzyl alcohol to benzaldehyde in water has been studied. The study consisted of

using a solar photocatalytic pilot plant at different operating conditions (TiO_2 photocatalyst type, Cu(II) initial concentration and irradiance of solar radiation). The possibility of reusing copper as a catalyst has been also tested by oxidizing the precipitated zero valent copper with an air flow blown into the pilot-plant in dark conditions.
At last, after the oxidation runs, analysis of solid has been carried out to clarify the nature of copper species at the end of the process.

The alcohol used for this investigation is benzyl alcohol, which should be oxidized to benzaldehyde.

2.1 Benzaldehyde and its derivatives

Benzaldehyde exists in nature, occurring in combined and uncombined forms in many plants. The best known natural source of benzaldehyde is amygdalin, in which it exists in a combined form as a glycoside and is present in bitter almonds. Benzaldehyde is an important starting material for the production of odorants and flavours. Being responsible for the odour of natural bitter almond oil, it is incorporated directly in perfumes, soaps, foods, drinks, and other products. Substantial amounts are used in the production of derivatives, such as cinnamaldehyde, that are also employed in the perfume and flavour industries. In the pharmaceutical industry, benzaldehyde is used as an intermediate in the production of fine chemicals[63].

Industrially, benzaldehyde is principally produced by:

Hydrolysis of benzal chloride[63]

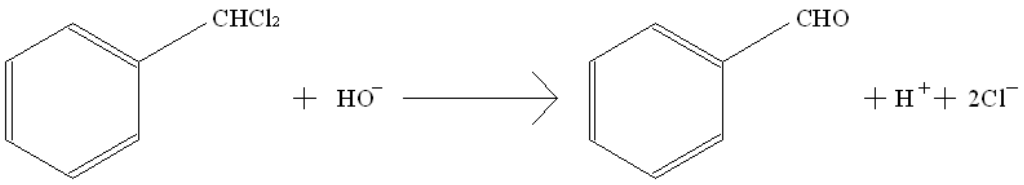

Fig 27 Hydrolysis of benzal chloride.

Benzal chloride and the alkaline hydrolyzing agent (e.g., calcium hydroxide, calcium, or sodium carbonate) react as counter currents in a flow reactor in an unreactive organic solvent

(e.g., toluene, xylene). A temperature of 125-145 °C and a pressure of 12-18 atm are maintained.

- Oxidation of toluene[63]

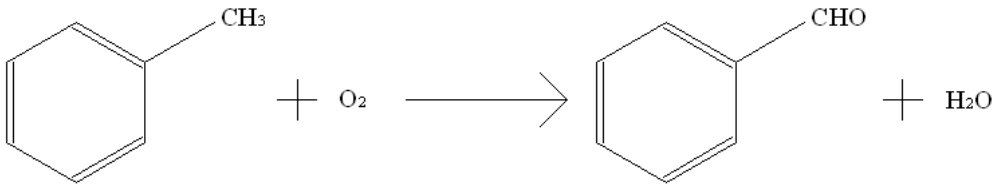

Fig 28 Oxidation of toluene.

The partial oxidation of toluene with oxygen to give benzaldehyde can be carried out in either the gas phase or liquid phase. Benzaldehyde itself is easily further oxidized to benzoic acid and other products. Conditions must therefore be carefully chosen to favour only partial oxidation. For the production of benzaldehyde, more important than gas-phase oxidation is the oxidation of toluene in the liquid phase by oxygen in the form of air or other gaseous mixtures. This is carried out at 80-250 °C, preferably in the presence of cobalt, nickel, manganese, iron, or chromium compounds (alone or in combination) as catalysts.

The process has been also tested with substituted benzyl alcohol. In particular, in table 3, are reported the alcohols used for this investigation and the corresponding aldehydes.

R	**ALCOHOL**	**ALDEHYDE**
-H	benzyl alcohol (BzA)	benzaldehyde (BzAD)
-OH	(2-, 3- and 4-)hydroxybenzyl alcohols (HBzA)	(2-, 3- and 4-)hydroxybenzaldehydes (HBzAD)
$-NO_2$	4-nitrobenzyl alcohol (NBzA)	4-nitrobenzaldehyde (NBzAD)
$-OCH_3$	(2- and 4-)methoxybenzyl alcohol (MBzA)	(2- and 4-)methoxybenzaldehydes (MBzAD)

Tab. 3 Substituted benzyl alcohols tested with the process TiO_2/Cu(II)/hv.

These substituted aldehydes, as benzaldehyde, are produced with processes that generally require:

- use of catalysts rather expensive and often harmful to the environment;
- severe operating conditions (high temperatures and pressures);
- use of chemical reagents with high environmental impact;
- use of solvents with high toxicity, flammable and expensive;
- system costs to ensure good safety level (highly flammable mixtures, ignition phenomena, etc...).

.

3 EXPERIMENTAL

3.1 Experimental set-up and procedures

3.1.1 Laboratory-scale experiments

All the experiments with UV lamp have been carried out at 25°C in a batch annular glass jacketed reactor with an outer diameter of 6.5 cm and a height of 40 cm wrapped with an aluminium foil and filled with 0.280 L of solution. At the top, the reactor has two inlets for feeding the reactants, for withdrawing samples and for the entry of a gas flow. In fact, in all the experiments, the solution has been preventively purged with nitrogen to remove the dissolved oxygen that could have competed with cupric ions for the reaction with the electrons. During the runs, a gaseous stream of nitrogen has been continuously fed to the irradiated solution to prevent any contact with oxygen as shown in figure 29.

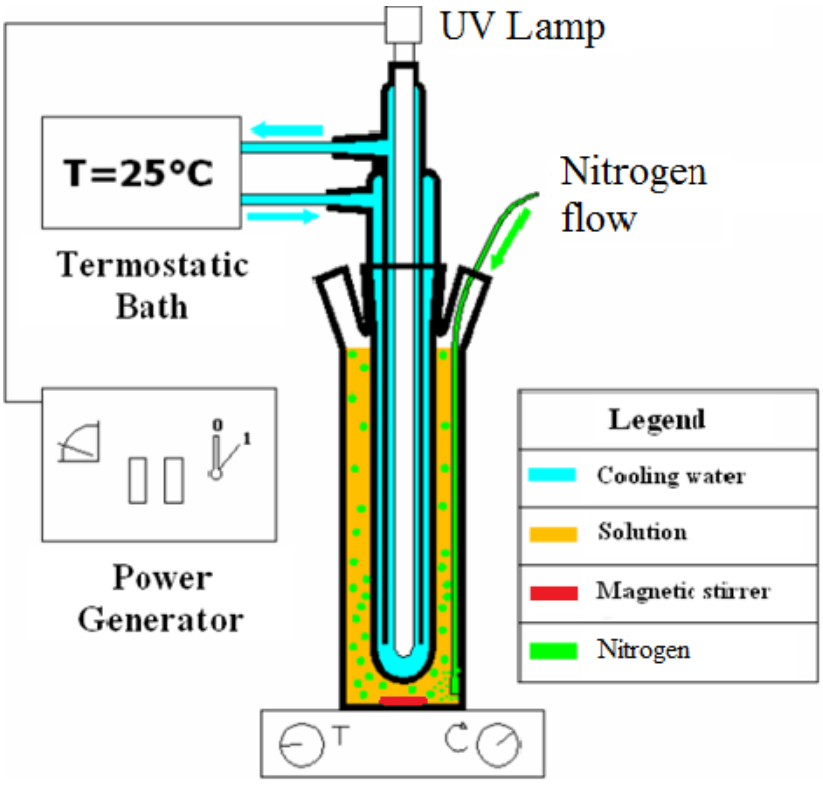

Fig. 29 Batch annular glass reactor.

The reactor has been equipped with a 125 W (power input) high-pressure lamp (by Helios Italquartz), mainly emitting at 305, 313 and 366 nm (manufacturer's data), enclosed in a glass sleeve, immersed in the solution, and mixed with a magnetic stirrer placed at the bottom.
The photon flow of the lamp at 305 nm was $1.47 \cdot 10^{-6}$ $E \cdot s^{-1}$ ($I°_{(305)}$, determined through hydrogen peroxide photolytic experiments[64]),at 313 nm, $1.56 \cdot 10^{-6}$ $E \cdot s^{-1}$ ($I°_{(313)}$, determined by valerophenone actinometry[65]) and at 366 nm, $4.10 \cdot 10^{-6}$ $E \cdot s^{-1}$ ($I°_{(366)}$, measured using a UV radiometer Delta Ohm HD 9021).
During the experimental run the samples have been collected with a syringe and have been immediately filtered and analysed.

To understand the effect of the irradiance on the TiO_2/Cu(II)/hv system, some experiments have been carried out in a Suntest solar simulator (Suntest XLS+ photoreactor, Atlas) equipped with a 765-250 W/m^2 Xenon lamp (61-24 W/m^2 from 300 nm to 400 nm, $1.4 \cdot 10^{20}$ - $5.5 \cdot 10^{19}$ photons/$m^2 \cdot s$) and a cooler to keep the temperature at 35°C. The UV irradiation, in the range of 300-400 nm, has been monitored by using a portable radiometer (Solar Light CO PMA 2100) fixed on the shaker inside the lamp influence zone, like shown in figure 30.

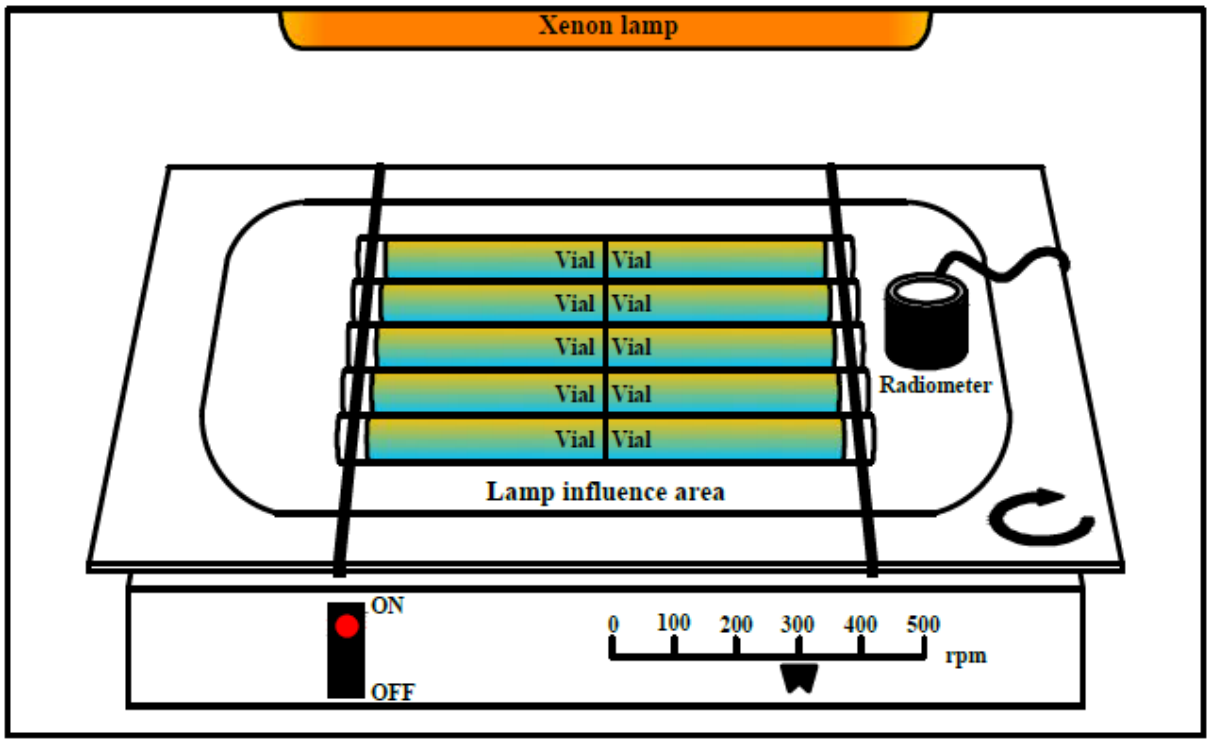

Fig. 30 System used for the experiments performed in the Suntest XLS+ photoreactor.

In this case, a volume of 700 ml of reacting solution has been prepared in a one liter flask and, after 30 minutes of stripping with nitrogen, has been rapidly poured in ten cylindrical glass vials, each of which has a capacity of 42 ml and a diameter of 25 mm. The vials have been rapidly closed with a screw cap, to prevent the entry of oxygen, and have been simultaneously exposed to the lamp radiation and agitated by a shaker like shown in figure 30. The temperature has been set to 35 °C. Each vial represented a sample to remove from the solar box at different reaction times. Once collected, all the samples have been rapidly filtered and analyzed.

3.1.2 Pilot-plant experiments

To clarify the effect of the solar radiation on the studied system, from May to July 2012, some experiments have been carried out in a solar pilot-plant, elsewhere described in its geometrical and functional characteristics[66], installed in the Plataforma Solar de Almería (37° latitude N, Spain).

In particular, the employed solar pilot-plant consisted of twelve Compound Parabolic Collectors (CPC) mounted on a static platform tilted at the same angle as the local latitude facing south. The total solution volume was 39 L, where only 22 L are exposed to solar radiation. The rest was distributed between the recirculation tank (9 L) and the hydraulic connections (8 L). The recirculation tank of the adopted CPC has been modified, as reported in figure 3L, in order to ensure the absence of oxygen, essential for performing the proposed process. For this purpose, the solutions, containing the catalysts and the substrate, have been preventively purged with nitrogen gaseous stream through two porous ceramic spargers, by closing the valve V_n, in order to remove the dissolved oxygen. During the experimental runs, a continuous nitrogen flow has been guaranteed to the reactor to prevent the entry of air in the reactor. However, it has been switched in the freeboard of the recirculation tank, by opening the valve V_n, to inhibit the stripping of organic substances from the solution. In latter, the bubbling of nitrogen has been strongly limited by the pressure drop due to the spargers.

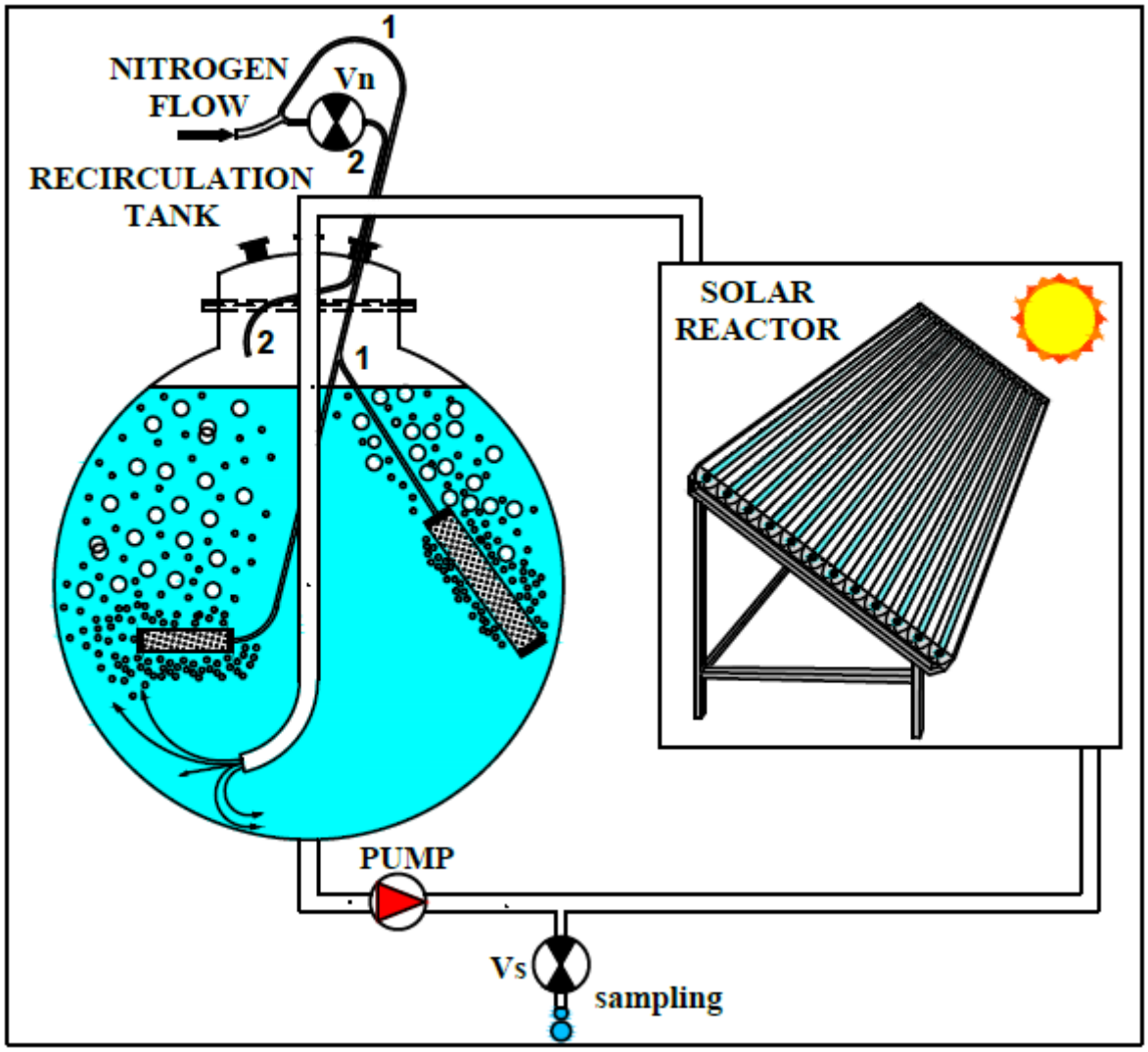

Fig. 31 Solar pilot-plant with a zoom on the recirculation tank.

To better follow up the concentration profiles of the compounds involved in the process, some experimental runs have been carried out for two days. In these cases, the irradiated part of the reactor has been covered and the recycling tank has been capped to respectively stop the photochemical reactions and to prevent the entry of oxygen.

Samples have been collected in a glass bottle at different reaction times, by opening the valve V_s, rapidly filtered to prevent the reoxidation of precipitate copper, and finally analyzed.

All the experimental data of these runs are reported in function of the accumulated energy per unit of volume (kJ/L), incident on the reactor at the corresponding time of the withdrawn sample (Q_n)[67]:

$$Q_n = Q_{n-1} + \Delta t_n \cdot \overline{UV_n} \cdot \frac{A_r}{V_t} \; ; \qquad \Delta t_n = t_n - t_{n-1}$$

$$Q_0 = 0 \quad \text{for} \quad t_0 = 0$$

where Q_{n-1} represent the accumulated energy (per unit of volume, kJ/L) taken during the experiment relative to the previous sampling; Δt_n, UV_n and V_t are, respectively, the elapsed time, the average UV-irradiance (measured by a global UV radiometer KIPP&ZONEN, model CUV 3 mounted on a platform tilted the same angle as the CPCs) which reaches the collector surface (A_r) between the two samplings and the total solution volume.

In particular, the UV radiation (300-400 nm), required for the performance of the process TiO_2/Cu(II)/hv, is only a small fraction of solar radiation that reaches the Earth's surface, as shown in figure 32 (green and blue lines), where is reported the solar spectra, obtained from "*American Society for Testing and Materials (ASTM)*".

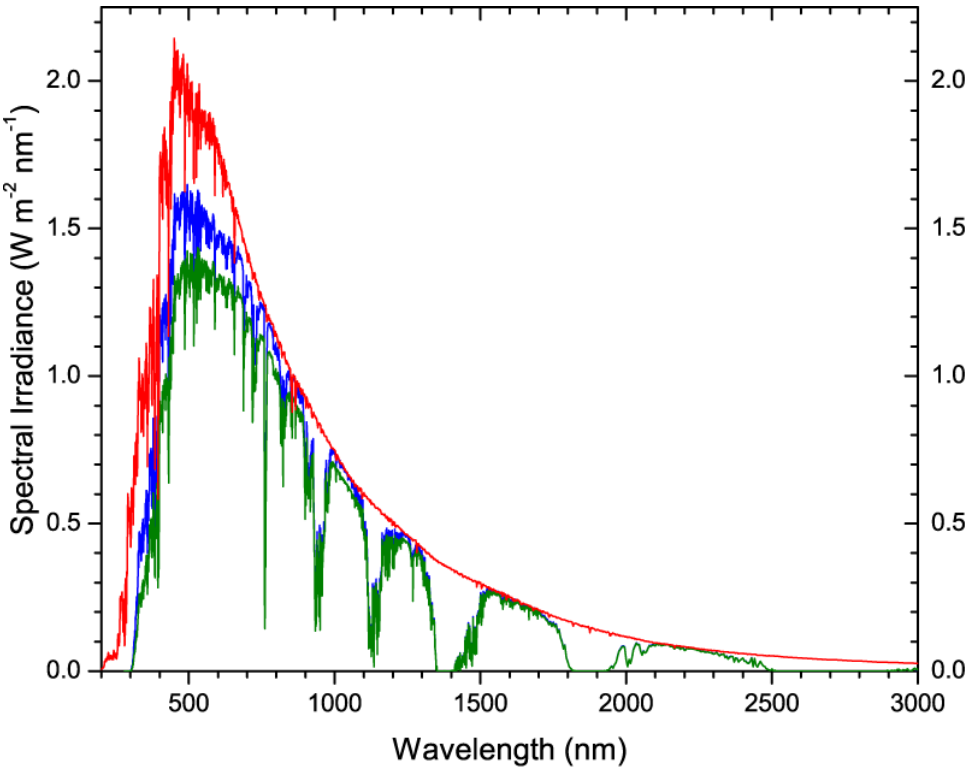

Fig. 32 Standard solar spectra for space and terrestrial use.

— Extraterrestrial spectra;

— Total global (hemispheircal) spectrum;

— Direct normal spectrum;

3.2 Analytical methods

At different reaction times, the concentrations of benzyl alcohol, benzaldehyde, benzoic acid, 2-hydroxy-benzyl alcohol, 3-hydroxy-benzyl alcohol, 4-hydroxy-benzyl alcohol, 2-hydroxy-benzaldehyde, 3-hydroxy-benzaldehyde, 4-hydroxy-benzaldehyde, 2-hydroxy-benzoic acid, 3-hydroxy-benzoic acid, and 4-hydroxy-benzoic acid have been evaluated by HPLC analysis. For this purpose, the HPLC apparatus (Agilent 1100) has been equipped with a diode array UV/Vis detector (λ= 215, 230, 250 nm) and Phenomenex (Gemini 5u or sinergy 4μ Hydro-RP 80A C18 150x3 mm) columns, using a mobile phase flowing at 0.7 mL min^{-1}. The mobile phase has been prepared by a buffer solution (A), H_2O (B) and CH_3CN (C). A linear gradient progressed from 15% C to 28% C and from 45% B to 32% B in 10 minutes with a subsequent re-equilibrium time of 3 minutes. One liter of buffer has been made by 10 mL of phosphoric acid solution (5.05 M), 50 mL of methyl alcohol and water for HPLC.

For the analysis of 4-nitro-benzyl alcohol, 4-nitro-benzaldehyde, 4-nitro-benzoic acid, 2-methoxy-benzyl alcohol, 2-methoxy-benzaldehyde, 2-methoxy-benzoic acid, 4-methoxy-benzyl alcohol, 4-methoxy-benzaldehyde, and 4-methoxy-benzoic acid, the columns of HPLC apparatus (Agilent 1100) have been changed as well as the mobile phase characteristics. In particular, sinergy 4μ Hydro-RP 80A or sinergy 4μ Polar-RP 80A (Phenomenex) columns have been used with a mobile phase of 50% buffer, 30% H_2O and 20% CH_3CN, flowing at 1.0 mL min^{-1}.

The concentration of dissolved copper ions has been measured by means of a colorimetric method using an analytical kit (based on oxalic acid bis-cyclohexylidene hydrazide, cuprizone®) purchased from Macherey-Nagel. An UV/Vis spectrometer (UNICAM-II spectrophotometer) has been used for the measurements at a wavelength of 585 nm.

Total organic carbon (TOC) has been monitored by Shimadzu Total Organic Carbon analyser model TOC-5050A, equipped with an auto sampler ASI 5000A.

The pH has been regulated with phosphoric or perchloric acid and monitored by means of an Orion 420A+ pH-meter (Thermo), for the laboratory scale experiments, and by a portable pH meter (Crison pH 25), for the pilot-plant experiments.

BET specific surface areas of the different catalysts have been measured by the singlepoint BET method using a Micrometrics Flow Sorb 2020 apparatus.

The Cu/Ti ratio for unknown solids, withdrawn at the end of some photocatalytic runs, has been estimated by an Energy Dispersive X-ray spectrometer system (SwiftED, Oxford Instruments) attached to a Scanning Electron Microscope (TM-1000, Hitachi).

Powder X-ray diffraction (XRD) patterns have been estimated using a X´PertPRO (PANalytical) diffractometer with nickel-filtered Cu Kα radiation. The X-ray generator has been operated at 45 kV and 40 mA. The powders have been scanned from $2\theta = 4^{o}$ to 90^{o} with a 0.02 step size and accumulating a total of 5 s per point.

X-ray photoelectron spectroscopy (XPS) analysis has been carried out under high vacuum chamber with a base pressure below $9x10^{-7}$ Pa at room temperature. Photoemission spectra have been recorded using a SPECS Gmbh system equipped with an UHV PHOIBOS 150 analyser with Al monochromatic anode operating at 12 kV and 200 W with a photon energy of $h\nu = 1486.74$ eV. A pass energy of 25 eV has been used for high-resolution scans. Binding energies (BE) have been referenced to C1s peak (284.6 eV) to take into account charging effects.

The XPS spectra have been then fitted using the XPS PeakFit software. The areas of the peaks have been computed by fitting the experimental spectra to Gaussian/Lorentzian curves after subtracting the background (Shirley function).

3.3 Materials

Four commercial microcrystalline TiO_2 powders have been used for the study of the effect of TiO_2 typology on the adopted system:

1. TiO_2 Degussa P25 (80% anatase, 20% rutile, BET specific surface area 50 $m^2\ g^{-1}$);
2. TiO_2 Aldrich (pure anatase phase, BET specific surface area 9.5 $m^2\ g^{-1}$, adsorption average pore width 88.5 Å);
3. TiO_2 Aldrich (pure rutile phase, BET specific surface area 2.5 $m^2\ g^{-1}$, adsorption average pore width 59.8 Å);
4. TiO_2 Aldrich (rutile phase with small amount of anatase, BET specific surface area 2.7 $m^2\ g^{-1}$, adsorption average pore width 63.6 Å).

The pH has been regulated with H_3PO_4 or $HClO_4$. Cu(II) ions have been introduced in the reactive solution as cupric sulfate pentahydrate ($CuSO_4$ x $5H_2O$) or cupric perchlorate hexahydrate ($Cu(ClO_4)_2$ x $6H_2O$). The cupric salts have been purchased from Sigma Aldrich with a purity ≥98.0% (w/w).

The provenience, the purity, and some characteristics of the organic reagents used in this work are listed in Appendix 1.

All the reagent have been used as received from the provider without any modifications.

4 PRELIMINARY LABORATORY EXPERIMENTS

Benzyl alcohol has been selected as substrate, copper sulphate as source of Cu(II) ions and H_3PO_4 as pH regulator, with the aim of studying, by using the batch annular reactor described in third chapter (figure 29), the possibility to carry out a selective oxidation process through the system TiO_2/Cu(II)/hv at different experimental conditions:

- type of TiO_2;
- TiO_2 load;
- Cu(II) concentration;
- pH;
- effect of concentration of anion.

Preliminary photodegradation runs (data not shown) in presence of benzyl alcohol and $CuSO_4$, without TiO_2 or the substrate and TiO_2 (pure anatase) without Cu(II) ions addition to the solution under nitrogen gaseous steam, and at pH=2.0, did not result into any consumption of benzyl alcohol even for long reaction times (more than 12 hours).

4.1 Effect of TiO_2 type

The results obtained during some runs of photoxidation of benzyl alcohol at pH = 2.0, with different TiO_2 commercial samples, at a load equal to 200 mg/L, are shown in figure 33. The diagrams show that the reactivity of benzyl alcohol is strongly influenced by the type of TiO_2 used in the experiment, whereas the specific surface area could not be taken as a predictor of the sample reactivity. In particular, the best results in terms of conversion, at a fixed reacting time, were observed when Aldrich TiO_2 (pure anatase) has been used in the run. In this case, after 120 min of reaction, the concentration of Cu(II) approaches to zero with a 75% conversion of the alcohol, despite of an initial ratio [benzyl alcohol/Cu(II)] = 1.

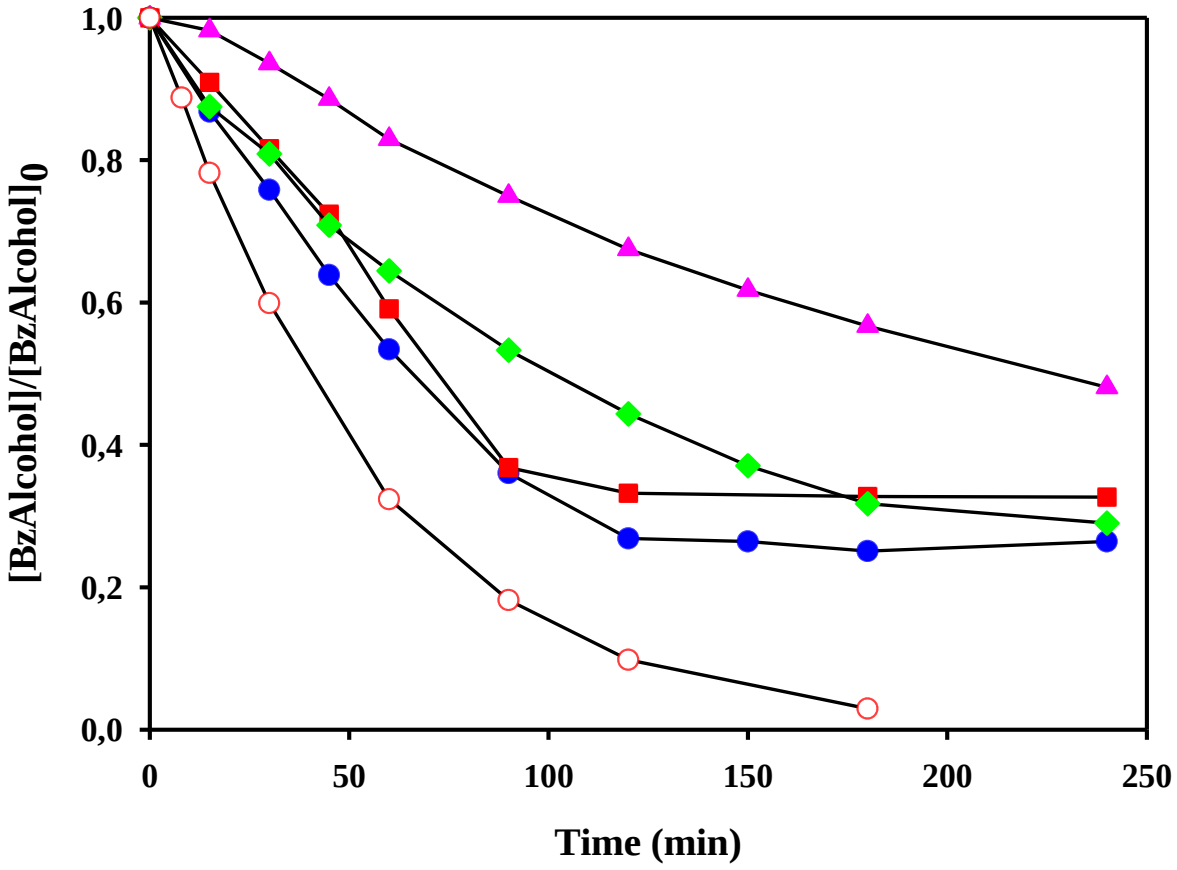

Fig. 33 Effect of TiO_2 type: Benzil alcohol oxidation.

$[Cu(II)]_0$ = 1,5mM. $[Benzyl\ Alcohol]_0$ = 1.5mM. pH = 2.0. T = 25 °C. $[TiO_2]_0$ = 200 mg/L.

Runs without oxygen: ● Aldrich (pure anatase, SA = 9.5 $m^2\ g^{-1}$),

■ P25 Degussa (80% anatase, SA = 50 $m^2\ g^{-1}$),

♦ Aldrich (pure rutile, SA = 2.5 $m^2\ g^{-1}$),

▲ Aldrich (prevalently rutile, SA = 2.7 $m^2\ g^{-1}$).

Run with oxygen without Cu(II): ○ Aldrich (pure anatase).

A similar reactivity, but with a lower conversion of benzyl alcohol (65%), is shown by a P25 Degussa sample in which anatase form is present at 80% with a specific surface area (50 m^2 g^{-1}) higher than the Aldrich sample (pure anatase, 9.5 m^2 g^{-1}). The catalysts, in which TiO_2 is present as rutile form, either prevalently or totally, show lower activities than the samples containing prevalently anatase.

The observed results can be explained through the fact that, for both crystallographic forms of TiO_2 (anatase and rutile), the valence band (VB) redox potentials are more positive (2.96 and 2.85 V vs NHE respectively)[68] than the $^{\bullet}OH/-OH$ and $^{\bullet}OH/H_2O$ redox couples (1.89 and 2.72 V vs NHE respectively)[69]. Consequently, both adsorbed water and hydroxyl groups can be oxidized to reactive hydroxyl radicals on both irradiated TiO_2 types surfaces[29]:

1) $Ti^{IV} - OH^- + h^+ \xrightarrow{hv} Ti^{IV} - OH^{\bullet}$

2) $Ti^{IV} - H_2O + h^+ \xrightarrow{hv} Ti^{IV} - OH^{\bullet} + H^+$

Nevertheless, the more negative redox potential (-0.27 V vs NHE) of the anatase conduction band (CB), makes it more competitive than the rutile one (-0.15 V vs NHE) for reduction reactions[68]. In this way, taking into account that the standard redox potential of $Cu^{2+}/Cu(0)$ couple is 0.337 V[70], cupric ions can be reduced to metal copper by anatase CB electrons more easily than by rutile CB electrons.

Another phenomenon to take into account to explain these results is the ability of different TiO_2 types to absorb the UV radiation emitted by the lamp. In this regard, four tests were performed to measure the adsorbance at 366 nm of the H_2O-TiO_2 mixture, by using a HD 9021 Delta Ohm radiometer, at varying loads of different TiO_2 samples. As shown in figure 34, pure anatase and P25 have the same behaviour and, at a load of 200 mg/L, adsorb more than 95% of UV radiation emitted by the lamp. Contemporary, also the other two TiO_2 samples (pure rutile and prevalently rutile) have a similar behaviour but, at a load of 200 mg/l, adsorb less than 50% of UV radiation.

In any case, as reported by others[71-72], several other properties of the tested photocatalysts such as particle geometry, crystallinity, density of surface functional groups, and defects should be considered to foresee the behaviour of the adopted TiO_2.

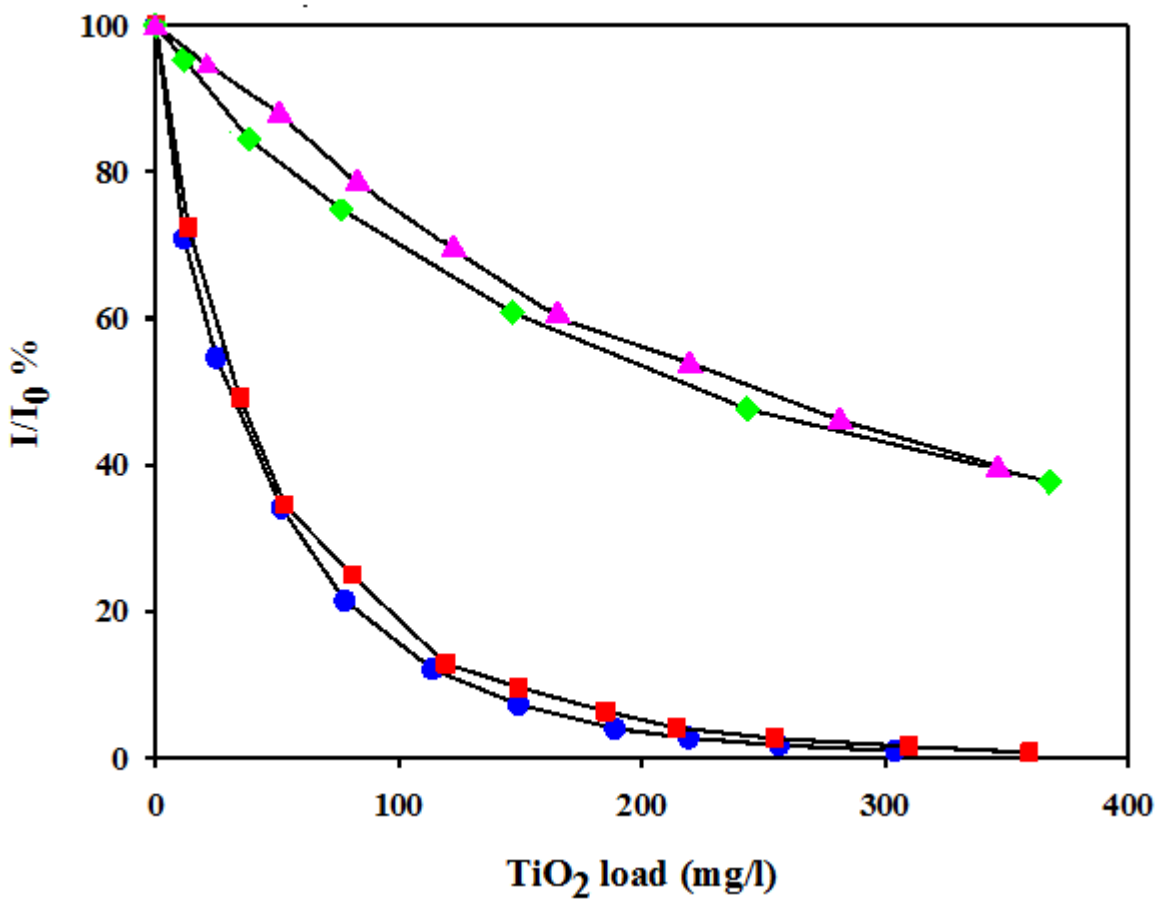

Fig. 34 Adsorbances of different TiO_2 types.

pH = 2.0. T = 25 °C.

Runs in presence of atmospheric oxygen: ● Aldrich (pure anatase, SA = 9.5 $m^2 g^{-1}$),

■ P25 Degussa (80% anatase, SA = 50 $m^2 g^{-1}$),

♦ Aldrich (pure rutile, SA = 2.5 $m^2 g^{-1}$),

▲ Aldrich (prevalently rutile, SA = 27 $m^2 g^{-1}$).

Moreover, since for each Cu(II) ion reduced to Cu(0), two photogenerated electrons are consumed and two positive holes have to be saturated, the experimental data invariably indicate the existence of secondary reactions in which other species, in competition with benzyl alcohol molecules, consume the positive holes thus reducing the consumption ratio [benzyl alcohol]/[Cu(II)], to a value lower than 1,0.

As it can be inferred from figure 35a, during the process, the substrate is mainly converted into benzaldehyde that partially undergoes to a further oxidation to benzoic acid (figure 35b). When the highest conversion of the substrate is achieved (72%), 35% of initial benzyl alcohol resulted to be converted into benzaldehyde and only 8% into benzoic acid for pure anatase TiO_2.

In order to better understand the importance of replacing oxygen with Cu(II) ions, the data related to a run in which the alcohol is in contact with oxygen, without any addition of Cu(II), in the presence of Aldrich TiO_2 (pure anatase) sample are presented in figures 33 and 35a (empty red circles). Although the system results to be capable of promptly converting benzyl alcohol (figure 33), the yield in benzaldehyde is very low (figure 35a). Similar results have been also obtained with different TiO_2 samples (data not shown).

The slight decrease of the concentration profiles of benzaldehyde for reaction times higher than 90 min (figure 35a: full red squares, full blue circles), when Cu(II) is totally converted to Cu(0), could be ascribed to its loss from the solution due to a stripping effect of the inlet nitrogen gaseous stream bubbling. An example of the importance of this effect is given in the same figure (figure 35a: empty blue squares) reporting the results collected by bubbling a nitrogen gas stream in a solution initially containing only benzaldehyde (in darkness and in absence of TiO_2 and Cu(II) ions).

During the runs, small amounts of undesired by-products, such as 2-hydroxy-benzyl-alcohol, 4-hydroxy-benzyl-alcohol, 2-hydroxy-benzaldehyde and 4-hydroxy-benzaldehyde, have been detected in the reacting solutions, as a result of hydroxyl radicals ($HO^{\bullet}$) attack to benzyl alcohol and benzaldehyde molecules. In fact, despite the elimination of oxygen from the system inhibited $HO^{\bullet}$ formation from H_2O_2 photolysis, the production of hydroxyl radicals through the adsorbed water and/or hydroxyl groups with positive holes (reactions 1 and 2) cannot be ruled out.

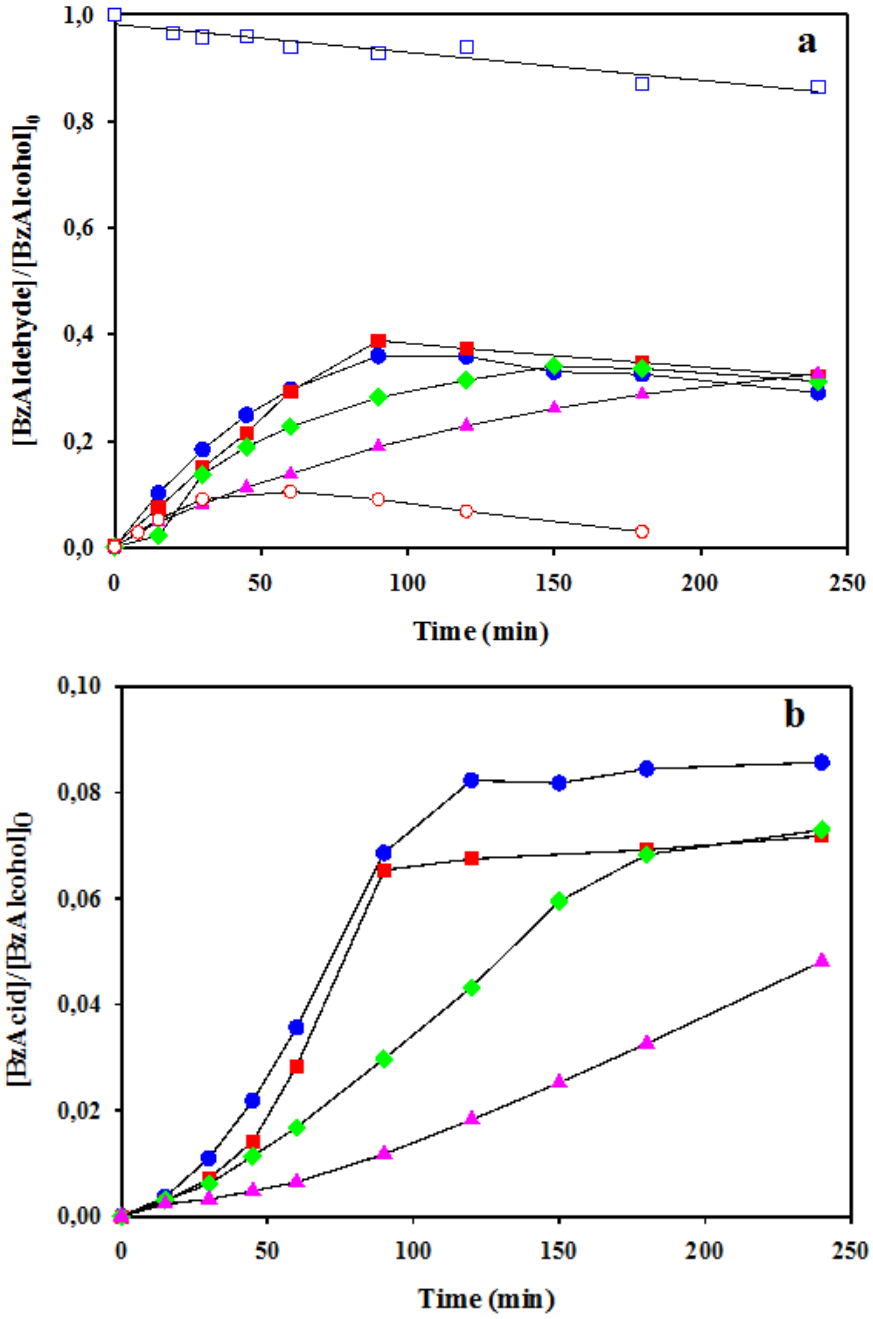

Fig. 35 Effect of TiO_2 type: Benzaldehyde (a) and Benzoic acid (b) production.

$[Cu(II)]_0$ = 1.5mM. [Benzyl Alcohol]$_0$ = 1.5mM. pH = 2.0. T = 25 °C. $[TiO_2]_0$ = 200 mg/L.

Only stripping with nitrogen at dark (□).

Runs without oxygen: ● Aldrich (pure anatase, SA = 9.5 m^2 g^{-1}),

■ P25 Degussa (80% anatase, SA = 50 m^2 g^{-1}),

♦ Aldrich (pure rutile, SA = 2.5 m^2 g^{-1}),

▲ Aldrich (prevalently rutile, SA = 2.7 m^2 g^{-1}).

Run with oxygen without Cu(II): ○ Aldrich (pure anatase).

During each run, the decrease of the concentration of cupric ions (figure 36) has been accompanied by the precipitation of a purple solid mixed with TiO_2 particles. According to what reported by some of the Authors in a previous paper[55], this solid could be Cu(0). When Cu(II) has been totally converted to Cu(0), i.e. at 120 min for P25 Degussa sample and TiO_2 Aldrich pure anatase (figure 36, full blue circles and red squares), no further consumption of benzyl alcohol (figure 33, full blue circles and red squares) neither production of both benzaldehyde and benzoic acid has been observed (figure 35a and b, full blue circles and red squares).

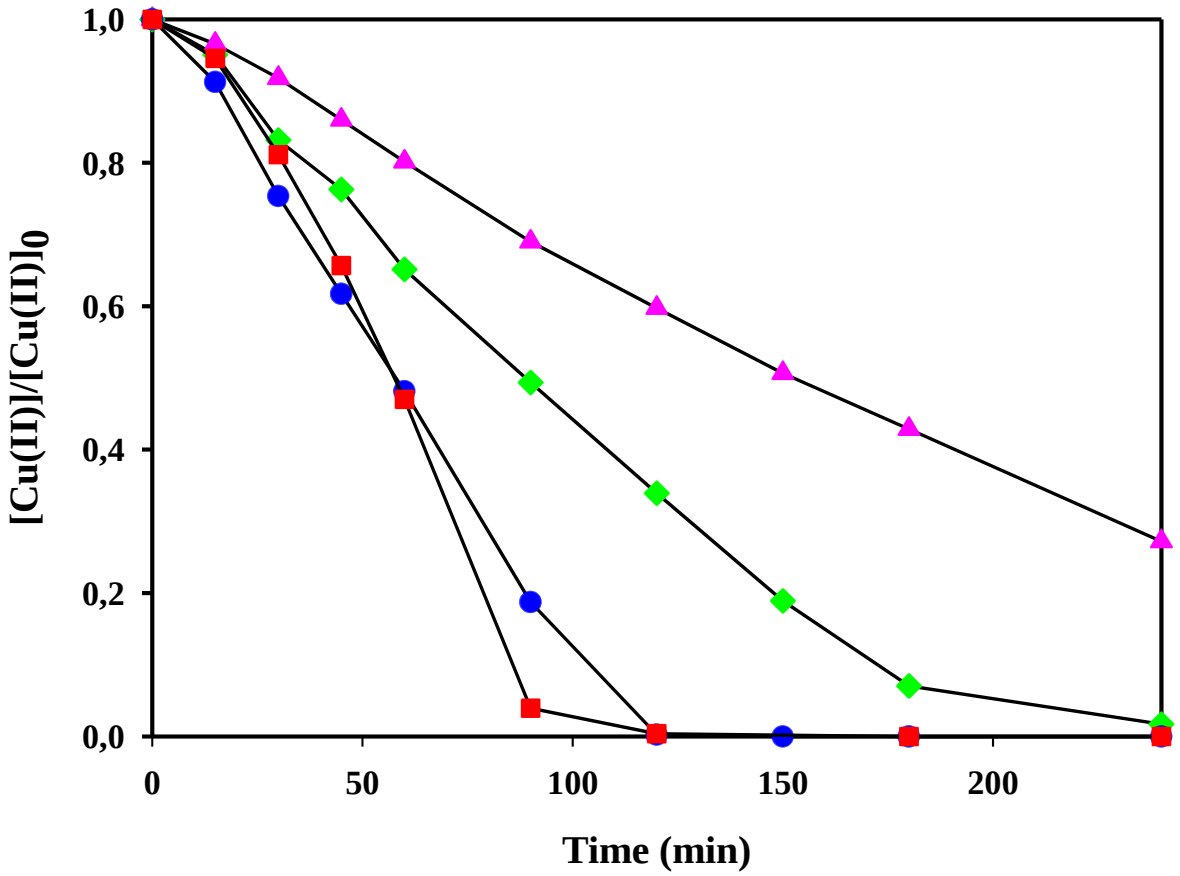

Fig. 36 Effect of TiO_2 type: Copper reduction.

$[Cu(II)]_0$ = 1.5mM. $[Benzyl\ Alcohol]_0$ = 1.5mM. pH = 2.0. T = 25 °C. $[TiO_2]_0$ = 200 mg/l.

Runs without oxygen: ● Aldrich (pure anatase, SA = 9.5 $m^2\ g^{-1}$),

■ P25 Degussa (80% anatase, SA = 50 $m^2\ g^{-1}$),

♦ Aldrich (pure rutile, SA = 2.5 $m^2\ g^{-1}$),

▲ Aldrich (prevalently rutile, SA = 2.7 $m^2\ g^{-1}$).

4.2 Effect of TiO_2 load

The effect of initial TiO_2 load has been successively investigated by carrying out some oxidation experiments in which different amounts of the photocatalyst (Aldrich pure anatase) per unit volume were added to the reacting solutions (figure 37 a and b).

As expected, an increase of the catalyst load from 50 mg/L to 200 mg/L results into a marked increase of the system. To better understand the effect of TiO_2 load, in figure 38 the benzyl alcohol oxidation rates have been reported, in correspondence with an alcohol consumption of 20% (blue columns) and 50% (cyan columns), for each experimental run reported in figure 37 a. As shown in the diagram, in both cases, there is almost linearity between the benzyl alcohol oxidation rate and TiO_2 load, for values in the range of 50-200 mg/L. An increase of TiO_2 load, for values higher than 200 mg/L, does not lead to an increase of system reactivity (data not shown) probably due to scattering and screening of radiation by the excess particles, which mask part of the photosensitive surface[30,73]. Moreover, as reported in figure 34, with load of 200 mg/L of pure anatase it is possible to adsorb 96% of the photon emitted by the lamp per unit of time.

As reported in figure 38, by increasing the conversion of benzyl alcohol decrease its oxidation rate. This phenomenon is due to the increasing of concentration of benzaldehyde which competes with benzyl alcohol in the adsorption on TiO_2 activated sites and in the reaction with the positives holes.

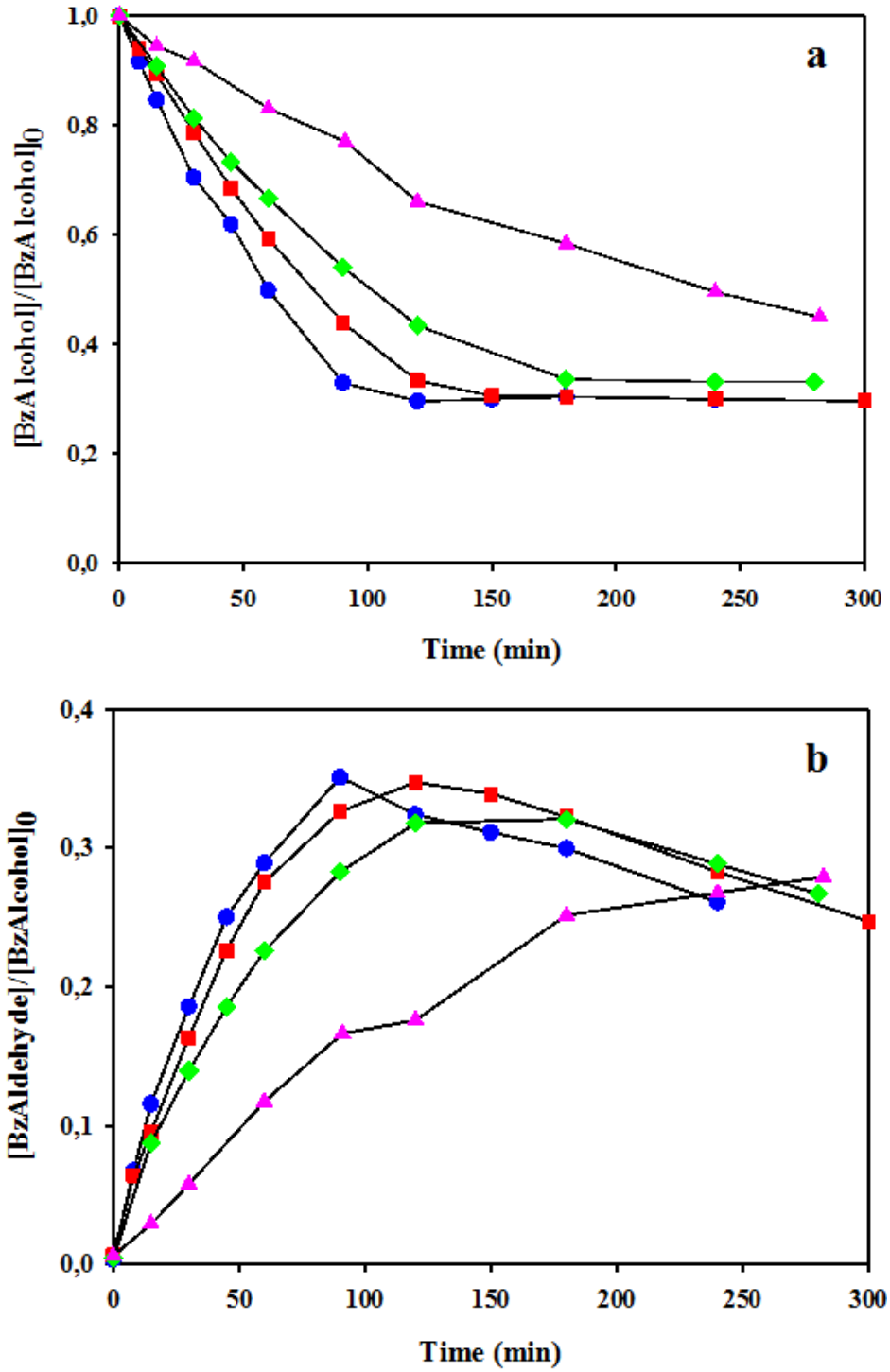

Fig. 37 Effect of initial TiO_2 load: Benzyl alcohol consumption (a) and benzaldehyde production (b).

$[Cu(II)]_0$ = 1.5mM. $[Benzyl\ Alcohol]_0$ = 1.5mM. pH = 2.0. T = 25 °C.

TiO_2 (Aldrich pure anatase): ● 200 mg/L, ■ 150 mg/L, ♦ 100 mg/L, ▲ 50 mg/L.

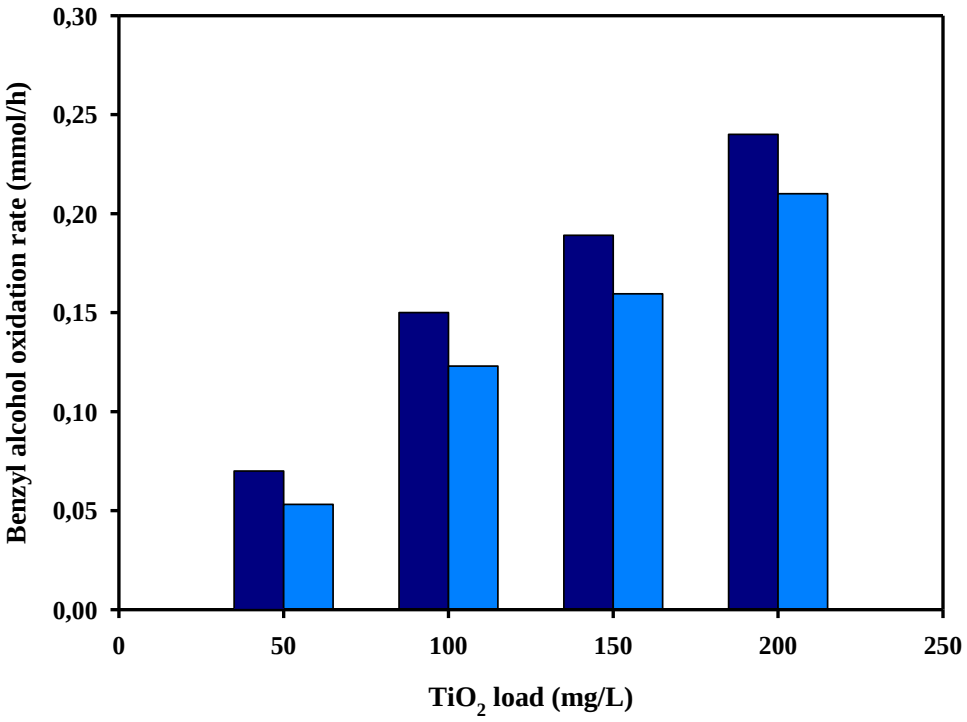

Fig. 38 Effect of initial TiO_2 load: Benzyl alcohol oxidation rate.

$[Cu(II)]_0$ = 1.5mM. $[Benzyl\ Alcohol]_0$ = 1.5mM. pH = 2.0. T = 25 °C.

■ 20% benzyl alcohol conversion;

■ 50% benzyl alcohol conversion.

4.3 Effect of Cu(II) initial concentration

Figures 39a and b show the results obtained in oxidation runs at pH = 2.0 with the same TiO_2 sample (Aldrich, pure anatase, 200 mg/L) but at different initial concentrations of Cu(II), added to the solution as $CuSO_4$.

A higher initial concentration of Cu(II) results into a decrease of the system reactivity as can be easily verified by comparing the half-life time of the substrate which changed from 50 to 90 min for $[Cu(II)]_0$ equal to 1.12 mM and 2.30 mM respectively. Moreover, for both runs, the selectivities to benzaldehyde, evaluated at 15 min (72%) and 90 min (57%), do not change significantly from the values calculated by using the data shown in figures 33 and 35a. A possible explanation for these findings may be a change of the light absorption properties of the reacting solutions, with an increasing inner filter effect at increasing Cu(II) initial concentrations. UV absorption measurements have been thus performed on the reacting solutions in order to evaluate the capability of cupric solutions to absorb the lamp radiation at the adopted wavelengths (305, 313 and 366 nm). However, the values, estimated for the molar extinction coefficients of cupric aquocomplexes at pH = 2,0, allowed ruling out the possibility of existence of any inner filter effect due to these species (data not reported).

The search of an explanation for the observed reduced reactivity of the oxidation of the alcohol at increasing Cu(II) concentrations revealed some difficulties which forced the attention on the fact that for the runs considered a parallel increase of sulphate ions had to be taken into account. That is, since cupric sulphate was used as Cu(II) salt to prepare the solution, it is evident that any increase of Cu(II) resulted into that of sulphates. Therefore, it has been necessary to understand the effect on the system reactivity exerted by these species.

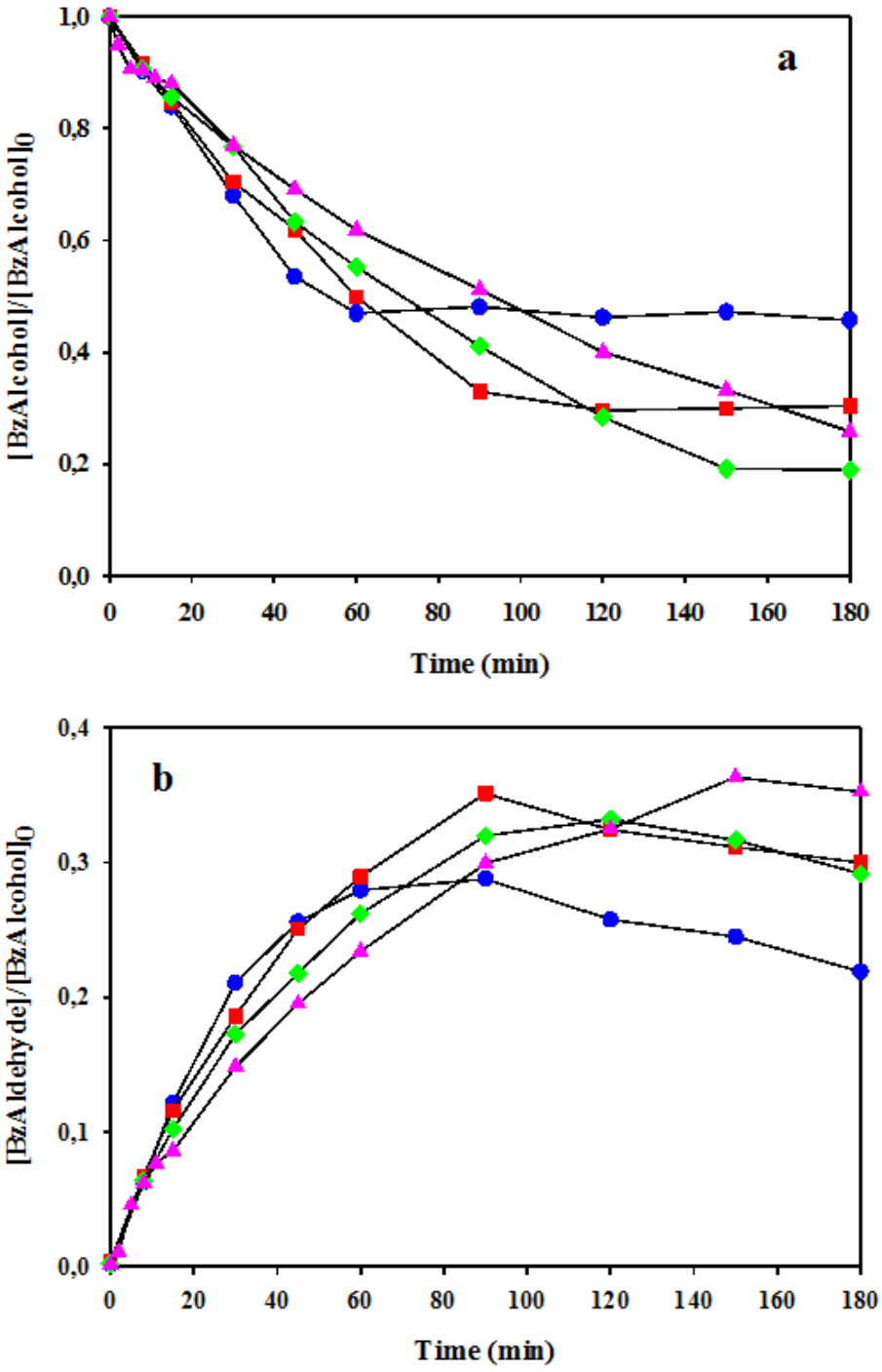

Fig. 39 Effect of initial Cu(II) concentration: Benzyl alcohol consumption (a) and Benzaldehyde production (b).

TiO_2 (Aldrich, pure anatase) = 200 mg/L. pH = 2.0. T = 25 °C. $[Benzyl\ alcohol]_0$ = 1.50 mM. $[Cu(II)]_0$: ● 1.12 mM, ■ 1.42 mM, ♦ 1.84 mM, ▲ 2.30 mM.

4.4 Effect of sulphate initial concentration

Some photocatalytic tests have been thus carried out varying the initial sulphate concentration with different additions of Na_2SO_4 salt (Fig. 40).

The results obtained in these experiments indicate that sulphate ions exert a marked inhibiting effect on the photoactivity of TiO_2, by decreasing the oxidation rate of benzyl alcohol and its conversion when their initial concentration increases (full symbols).

This behaviour can be ascribed, as reported by others[74-76], for the reaction between sulphate species and the positive holes (h^+) with the formation of sulphate ion radicals ($SO_4^{\bullet -}$) on the illuminated titanium dioxide surface:

3) $SO_4^{2-} + h^+ \longrightarrow SO_4^{\bullet -}$

and for a radical scavenging effect of sulphate ions:

4) $SO_4^{2-} + HO^{\bullet} \longrightarrow SO_4^{\bullet -} + HO^-$

$SO_4^{\bullet -}$ species are reported to be less reactive than the hydroxyl radicals towards organic molecules[74].

In any case, as reported by Abdullah and coworkers[77], a catalyst deactivation, by the adsorbed sulphate ions which can block the TiO_2 active sites, cannot be ruled out.

The selectivity to benzaldehyde, which increases at increasing sulphate concentration (empty symbols), confirms the capability of sulphate ions to scavenge very reactive and unselective hydroxyl radicals.

In conclusion, the presence of SO_4^{2-} ions exert a dual function:

- are in competition with benzyl alcohol for the adsorption on TiO_2 surface and for the reaction with the positive holes, decreasing the process reactivity;
- radical scavengers against the $HO^{\bullet}$ radicals, increasing the process selectivity.

Therefore, the results reported in figure 39a and 39b could not be attributed only to the effect of Cu(II) concentration but also to a combination of the latter and the concentration of sulphate ions. In particular, the negative effect of sulphate on the system reactivity prevailed over the effect exerted by Cu(II).

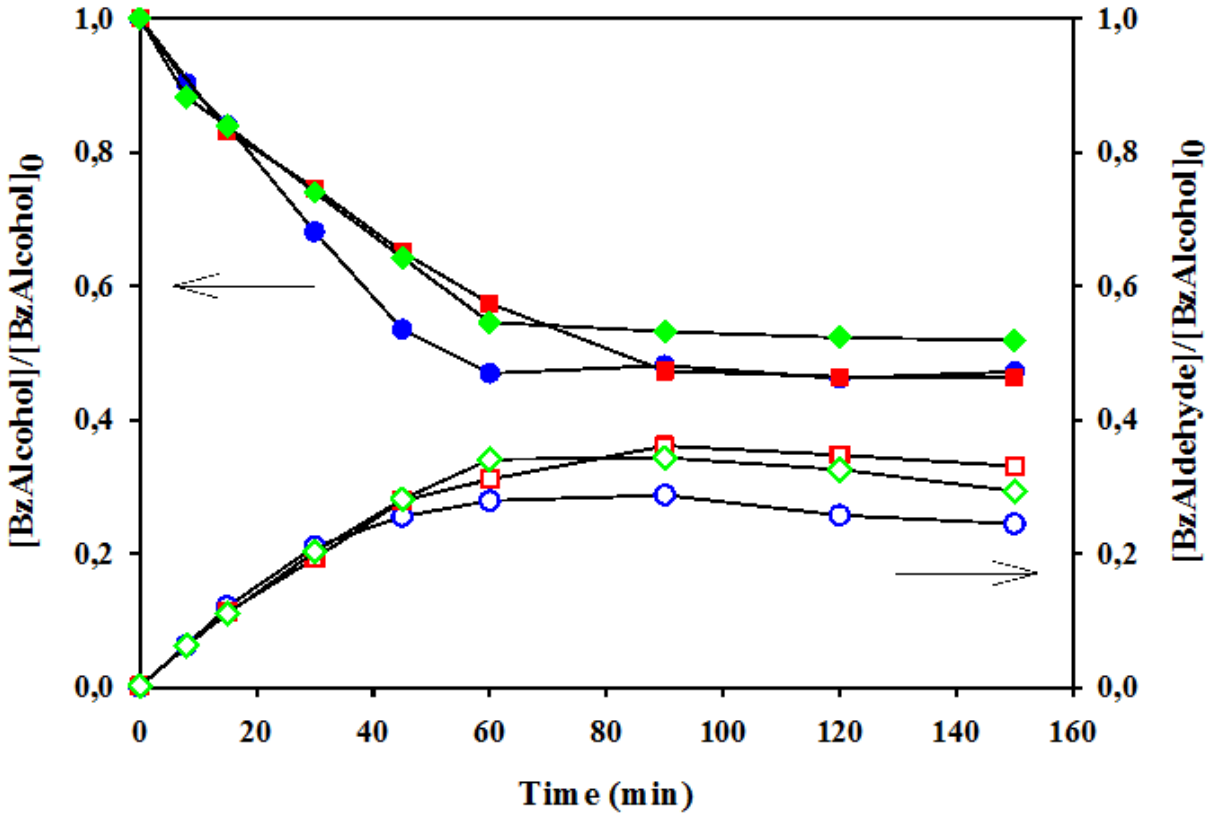

Fig. 40 Effect of initial sulphate concentration.

$[\text{Benzyl alcohol}]_0$ = 1.50 mM. $[\text{Cu(II)}]_0$ = 1.15 mM.

TiO_2 (Aldrich, pure anatase) = 200 mg/L. pH = 2.0. T = 25 °C.

Full symbols: benzyl alcohol consumption, empty symbols: Benzaldehyde production.

$[SO_4^{2-}]$: (●;○) 1.15 mM, (■;□) 1.9 mM, (♦;◊) 2.4 mM.

4.5 Effect of pH

Figures 41a and 41b report the results obtained from varying the pH of the solution, between 2.0 and 4.0.

During the tests, increasing the pH from 2.0 to 4.0, a decrease in thebenzyl alcohol consumption as well as the benzaldehyde formation rates occurred. These results have two main causes. First of all, TiO_2 surface may be characterized by an amphoteric behaviour, that is either positive or negative charge could be present on it as function of pH:

5) $\equiv TiOH_2^+ \rightleftarrows \equiv TiOH + H^+$

6) $\equiv TiOH \rightleftarrows \equiv TiO^- + H^+$

The pH's value at which TiO_2 has a net zero surface charge is defined pH_{zpc}. The surface has a net positive charge for pH < pH_{zpc}, whereas for pH > pH_{zpc}, the surface has a net negative charge.

It could be assumed, according to a pH_{zpc} equal to 4.2 for the adopted TiO_2 Aldrich sample[71], that an increase of the pH from 2.0 to 4.0 reduces the concentration of positive charges on the catalyst surface partially inhibiting the adsorption (and the reactivity) of benzyl alcohol (pKa = 15.2[78]).

On the other hand, since phosphoric acid has been used to adjust the pH of the reacting solutions, in the pH range 2.0–4.0, the prevalent species present is $H_2PO_4^-$. The capability of $H_2PO_4^-$ ion to react with the positive holes formed on the catalyst after radiation is well known[72]:

7) $H_2PO_4^- + h^+ \longrightarrow H_2PO_4^{\bullet}$

It is clear that for any increase of pH resulting into a higher concentration of this ion, a marked inhibition of the direct oxidation of the substrate could be expected.

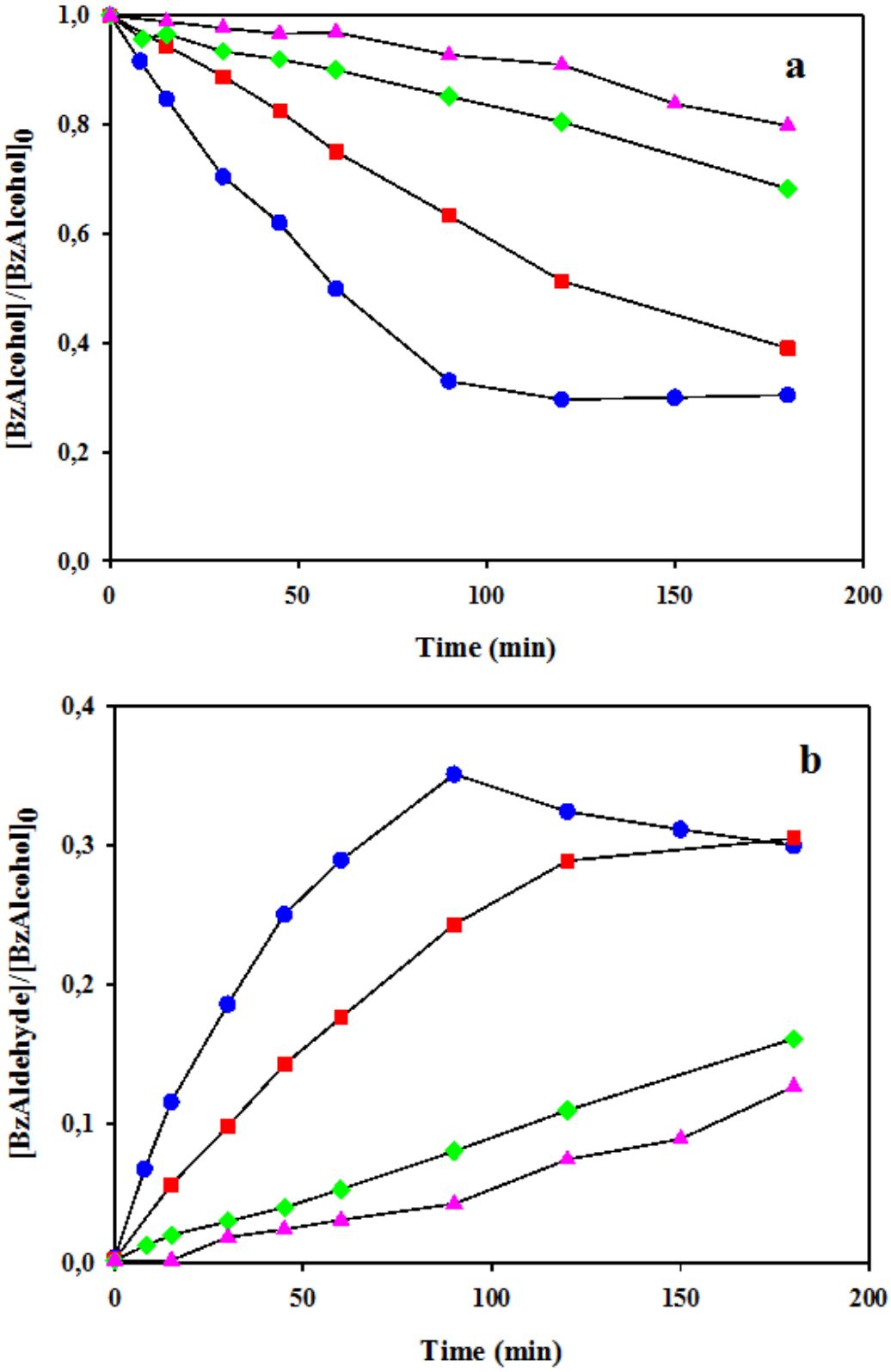

Fig. 41 Effect of pH: benzyl alcohol consumption (a) and benzaldehyde production (b). [Benzyl alcohol]$_0$ = 1.50 mM. [Cu(II)]$_0$ = 1.50 mM. TiO_2 (Aldrich, pure anatase) = 200 mg/L. ● pH = 2.0; ■ pH = 2.5; ♦ pH = 3.0; ▲ pH = 4.0.

In order to confirm these hypothesis, some further photo-oxidation tests have been performed, with and without an addition of NaH_2PO_4 (2.44 mM) salt in benzyl alcohol solutions (1.60 mM), at pH = 2.0 (regulated with H_3PO_4), in the presence of TiO_2 (200 mg/L, Aldrich, pure anatase), and with an initial Cu(II) concentration equal to 1,15 mM (data not shown). After 120 min of reaction, when Cu(II) has been completely reduced to Cu(0), benzyl alcohol total conversions of 55.0% (without NaH_2PO_4) and 45.8% (with NaH_2PO_4) have been achieved respectively. Moreover, the percentage of the substrate converted into benzaldehyde has been 25.7% (without NaH_2PO_4) and 32.7% (with NaH_2PO_4), thus indicating a capability of dihydrogen phosphate ions to behave as a radical scavenging towards hydroxyl radicals[72]:

8) $H_2PO_4^- + HO^\bullet \longrightarrow H_2PO_4^\bullet - HO^-$

4.6 Summary

Starting from previously discussed data, collected at different experimental conditions, the simplified pictorial scheme of the mechanism for the selective photooxidation of benzyl alcohol to benzaldehyde and benzoic acid by TiO_2 photocatalysis could be depicted (figure 42).

The irradiation of the photocatalytic surface leads to the formation of positive holes (h^+) in the valence band (VB) and electrons (e^-) in the conduction band (CB). First of all, the positive holes react with benzyl alcohol (substrate) and benzaldehyde (intermediate) to produce benzaldehyde and benzoic acid respectively. Surface hydroxyl radicals are also formed by the reaction of water molecules with the holes. Hydroxyl radicals attack both benzyl alcohol and benzaldehyde to form undesired by-products (2- and 4-hydroxy-benzyl alcohols, 2- and 4-hydroxy benzaldehyde). Finally, the holes can be trapped by sulphate and dihydrogenphosphate ions to generate less reactive $SO_4^\bullet$ and $H_2PO_4^\bullet$ species. The electrons in the conduction band react with Cu(II) ions which are reduced to Cu(I) and Cu(0).

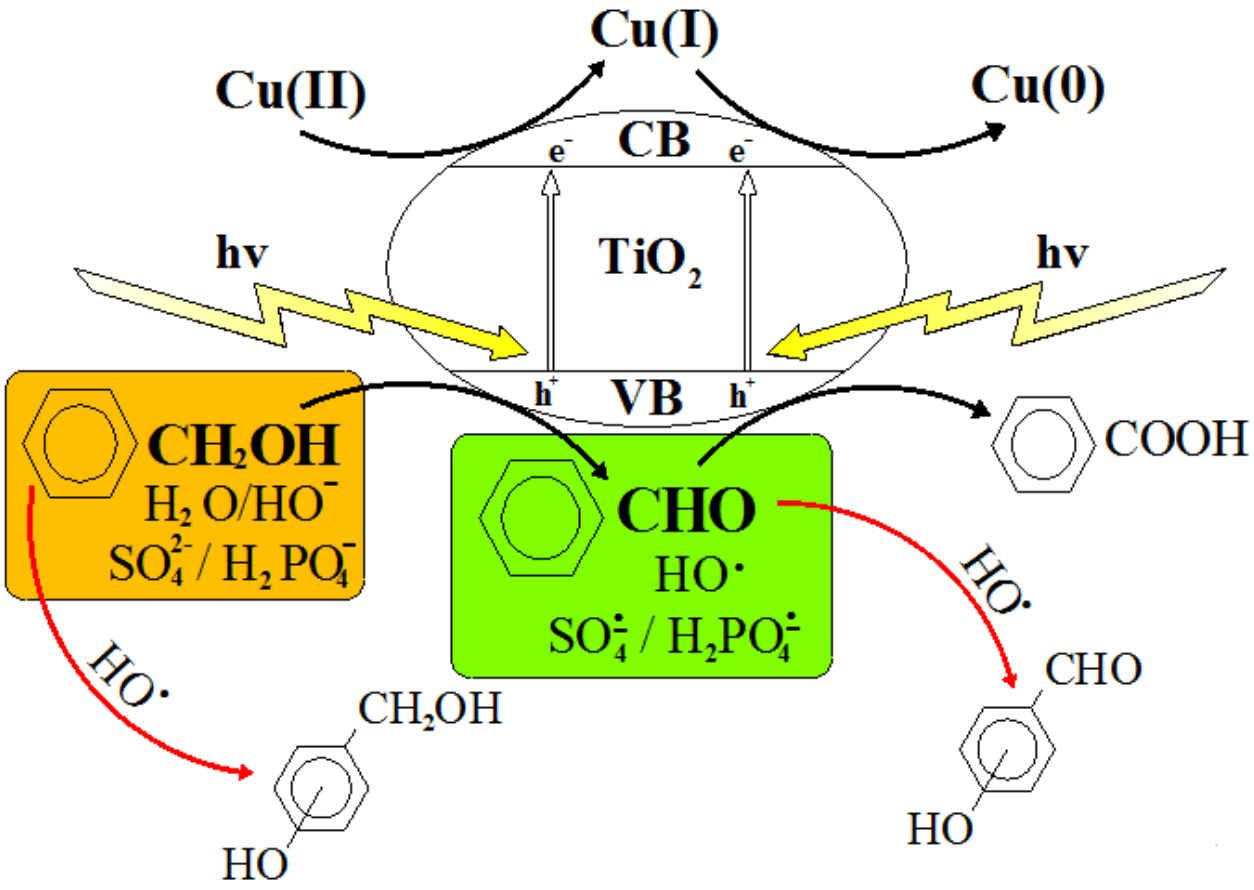

Fig. 42 Mechanism of selective oxidation of Benzyl alcohol by TiO_2/Cu(II)/UV.

5 MODELING OF TiO_2/Cu(II)/hv SYSTEM FOR THE BENZYL ALCOHOL SELECTIVE OXIDATION

On the basis of the previous results, a new kinetic model has been developed to describe the TiO_2/Cu(II)/hv process for the selective oxidation of benzyl alcohol in benzaldehyde. No examples have been found in the literature about the modeling of a similar process. Therefore, to account for and to validate main involved reactions described in the previous chapter, the process has been studied through a quantitative description of the oxidation process of benzyl alcohol (BA) to benzaldehyde (BHA) and benzaldehyde to benzoic acid (BAC) in aqueous media.

During all the experimental runs reported in this chapter, after the lamp has been turned on, the nitrogen flow has been sent in the freeboard of the glass reactor (figure 29). In this way, the absence of oxygen during the experimental runs has been guaranteed. Contemporary, the kinetic model has been simplified by removing the contribution of the disappearance of organic compounds, such as benzaldehyde, through stripping.

5.1 Kinetic scheme

The kinetic scheme related to the selective oxidation of BA and BHA has been built by considering the following reaction steps.

TiO_2 irradiation generates the photoelectrons and positive holes which are responsible for the system reactivity:

$r_1)\ TiO_2 + hv \xrightarrow{\Phi_{TiO_2}} h^+_{VB} + e^-_{CB}$ $\qquad \Phi_{TiO_2} = 6.0 \cdot 10^{-2}\ \text{mol E}^{-1}$ [58]

A very fast recombination (r2) competes with the reactions in which photoelectrons and positive holes are involved (r3-4, r8-9,r20-r22, r25-r26):

$r_2)\ h^+_{VB} + e^-_{CB} \xrightarrow{k_{rec}} heat$ $\qquad k_{rec} = 3.0 \cdot 10^{10}\ M^{-1}\ \text{s}^{-1}$ [79]

OH radicals are generated by the interaction between positive holes and either H_2O adsorbed molecules or HO^- groups present on TiO_2 surface:

$r_3)\ (H_2O)_{ads} + h^+_{VB} \xrightarrow{k_{H_2O/h}} HO^\bullet + H^+$ $\qquad k_{H_2O/h}$ (unknown parameter)

$r_4)\ (HO^-)_{ads} + h^+_{VB} \xrightarrow{k_{HO/h}} HO^\bullet$ $\qquad k_{HO/h}$ (unknown parameter)

BA, BHA, and BAC adsorb on the same type catalyst active site, defined by s*. For the equilibrium adsorption constants of the BA (K_{ads}), BHA (K'_{ads}), and BAC (K''_{ads}) species on TiO_2 catalysts the following values are reported as $3.22\cdot10^2$ M^{-1}[80], $4.67\cdot10^3$ M^{-1}[33] and $1.0\cdot10^3$ M^{-1}[81] respectively.

However, several reports appeared in the literature showing that the value of the equilibrium adsorption constants determined in TiO_2 photo-assisted systems are generally larger than those measured separately under dark conditions[82-84]. In particular, for BA and similar molecules, the values measured under irradiation are about 12 times larger than those found in the dark[80,85]. Therefore, in the present work the following values have been taken into consideration:

$r_5)\ BA + s^* \overset{K_{ads}}{\Longleftrightarrow} BA_{ads}$ $\qquad K_{ads} = 3.9\cdot10^3\ M^{-1}$

$r_6)\ BHA + s^* \overset{K'_{ads}}{\Longleftrightarrow} BA_{ads}$ $\qquad K'_{ads} = 5.6\cdot10^4\ M^{-1}$

$r_7)\ BAC + s^* \overset{K''_{ads}}{\Longleftrightarrow} BAC_{ads}$ $\qquad K''_{ads} = 1.2\cdot10^4\ M^{-1}$

BA and BHA adsorbed on the catalyst react with positive holes giving rise to the formation of BHA and BAC respectively:

$r_8)\ BA_{ads} + 2h^+_{VB} \xrightarrow{k_{BA/h}} BHA_{ads}$ $\qquad k_{BA/h}$ (unknown parameter)

$r_9)\ BHA_{ads} + 2h^+_{VB} \xrightarrow{k_{BHA/h}} BAC_{ads}$ $\qquad k_{BHA/h}$ (unknown parameter)

Alternatively, BA and BHA are attacked, on the aromatic ring, by hydroxyl radicals leading to the formation of by-products (hydroxylated aromatic species):

$r_{10})\ BA_{ads} + HO^{\bullet} \xrightarrow{k_{BA/HO}} P$ $\qquad k_{BA/HO} = 8.40 \cdot 10^{10}\ M^{-1}\ s^{-1}$ [86]

$r_{11})\ BHA_{ads} + HO^{\bullet} \xrightarrow{k_{BHA/HO}} P$ $\qquad k_{BA/HO} = 4.40 \cdot 10^{10}\ M^{-1}\ s^{-1}$ [86]

Moreover, an unselective attack of HO radicals occurs on the species present in the reacting medium with a consequent formation of polymeric species. In particular, HO radicals directly attack either aldehydic or benzylic groups with the formation of radicals ($B_x^{\bullet}$, $B_y^{\bullet}$) which may add to other molecules of BHA or BA starting some polymerization processes [87-88]:

$r_{12})\ BA_{ads} + HO^{\bullet} \xrightarrow{k_c} B_y^{\bullet}$ $\qquad k_c$ (unknown parameter)

$r_{13})\ B_y^{\bullet} + BA_{ads} \xrightarrow{k_d} PS_y^{\bullet} \xrightarrow{BA_{ads}/k_d} PS$ $\qquad k_d$ (unknown parameter)

$r_{14})\ 2B_y^{\bullet} \xrightarrow{k_{t1}} PS$ $\qquad k_{t1}$ (unknown parameter)

$r_{15})\ BHA_{ads} + HO^{\bullet} \xrightarrow{k_a} B_x^{\bullet}$ $\qquad k_a$ (unknown parameter)

$r_{16})\ B_x^{\bullet} + BHA_{ads} \xrightarrow{k_b} PS_x^{\bullet} \xrightarrow{BHA_{ads}/k_b} PS$ $\qquad k_b$ (unknown parameter)

$r_{17})\ 2B_x^{\bullet} \xrightarrow{k_{t2}} PS$ $\qquad k_{t2}$ (unknown parameter)

where k_c and k_a, as have been described, have to be considered as an aliquot of the kinetic constants of HO radicals to benzyl alcohol and benzaldehyde respectively.
The possibility that HO radicals may react with adsorbed BAC to give undesired hydroxylated by-products has been also considered:

$r_{18})\ BAC_{ads} + HO^{\bullet} \xrightarrow{k_{BAC/HO}} P$ $\qquad k_{BAC/HO} = 4.30 \cdot 10^{9}\ M^{-1}\ s^{-1}$ [86]

The hydroxylated aromatic products obtained in the reactions (r_{10}), (r_{11}), and (r_{18}) were lumped into a single undesired by-product indicated with the symbol "P".
The catalytic cycle is closed by the photoreduction of Cu(II) ions to Cu(0) species:

$r_{19})\ Cu(II) + e_{CB}^{-} \xrightarrow{k_{Cu(II)/e}} Cu(I)$ $\qquad k_{Cu(II)/e} = 8.88 \cdot 10^{5}\ M^{-1}\ s^{-1}$ [55]

$r_{20})\ Cu(I) + e_{CB}^{-} \xrightarrow{k_{Cu(I7)/e}} Cu(0)$ $\qquad k_{Cu(I)/e} = 8.88 \cdot 10^{5}\ M^{-1}\ s^{-1}$ [55]

Cu(I) is also re-oxidated to Cu(II) by positive holes:

r_{21}) $Cu(I) + h^+_{VB} \xrightarrow{k_{Cu(I)/h}} Cu(II)$ $k_{Cu(I)/h}$ (unknown parameter)

The proposed model takes into account also the effects due to two anionic species (SO_4^{2-} and $H_2PO_4^-$) which are present in the system since the Cu(II) ions are introduced in the solution as $CuSO_4$ and the pH is adjusted with H_3PO_4.
It is known from the literature that when SO_4^{2-} and $H_2PO_4^-$ species are present in the reacting solution, they may compete with the substrate for the adsorption on the catalyst sites[73,89]

r_{22}) $SO_4^{2-} + s^* \overset{K'''_{ads}}{\Longleftrightarrow} {SO_4^{2-}}_{ads}$ K'''_{ads} (unknown parameter)

r_{23}) $H_2PO_4^- + s^* \overset{K''''_{ads}}{\Longleftrightarrow} {H_2PO_4^-}_{ads}$ K''''_{ads} (unknown parameter)

Alternatively, these species may compete with the substrate for the reaction with positive holes on the catalyst[72,74]:

r_{24}) ${SO_4^{2-}}_{ads} + h^+_{VB} \xrightarrow{k_{SO_4/h}} {SO_4^{\bullet -}}_{ads}$ $k_{SO_4/h}$ (unknown parameter)

r_{25}) ${H_2PO_4^-}_{ads} + h^+_{VB} \xrightarrow{k_{H_2PO_4/h}} {H_2PO_4^{\bullet}}_{ads}$ $k_{H_2PO_4/h}$ (unknown parameter)

Furthermore, they behave as HO radical scavengers giving rise to the formation of other (less reactive) radical species:

r_{26}) ${SO_4^{2-}}_{ads} + HO^{\bullet} + H^+ \xrightarrow{k_{SO_4/HO}} {SO_4^{\bullet -}}_{ads} + H_2O$ $k_{SO_4/HO} = 1.19 \cdot 10^6\ M^{-1}\ s^{-1}$ [86]

r_{27}) ${H_2PO_4^-}_{ads} + HO^{\bullet} \xrightarrow{k_{H_2PO_4/HO}} {H_2PO_4^{\bullet}}_{ads} + HO^-$ $k_{H_2PO_4/HO} = 2.0 \cdot 10^4\ M^{-1}\ s^{-1}$ [86]

For the sake of simplicity, these two anionic species (SO_4^{2-} and $H_2PO_4^-$) are considered as a single pseudo-component (BC):

r_{28}) $BC + s^* \overset{K_{BC}}{\Longleftrightarrow} BC_{ads}$ K_{BC} (unknown parameter)

r_{29}) $BC_{ads} + h^+_{VB} \xrightarrow{k_{BC/h}} ...$ $k_{BC/h}$ (unknown parameter)

r_{30}) $BC_{ads} + HO^{\bullet} \xrightarrow{k_{BC/HO}} ...$ $k_{BC/HO}$ has been assumed in this work as a mean value of $k_{SO_4/HO}$ and $k_{H_2PO_4/HO}$. ($k_{BC/HO} = 7.0 \cdot 10^5\ M^{-1}\ s^{-1}$)

5.2 Mass balances

On the basis of the proposed mechanism, the following material balance equations can be written for each species present in the reacting system.

5.2.1 Hydroxyl radicals

By considering the reactions r_3-r_4, r_{10}-r_{11}, r_{18} and r_{30}, it has been possible to derive the mass balance on HO radicals:

$$eq_1) \qquad \frac{d[HO^{\bullet}]}{dt} = k_m[h^+_{VB}] - k_{BA/HO} \cdot [HO^{\bullet}] \cdot [BA_{ads}] - k_{BHA/HO} \cdot [HO^{\bullet}] \cdot [BHA_{ads}] + - k_{BAC/HO} \cdot [HO^{\bullet}] \cdot [BAC_{ads}] - k_{BC/HO} \cdot [HO^{\bullet}] \cdot [BC_{ads}]$$

where $k_m = k_{H_2O/h} \cdot [H_2O] + k_{HO/h} \cdot [HO^-]$.

In the equation eq_1, the constants $k_{BA/HO}$ and $k_{BHA/HO}$ account for the overall attack of HO radical species to both aromatic ring positions and benzylic or aldehydic groups respectively.

5.2.2 Polymeric radicals

By considering the reactions r_{12}-r_{14}, and r_{15}-r_{17}, it has been possible to derive the mass balance on $B^{\bullet}_x$ and $B^{\bullet}_y$ polymeric radicals:

$$eq_2) \qquad \frac{d[B^{\bullet}_x]}{dt} = k_a \cdot [HO^{\bullet}] \cdot [BHA_{ads}] - 2 \cdot k_{t2} \cdot [B^{\bullet}_x]^2$$

$$eq_3) \qquad \frac{d[B^{\bullet}_y]}{dt} = k_c \cdot [HO^{\bullet}] \cdot [BA_{ads}] - 2 \cdot k_{t1} \cdot [B^{\bullet}_y]^2$$

where $k_a = S_a \cdot k_{BHA/HO}$ and $k_c = S_c \cdot k_{BA/HO}$, being S_a and S_c the selectivities of HO radical attack to aldehydic and benzylic groups respectively.

5.2.3 Conduction band electrons and valence band holes

The mass balance of photogenerated electrons and valence band holes, reported in equations eq_4 and eq_5, have been obtained by considering the reaction series r_1-r_2, r_{19}-r_{20}, and r_1-r_2, r_3-r_4, r_8-r_9, r_{21} and r_{29} respectively:

eq_4)
$$\frac{d[e_{CB}^-]}{dt} = F - k_{rec} \cdot [e_{CB}^-] \cdot [h_{VB}^+] - k_{Cu(II)/e} \cdot [e_{CB}^-] \cdot [Cu(II)] + - k_{Cu(I)/e} \cdot [e_{CB}^-] \cdot [Cu(I)]$$

eq_5)
$$\frac{d[h_{VB}^+]}{dt} = F - k_{rec} \cdot [e_{CB}^-] \cdot [h_{VB}^+] - k_m \cdot [h_{VB}^+] - k_{Cu(I)/h} \cdot [h_{VB}^+] \cdot [Cu(I)] + -2 \cdot k_{BA/h} \cdot [h_{VB}^+] \cdot [BA_{ads}] - 2 \cdot k_{BHA/h} \cdot [h_{VB}^+] \cdot [BHA_{ads}] - 2 \cdot k_{BC/h} \cdot [h_{VB}^+] \cdot [BC_{ads}]$$

Where the term F represents the electron-hole pair generation term by photolysis which can be written as[90-91]:

eq_6)
$$F = \frac{\phi_{TiO_2}}{V} \cdot \sum_{i=0}^{3} I_{\lambda i}^0 \cdot \left(1 - \exp\left(-2.3 \cdot L \cdot \varepsilon_{TiO_2} \frac{m_{TiO_2}}{V}\right)\right)$$

where the term ϕ_{TiO_2} is the *quantum yield*, which for TiO_2 is equal to 0.06 mol·E^{-1}[90], V is the irradiated volume of the reactor (0.280 l), L is the reactor path length (1.10 cm), $I_{\lambda i}^0$ the power emitted by the lamp at the three different wavelengths (I_{305}^0=1.47·10^{-6} E·s^{-1}, I_{313}^0 = 1.56·10^{-6} E·s^{-1} and I_{366}^0=4.10·10^{-6} E·s^{-1}), $\varepsilon_{TiO_2}$the molar absorption coefficient of TiO_2 suspension, 9.50 l·g^{-1}·cm^{-1}[92] and $\frac{m_{TiO_2}}{V}$ the TiO_2 load expressed in g·l^{-1}.

Equation eq_6 is correct under the assumption (verified) that, in the wavelength range 303-366 nm, the absorption of the other substances present in the solution is negligible compared to that of the titanium dioxide:

$$\varepsilon_{BA} \cdot [BA] + \varepsilon_{BHA} \cdot [BHA] + \varepsilon_{BAC} \cdot [BAC] + \varepsilon_{Cu(II)} \cdot [Cu(II)] \ll \varepsilon_{TiO_2} \frac{m_{TiO_2}}{V}$$

5.2.4 Cuprous and cupric ions

The mass balance of Cu(II) and Cu(I) ions, reported in equation eq_7 and eq_8, have been obtained by considering the reaction series r_{19}, r_{21} and r_{19}-r_{21} respectively:

eq_7) $$\frac{d[Cu(II)]}{dt} = -k_{Cu(II)/e} \cdot [e_{CB}^-] \cdot [Cu(II)] + k_{Cu(I)/h} \cdot [h_{VB}^+] \cdot [Cu(I)]$$

eq_8) $$\frac{d[Cu(I)]}{dt} = k_{Cu(II)/e} \cdot [e_{CB}^-] \cdot [Cu(II)] - k_{Cu(I)/h} \cdot [h_{VB}^+] \cdot [Cu(I)] + - k_{Cu(I)/e} \cdot [e_{CB}^-] \cdot [Cu(I)]$$

5.2.5 Benzyl alcohol, benzaldehyde and benzoic acid

The benzyl alcohol mass balance (eq_9) has been derived from reactions r_8, r_{10} and r_{12}:

eq_9) $$\frac{d[BA_{ads}]}{dt} = -k_{BA/h} \cdot [h_{VB}^+] \cdot [BA_{ads}] - k_{BA/HO} \cdot [HO^\bullet] \cdot [BA_{ads}] - k_d \cdot [BA_{ads}] \cdot [B_y^\bullet]$$

Equation eq_{10} represents the benzaldehyde mass balance, obtained on the basis of reactions r_8-r_9, r_{11} and r_{16}:

eq_{10}) $$\frac{d[BHA_{ads}]}{dt} = k_{BA/h} \cdot [h_{VB}^+] \cdot [BA_{ads}] - k_{BHA/h} \cdot [h_{VB}^+] \cdot [BHA_{ads}] + -k_{BHA/HO} \cdot [HO^\bullet] \cdot [BHA_{ads}] - k_b \cdot [BHA_{ads}] \cdot [B_x^\bullet]$$

The benzoic acid mass balance, reported in equation eq_{11}, has been derived from reactions r_9 and r_{18}:

eq_{11}) $$\frac{d[BAC_{ads}]}{dt} = k_{BAC/h} \cdot [h_{VB}^+] \cdot [BHA_{ads}] - k_{BAC/HO} \cdot [HO^\bullet] \cdot [BAC_{ads}]$$

5.2.6 Sulphate and dihydrogenphosphate anions

For the sake of simplicity, the anionic species SO_4^{2-} and $H_2PO_4^-$ have been considered as a single pseudo-component BC, whose mass balance has been obtained by considering the reactions r_{29}-r_{30} and is reported in the follow equation:

eq$_{12}$) $$\frac{d[BC_{ads}]}{dt} = -k_{BC/h} \cdot [h^+_{VB}] \cdot [BC_{ads}] - k_{BC/HO} \cdot [HO^\bullet] \cdot [BC_{ads}]$$

5.2.7 Hydroxylated aromatic species

As it has been done with the anionic species, also the hydroxylated aromatic compounds, resulting from the HO radicals attack to BA_{ads}, BHA_{ads} and BAC_{ads} molecules (r_{10}, r_{11} and r_{18} respectively), have been considered as a single pseudo-component P:

eq$_{13}$) $$\frac{d[P]}{dt} = k_{BA/HO} \cdot [HO^\bullet] \cdot [BA_{ads}] + k_{BHA/HO} \cdot [HO^\bullet] \cdot [BHA_{ads}] + + k_{BAC/HO} \cdot [HO^\bullet] \cdot [BAC_{ads}]$$

5.2.8 Adsorbed species

In some reported equation (in particular eq$_1$-eq$_3$, eq$_5$ and eq$_9$-$_{13}$) appear the concentrations of adsorbed BA, BHA, BAC and BC species, which have been calculated on the basis of Langmuir-Hinshelwood model:

eq$_{14}$) $$[BA_{ads}] = \frac{\alpha \cdot \frac{m_{TiO_2}}{V} \cdot K_{ads} \cdot [BA]}{1 + K_{ads} \cdot [BA] + K'_{ads} \cdot [BHA] + K''_{ads} \cdot [BAC] + K_{BC} \cdot [BC]}$$

eq$_{15}$) $$[BHA_{ads}] = \frac{\alpha \cdot \frac{m_{TiO_2}}{V} \cdot K'_{ads} \cdot [BHA]}{1 + K_{ads} \cdot [BA] + K'_{ads} \cdot [BHA] + K''_{ads} \cdot [BAC] + K_{BC} \cdot [BC]}$$

eq$_{16}$) $$[BAC_{ads}] = \frac{\alpha \cdot \frac{m_{TiO_2}}{V} \cdot K''_{ads} \cdot [BAC]}{1 + K_{ads} \cdot [BA] + K'_{ads} \cdot [BHA] + K''_{ads} \cdot [BAC] + K_{BC} \cdot [BC]}$$

eq$_{17}$) $$[BC_{ads}] = \frac{\alpha \cdot \frac{m_{TiO_2}}{V} \cdot K_{BC} \cdot [BC]}{1 + K_{ads} \cdot [BA] + K'_{ads} \cdot [BHA] + K''_{ads} \cdot [BAC] + K_{BC} \cdot [BC]}$$

The term $\alpha \cdot \frac{m_{TiO_2}}{V}$ indicates the total concentration of total active sites which depends upon the catalyst load $\left(\frac{m_{TiO_2}}{V}\right)$. A value of $\alpha = 1.02 \cdot 10^5\ mol \cdot g^{-1}$ total moles of active sites per unit mass of catalyst was calculated through the formulas $\alpha = \frac{A_{SP}}{N_a \cdot S^0_{sat}}$ where $A_{SP} = 9.5\ m^2\ g^{-1}$ is the specific surface area (measured by the singlepoint BET method) of the adopted TiO_2 (Aldrich, pure anatase), $N_a = 6.022 \cdot 10^{23}$ is the Avogadro's number, and $S^0_{sat} = 1.55 \cdot 10^{-18}\ m^2$ is the surface area of TiO_2 covered by one molecule of adsorbed BA[80].
The initial concentration of the pseudo-component BC has been calculated and is given by:

$$[BC]_0 = \frac{10^{-pK_{a(H_3PO_4/H_2PO_4^-)}} \cdot [H_3PO_4]_0}{1+10^{-pH}} + \frac{1}{1+\frac{10^{pK_{a(HSO_4^-/SO_4^{2-})}}}{10^{pH}}} \cdot [Cu(II)]_0$$

The first term is related to the concentration of di-hydrogenphosphates ions in the solution, due to the use of phosphoric acid ($pK_{a(H_3PO_4/H_2PO_4^-)} = 2.12$), to regulate the pH. The second one represents the concentration of sulfate ($pK_{a(HSO_4^-/SO_4^{2-})} = 1.92$) present in the reacting medium as the result of the addition of cupric sulfate to the solution.

5.2.9 Steady-state hypothesis

Applying the steady-state hypothesis on HO, B_x, and B_y radicals, equations eq_1-eq_3 are modified as following:

$eq_{18})$ $$[HO^\bullet]_{ss} = \frac{k_m \cdot [h^+_{VB}]}{k_{BA/HO} \cdot [BA_{ads}] + k_{BHA/HO} \cdot [BHA_{ads}] + k_{BAC/HO} \cdot [BAC_{ads}] + k_{BC/HO} \cdot [BC_{ads}]}$$

$eq_{19})$ $$[B^\bullet_x]_{ss} = \sqrt{\frac{k_a \cdot [HO^\bullet] \cdot [BHA_{ads}]}{2 \cdot k_{t2}}} = k_z \cdot ([HO^\bullet]_{ss} \cdot [BHA_{ads}])^{0.5}$$

$eq_{20})$ $$[B^\bullet_y]_{ss} = \sqrt{\frac{k_c \cdot [HO^\bullet] \cdot [BA_{ads}]}{2 \cdot k_{t1}}} = k_w \cdot ([HO^\bullet]_{ss} \cdot [BHA_{ads}])^{0.5}$$

with $k_z = \left(\frac{k_a}{2 \cdot k_{t2}}\right)^{0.5}$ and $k_x = \left(\frac{k_c}{2 \cdot k_{t1}}\right)^{0.5}$.

By considering steady state concentration of the radical species, represented in equations eq$_{17}$-eq$_{19}$, the BA_{ads}, BHA_{ads}, BAC_{ads}, BC_{ads}, and P mass balances (eq$_9$-eq$_{13}$) become:

eq$_{21}$)
$$\frac{d[BA_{ads}]}{dt} = -k_{BA/h} \cdot [h^+_{VB}] \cdot [BA_{ads}] +$$

$$-k_{BA/HO} \cdot \frac{k_m \cdot [h^+_{VB}] \cdot [BA_{ads}]}{k_{BA/HO} \cdot [BA_{ads}] + k_{BHA/HO} \cdot [BHA_{ads}] + k_{BAC/HO} \cdot [BAC_{ads}] + k_{BC/HO} \cdot [BC_{ads}]} +$$

$$- k_y \cdot ([BA_{ads}])^{1.5} \cdot \left(\frac{k_m [h^+_{VB}]}{k_{BA/HO} \cdot [BA_{ads}] + k_{BHA/HO} \cdot [BHA_{ads}] + k_{BAC/HO} \cdot [BAC_{ads}] + k_{BC/HO} \cdot [BC_{ads}]} \right)^{0.5}$$

eq$_{22}$)
$$\frac{d[BHA_{ads}]}{dt} = k_{BA/h} \cdot [h^+_{VB}] \cdot [BA_{ads}] - k_{BHA/h} \cdot [h^+_{VB}] \cdot [BHA_{ads}] +$$

$$-k_{BHA/HO} \cdot \frac{k_m \cdot [h^+_{VB}] \cdot [BHA_{ads}]}{k_{BA/HO} \cdot [BA_{ads}] + k_{BHA/HO} \cdot [BHA_{ads}] + k_{BAC/HO} \cdot [BAC_{ads}] + k_{BC/HO} \cdot [BC_{ads}]} +$$

$$- k_x \cdot ([BHA_{ads}])^{1.5} \cdot \left(\frac{k_m [h^+_{VB}]}{k_{BA/HO} \cdot [BA_{ads}] + k_{BHA/HO} \cdot [BHA_{ads}] + k_{BAC/HO} \cdot [BAC_{ads}] + k_{BC/HO} \cdot [BC_{ads}]} \right)^{0.5}$$

where $k_x = k_b \cdot k_z$ and $k_y = k_d \cdot k_w$

eq$_{23}$)
$$\frac{d[BAC_{ads}]}{dt} = k_{BAC/h} \cdot [h^+_{VB}] \cdot [BHA_{ads}] +$$

$$-k_{BAC/HO} \cdot \frac{k_m \cdot [h^+_{VB}] \cdot [BAC_{ads}]}{k_{BA/HO} \cdot [BA_{ads}] + k_{BHA/HO} \cdot [BHA_{ads}] + k_{BAC/HO} \cdot [BAC_{ads}] + k_{BC/HO} \cdot [BC_{ads}]}$$

eq$_{24}$)
$$\frac{d[BC_{ads}]}{dt} = k_{BC/h} \cdot [h^+_{VB}] \cdot [BC_{ads}] +$$

$$-k_{BC/HO} \cdot \frac{k_m \cdot [h^+_{VB}] \cdot [BC_{ads}]}{k_{BA/HO} \cdot [BA_{ads}] + k_{BHA/HO} \cdot [BHA_{ads}] + k_{BAC/HO} \cdot [BAC_{ads}] + k_{BC/HO} \cdot [BC_{ads}]}$$

$$eq_{25}) \qquad \frac{d[P]}{dt} = \frac{k_m \cdot [h^+_{VB}] \cdot (k_{BA/HO} \cdot [BA_{ads}] + k_{BHA/HO} \cdot [BHA_{ads}] + k_{BAC/HO} \cdot [BAC_{ads}])}{k_{BA/HO} \cdot [BA_{ads}] + k_{BHA/HO} \cdot [BHA_{ads}] + k_{BAC/HO} \cdot [BAC_{ads}] + k_{BC/HO} \cdot [BC_{ads}]}$$

5.3 Integration

The mathematical model of the selective oxidation of benzyl alcohol by means of the TiO_2/Cu(II)/hv system, as it has been developed, is thus characterized by a set of 9 ordinary differential equations (ODEs), where 8 parameters (k_m, $k_{Cu(I)/h}$, $k_{BA/h}$, $k_{BHA/h}$, $k_{BC/h}$, K_{BC}, k_x, k_y) appear, with values unknown in literature.

$$\begin{cases} \frac{d[e^-_{CB}]}{dt} = \dots & eq_4 \\ \frac{d[h^+_{VB}]}{dt} = \dots & eq_5 \\ \frac{d[Cu(II)]}{dt} = \dots & eq_7 \\ \frac{d[Cu(I)]}{dt} = \dots & eq_8 \\ \frac{d[BA_{ads}]}{dt} = \dots & eq_{21} \\ \frac{d[BHA_{ads}]}{dt} = \dots & eq_{22} \\ \frac{d[BAC_{ads}]}{dt} = \dots & eq_{23} \\ \frac{d[BC_{ads}]}{dt} = \dots & eq_{24} \\ \frac{d[P]}{dt} = \dots & eq_{25} \end{cases}$$

Fig. 43 Set of 9 ODEs that describe the selective oxidation of benzyl alcohol by means TiO_2/Cu(II)/hv system

Once integrated, this set of differential equations (figure 43) makes it possible to calculate the concentration of each species participating in the process against time. Unfortunately, there are too many unknown parameters to be estimated (figure 44a) from the data collected in runs starting from an aqueous solution of benzyl alcohol, copper sulfate, and titanium dioxide. To overcome the difficulties associated with this assessment, the results collected by following the evolution of a simpler subsystem have been firstly taken into account.

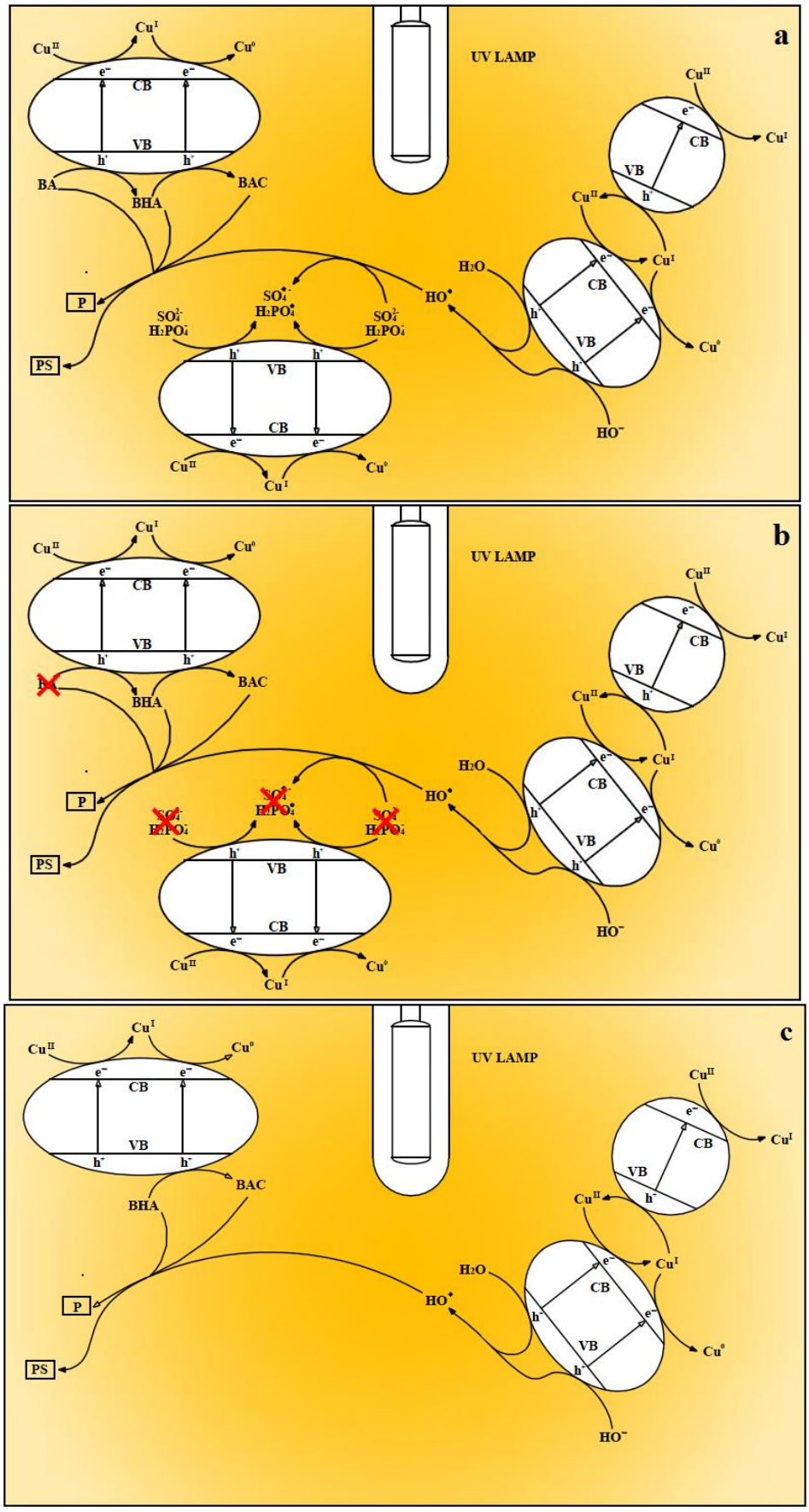

Fig. 44

In particular, studying the oxidation of benzaldehyde, in absence of benzyl alcohol, sulphate, and dihydrogenphosphate ions (figure 44b) by means of the TiO_2/Cu(II)/hv system, the number of unknown parameters to estimate and of ODEs is reduced and the mathematical model is simplified, as can be seen from figure 44c.

5.3.1 Benzaldehyde oxidation

In all the experiments used for the optimization of this subsystem, copper(II) has been introduced in the reacting system as cupric perchlorate (not as cupric sulfate) and the pH has been regulated with perchloric acid (not as phosphoric acid) due to the fact that the adsorption of perchlorate anions does not occur on TiO_2 surface, according to the results of previous investigations reported by others[77]. These studies demonstrate that perchlorates have negligible effects on the rates of photocatalytic oxidation of organics over illuminated titanium dioxide.

In this way, benzaldehyde oxidation subsystem is characterized only by 7 ODEs because, in absence of benzyl alcohol ($[BA]_0 = 0$), sulphate, and dihydrogenophosphate ions ($[BC]_0 = 0$), equations eq_{21} and eq_{24} are deleted. For the same reason, the ODEs describing the mass balances on h^+_{VB}, BHA_{ads}, BAC_{ads}, and P species (eq_5, eq_{22}-eq_{23} and eq_{25}) have been respectively modified by neglecting the terms including BA_{ads} and BC concentrations:

eq_{26})
$$\frac{d[h^+_{VB}]}{dt} = F - k_{rec} \cdot [e^-_{CB}] \cdot [h^+_{VB}] - k_m \cdot [h^+_{VB}] + \\ -k_{Cu(I)/h} \cdot [h^+_{VB}] \cdot [Cu(I)] - 2 \cdot k_{BHA/h} \cdot [h^+_{VB}] \cdot [BHA_{ads}]$$

eq_{27})
$$\frac{d[BHA_{ads}]}{dt} = - k_{BHA/h} \cdot [h^+_{VB}] \cdot [BHA_{ads}] + \\ -k_{BHA/HO} \cdot \frac{k_m \cdot [h^+_{VB}] \cdot [BHA_{ads}]}{k_{BHA/HO} \cdot [BHA_{ads}] + k_{BAC/HO} \cdot [BAC_{ads}] + k_{BC/HO} \cdot [BC_{ads}]} + \\ - k_x \cdot ([BHA_{ads}])^{1.5} \cdot \left(\frac{k_m [h^+_{VB}]}{k_{BHA/HO} \cdot [BHA_{ads}] + k_{BAC/HO} \cdot [BAC_{ads}] + k_{BC/HO} \cdot [BC_{ads}]} \right)^{0.5}$$

eq$_{28}$)
$$\frac{d[BAC_{ads}]}{dt} = k_{BAC/h} \cdot [h^+_{VB}] \cdot [BHA_{ads}] + -k_{BAC/HO} \cdot \frac{k_m \cdot [h^+_{VB}] \cdot [BAC_{ads}]}{k_{BHA/HO} \cdot [BHA_{ads}] + k_{BAC/HO} \cdot [BAC_{ads}] + k_{BC/HO} \cdot [BC_{ads}]}$$

eq$_{29}$)
$$\frac{d[P]}{dt} = \frac{k_m \cdot [h^+_{VB}] \cdot (k_{BHA/HO} \cdot [BHA_{ads}] + k_{BAC/HO} \cdot [BAC_{ads}])}{k_{BHA/HO} \cdot [BHA_{ads}] + k_{BAC/HO} \cdot [BAC_{ads}] + k_{BC/HO} \cdot [BC_{ads}]}$$

On the other hand, the ODEs describing the mass balances on e^-_{CB}, Cu(II), and Cu(I) species are those previously reported (eq$_4$, eq$_7$-eq$_8$).

The described set of ODEs has been solved by using the MATLAB routine "ode45", which is based on the Runge-Kutta method with adaptive step-size.

For the selective oxidation of BHA, four unknown parameters ($k_{BHA/h}$, k_m, $k_{Cu(I)/h}$, and k_x) are included in the set of mass balance equations. The kinetic parameters have been estimated through the adoption of an iterative optimization procedure (Marquardt approach) which minimizes the squares of the differences between calculated and experimental concentrations of each species (objective function)[93]:

$$\phi = \sum_{l=1}^{m} \sum_{j=1}^{n} \sum_{i=1}^{h} \left(y_{i,j,l} - c_{ijl}\right)^2$$

where the terms *y* and *c* are the calculated and experimental concentrations. Whereas m, n, and h are the number of experimental data recorded in each experiment, the number of the involved species (BHA, BAC, and Cu(II)), and the number of the experiments used in the optimization procedure respectively.

The experimental data collected in four oxidation runs (pH = 2.0, m_{TiO_2} 56.6 mg), at different benzaldehyde and Cu(II) starting concentrations (t=0, $[BHA]_0$ = 0.74–0.40 mM, $[Cu(II)]_0$ = 1.69–0.44 mM, whereas $[BAC]_0 \neq 0$, being present in small amounts, experimentally measured, in the commercial BHA samples), have been simultaneously used in this procedure. In table 4, the estimated values for the four constants are reported along with their uncertainties. It is noteworthy to observe that the values of some of them do not seem

completely satisfactory, in one case being as high as, approximately, 18% of the estimated value.

$k_{BHA/h}$ $(M^{-1} \cdot s^{-1})$	k_m $(M^{-1} \cdot s^{-1})$	$k_{Cu(I)/h}$ $(M^{-1} \cdot s^{-1})$	k_x $(M^{-1} \cdot s^{-1})$
$3.00 \cdot 10^4$ $\pm$ $3.15 \cdot 10^3$	$8.48 \cdot 10^{-1}$ $\pm$ $7.23 \cdot 10^{-2}$	$4.65 \cdot 10^3$ $\pm$ $9.52 \cdot 10^2$	$4.12 \cdot 10^3$ $\pm$ $7.32 \cdot 10^2$

Tab.4 Values estimated for the four unknown parameters along with their uncertainties.

A visual comparison of the calculated and experimental concentration data for the Cu(II), BHA, and BAC species is shown in the figures and are reported in figures 45a-d. A good capability of the model to simulate the system behavior appears from the analysis of these figures.

This conclusion is confirmed on a quantitative basis as well as by the overall percentage standard deviations and those of BHA, BAC, and Cu(II) species (reported in table 5) which are lower than those associated to the experimental determination of the concentrations of the measured species.

Figure	$[BHA]_0$ (mM)	$[Cu(II)]_0$ (mM)	σ_{BHA} (%)	$\sigma_{Cu(II)}$ (%)	σ_{BAC} (%)	σ_{tot} (%)
45a	0.467	1.69	0.05	0.17	2.55	2.77
45b	0.418	0.948	1.94	1.21	2.23	5.39
45c	0.401	0.440	1.34	1.23	0.19	2.76
45d	0.740	0.862	0.40	0.72	1.59	2.70

Tab. 5 Percentage standard deviations on the BHA, BAC and Cu(II) species, for each experimental run utilized in the optimization procedure.

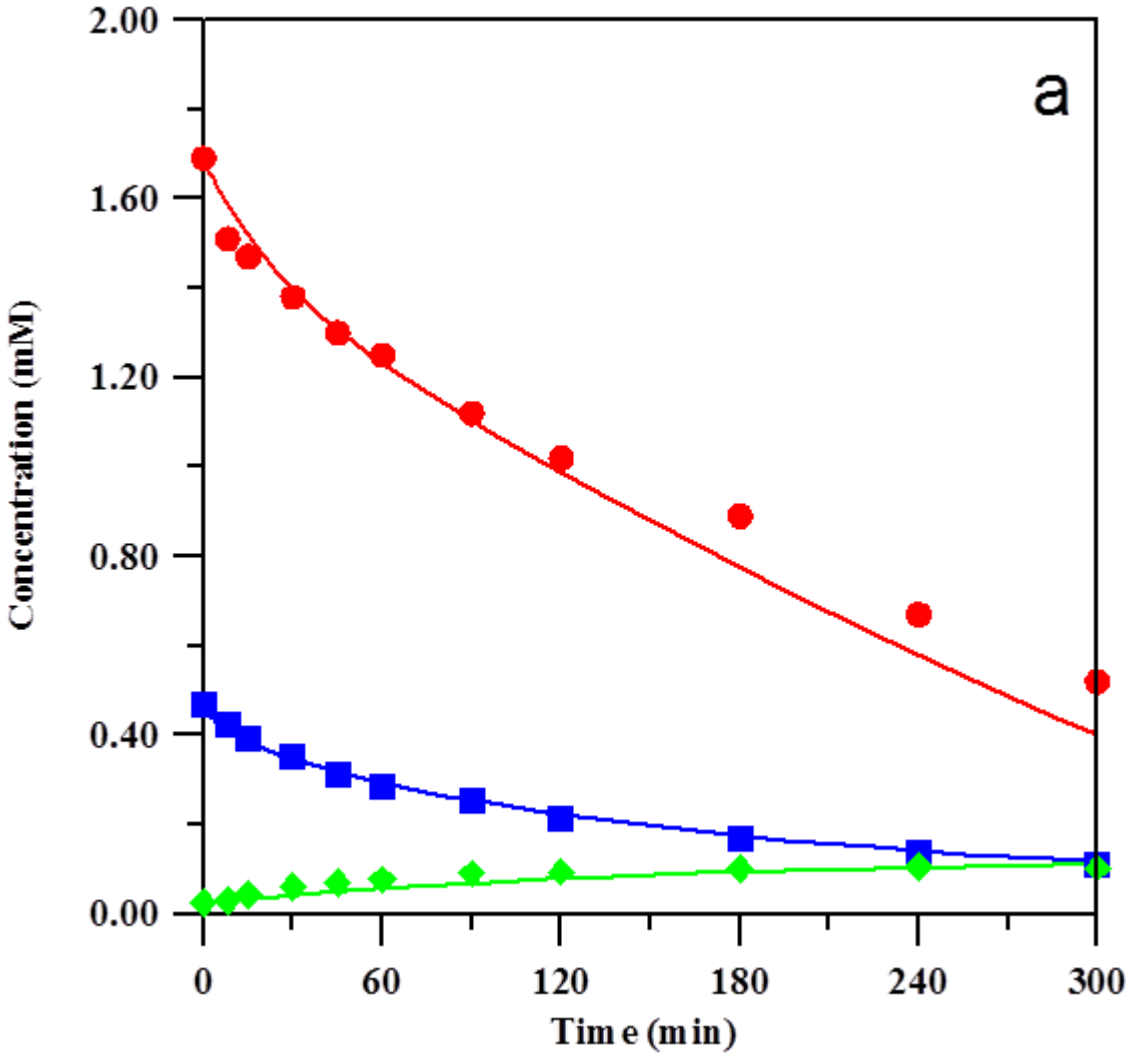

Fig. 45a Predicted (solid lines) and experimental (symbols) concentration-time profile for BHA selective oxidation.

pH = 2.0. T = 25 °C. m_{TiO_2}=56.6 mg.

$[BHA]_0$ = 0.467 mM, $[Cu(II)]_0$ = 1.69 mM.

Cu(II): —●, BHA: —■, BAC: —◆.

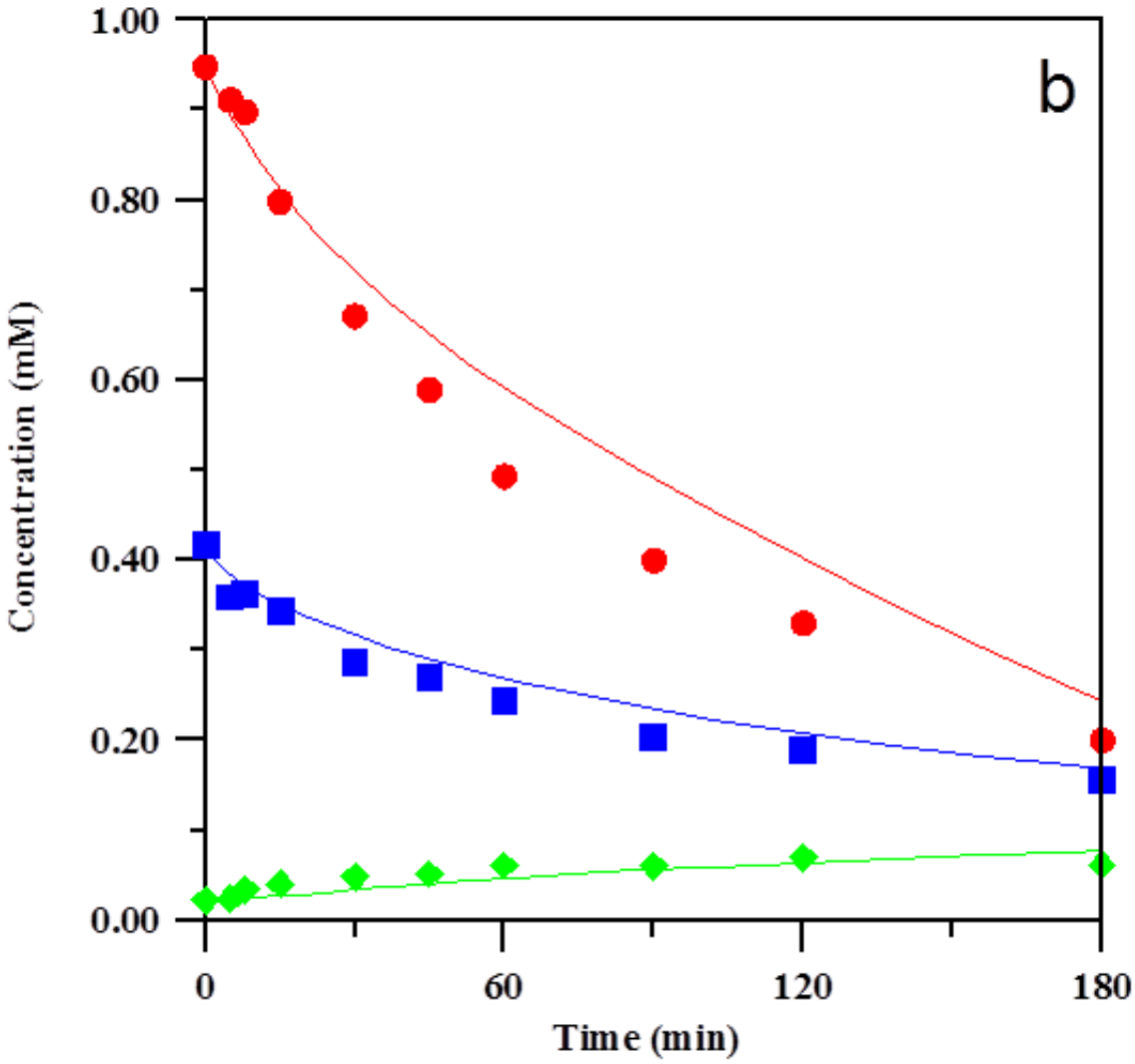

Fig. 45b Predicted (solid lines) and experimental (symbols) concentration-time profile for BHA selective oxidation.

pH = 2.0. T = 25 °C. m_{TiO_2}=56.6 mg.

$[BHA]_0$ = 0.418 mM, $[Cu(II)]_0$ = 0.948 mM.

Cu(II): —●—, BHA: —■—, BAC: —◆—.

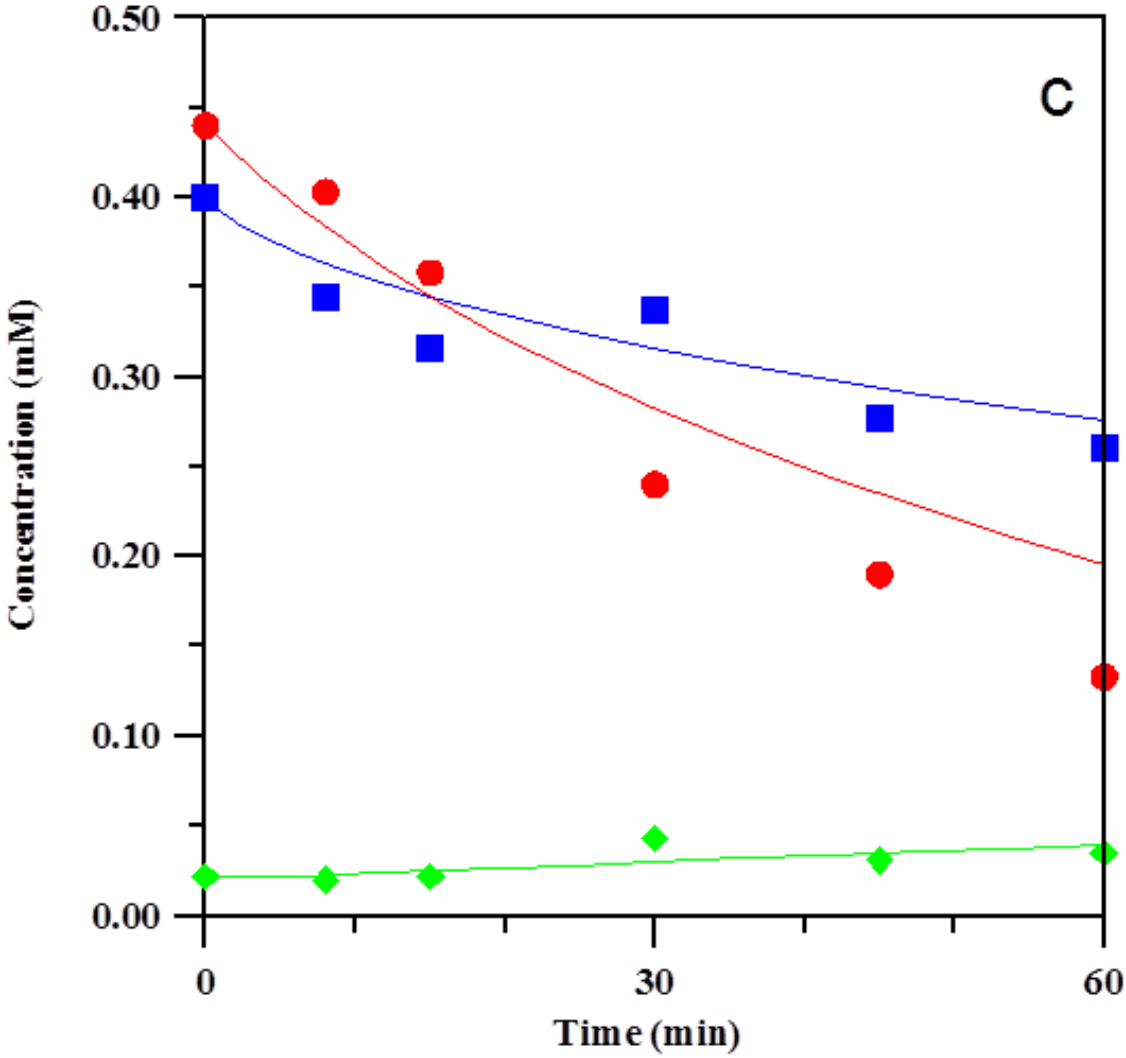

Fig. 45c Predicted (solid lines) and experimental (symbols) concentration-time profile for BHA selective oxidation.

pH = 2.0. T = 25 °C. m_{TiO_2}=56.6 mg.

$[BHA]_0$ = 0.401 mM, $[Cu(II)]_0$ = 0.440 mM.

Cu(II): —●—, BHA: —■—, BAC: —◆—.

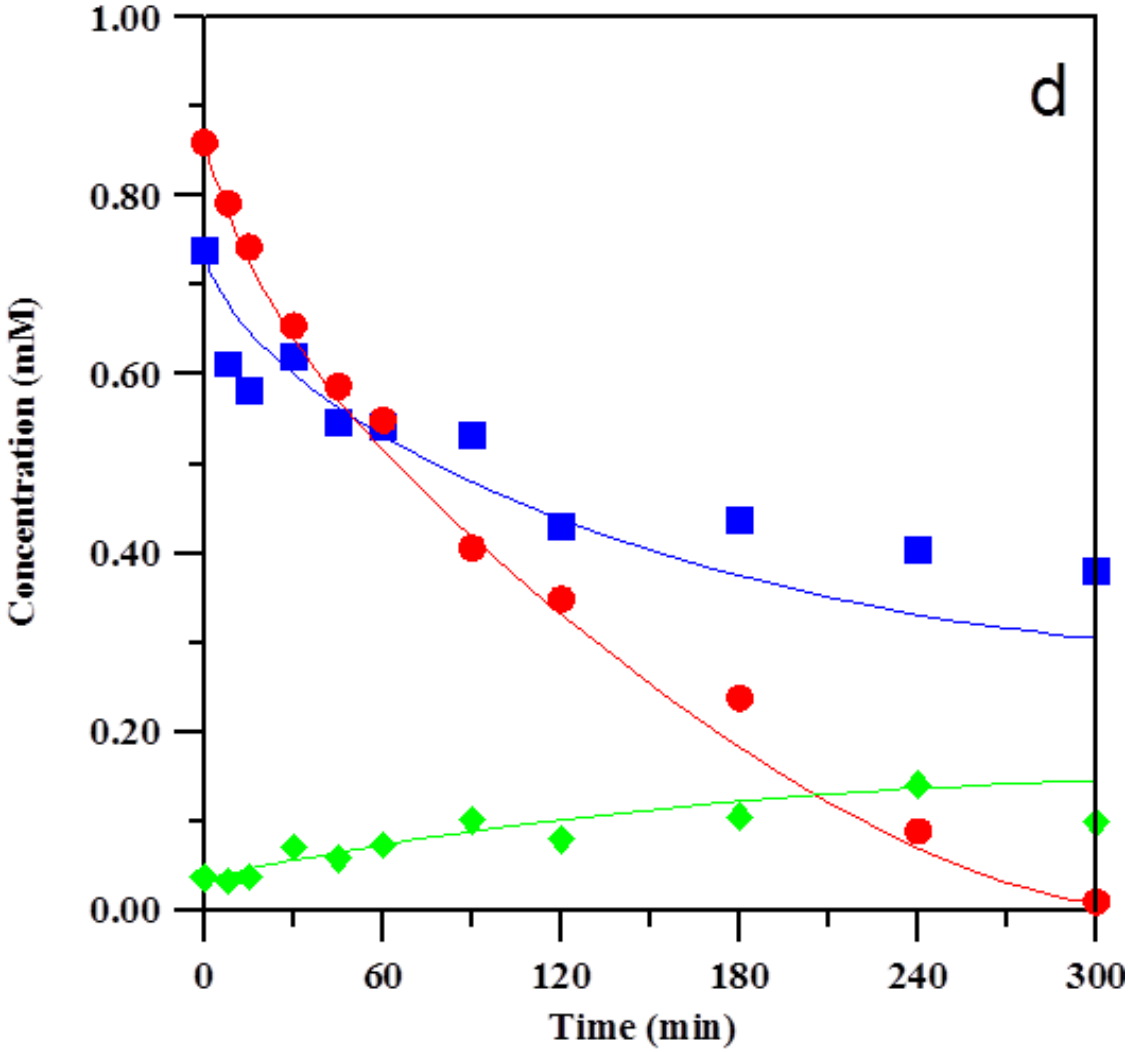

Fig. 45d Predicted (solid lines) and experimental (symbols) concentration-time profile for BHA selective oxidation.

pH = 2.0. T = 25 °C. m_{TiO_2}=56.6 mg.

$[BHA]_0$ = 0.740 mM, $[Cu(II)]_0$ = 0.862 mM.

Cu(II): —●—, BHA: —■—, BAC: —◆—.

5.3.2 Benzyl alcohol oxidation

For the analysis of the data collected during the oxidation runs of benzyl alcohol, an approach similar to that previously used for benzaldehyde oxidation has been adopted. The above-described model, developed for BHA oxidation, has been properly modified based on the results collected during the oxidation of BA. First of all, because $[BA]_0 \neq 0$ for t = 0, the ordinary differential equation eq_{21} has been considered in addition to those already included. Moreover, it has been also taken into account the possibility of using this model for the results of some experimental runs in which sulfates ions, added as $CuSO_4 \cdot 5H_2O$ instead of $Cu(ClO_4)_2 \cdot 6H_2O$, and dihydrogenphosphates species, added as H_3PO_4 for regulating the pH instead of $HClO_4$, were present in the reacting medium (at t = 0, $[BC]_0 \neq 0$). For this purpose, the equation eq_{24} has been taken into account.

It is clear that, also in this case, some kinetic constants were present whose values were known ''a priori'' ($k_{BA/h}$, K_{BC}, $k_{BC/h}$, and k_y) and an optimization procedure has been utilized to estimate them[93], by minimizing the objective function shown in paragraph 5.3.1. In this case the species involved in the optimization procedure have been BA, BHA, and Cu(II).

The results of six oxidation runs (pH = 2.0 and m_{TiO_2} = 56.6 mg), at different benzyl alcohol and Cu(II) starting concentrations ($[BA]_0$ = 1.66–1.42 mM, $[Cu(II)]_0$ = 1.95–1.12 mM, and $[BC]_0$ = 0–10.98 mM), have been simultaneously used in this procedure.

The best estimated values obtained along with their uncertainties are shown in table 6.

$k_{BA/h}$ $(M^{-1} \cdot s^{-1})$	K_{BC} (M^{-1})	$k_{BC/h}$ $(M^{-1} \cdot s^{-1})$	k_y $(M^{-1} \cdot s^{-1})$
$3.80 \cdot 10^5$	95.3	$1.47 \cdot 10^6$	$6.47 \cdot 10^3$
$\pm$	$\pm$	$\pm$	$\pm$
$3.25 \cdot 10^3$	24.3	$4.33 \cdot 10^5$	$1.97 \cdot 10^3$

Tab.6 Values estimated for the four unknown parameters along with their uncertainties.

The value for the adsorption equilibrium constant for the pseudocomponent BC ($K_{BC} = 95.3 \pm 24.3\ M^{-1}$) falls in the range $1.5 \leq \log K \leq 2.0$, reported by others[94], for the adsorption of SO_4^{2-} species on commercial TiO_2 pure anatase (same TiO_2 crystallographic phase used in the experimental runs).

Unfortunately, no data for the kinetic constants of the reactions of photo-produced TiO_2–holes with aromatic molecules have been found for comparison purposes.

Also in this case, visual comparisons of the calculated and experimental concentration data for Cu(II), benzyl alcohol, benzaldehyde, and benzoic acid are shown (figures 44a-f). The model is capable of simulating the concentration trend for BA, BHA, and Cu(II) species in all the runs analyzed. On the other hand, the calculated concentration of BAC results underestimated as already observed during the oxidation runs of BHA.

To validate the mathematical model and the best estimated values of the parameters found with the applied procedure, the results of two additional selective oxidation runs of BA with different TiO_2 initial load (m_{TiO_2} = 28.1–42.5 mg) have been analyzed by means of this model *without any further adjustment of the parameters*. A comparison of calculated and experimental data is shown in figures 46g-h. A good agreement is observed between calculated and experimental concentration data thus indicating a good capability of the proposed model to simulate the system behavior at varying initial conditions.

Less satisfactorily, although still appreciable, the prediction of BAC concentration profiles, shown in figures 45 and 46, seems to suggest the existence of some model inadequacies probably due to simplifying assumptions done or to the very low concentrations, experimentally measured, of BAC. Moreover, the proposed kinetic model relies on the implicit assumption that the unknown intermediates formed during the oxidation process have a negligible effect on the consumption or production rates of the measured species. This assumption, done to overcome the difficulties due to the lack of knowledge of the structures and reactivity of these intermediates, could be responsible of large percentage standard deviations found in some cases. The overall percentage standard deviations and those of BA, BHA, and Cu(II) measured species are reported in table 7.

Figure	$[BA]_0$ (mM)	$[Cu(II)]_0$ (mM)	$[BC]_0$ (mM)	m_{TiO_2} (mg)	σ_{BA} (%)	σ_{BHA} (%)	$\sigma_{Cu(II)}$ (%)	σ_{tot} (%)
46a	1.65	1.80	10.90	56.6	2.84	2.57	2.57	7.71
46b	1.42	1.50	0	56.6	0.96	1.72	1.72	5.11
46c	1.62	1.73	10.86	56.6	1.14	2.43	2.43	7.48
46d	1.46	1.50	10.75	56.6	1.91	2.19	2.19	8.04
46e	1.53	1.95	10.98	56.6	2.58	0.21	0.21	8.68
46f	1.66	1.12	10.56	56.6	1.66	0.11	0.11	9.35
46g	1.48	1.57	10.79	28.1	0.38	0.71	0.71	6.22
46h	1.51	1.62	10.81	42.5	1.37	0.70	0.70	2.76

Tab.7 Percentage standard deviations on the BA, BAH and Cu(II) species, for each experimental run utilized in the optimization and validation procedure.

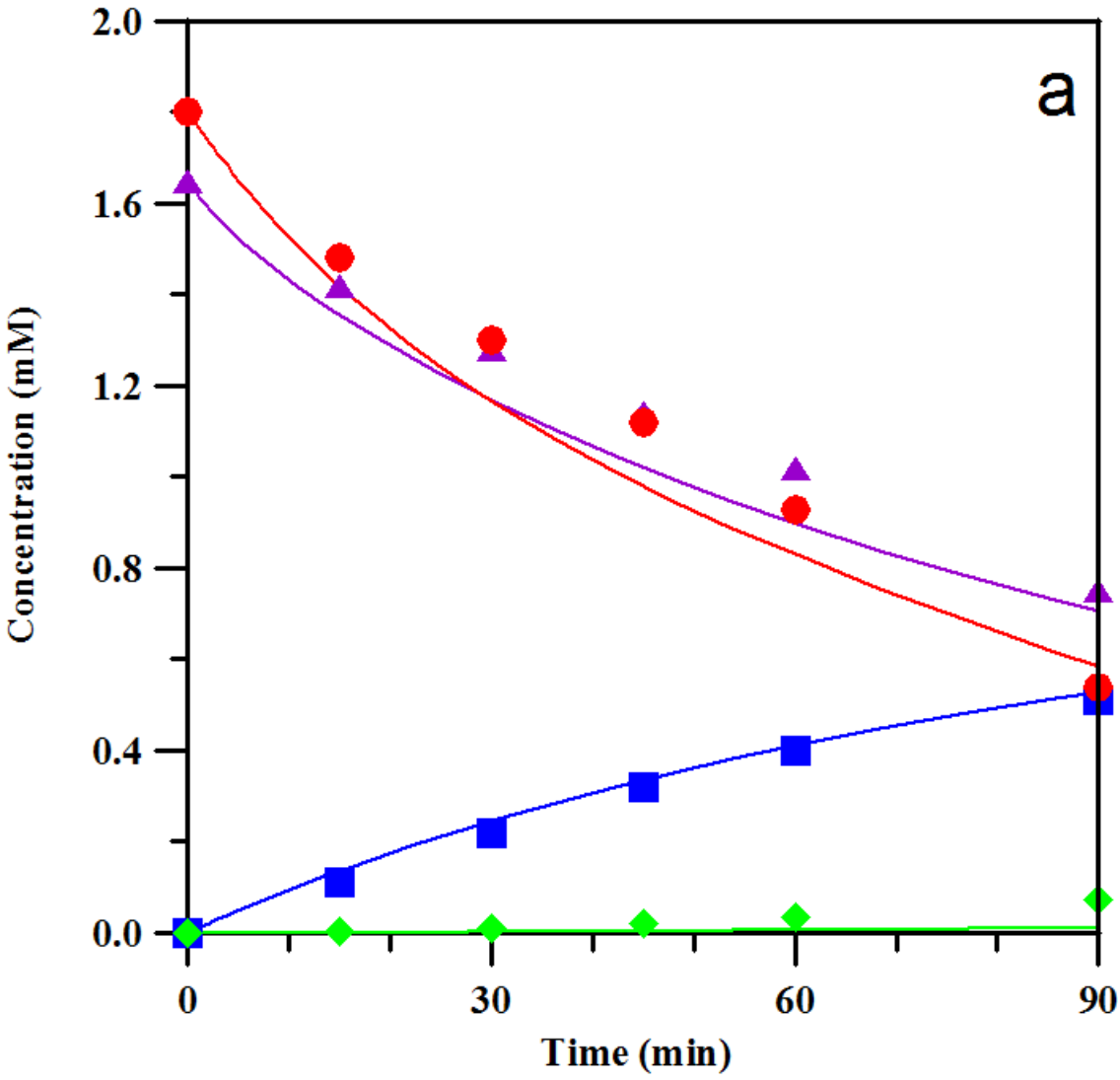

Fig. 46a Predicted (solid lines) and experimental (symbols) concentration-time profile for BA selective oxidation.

pH = 2.0. T = 25 °C. m_{TiO_2}=56.6 mg.

$[BA]_0$ = 1.65 mM, $[Cu(II)]_0$ = 1.80 mM, $[BC]_0$ = 10.90 mM

BA: —▲—,Cu(II): —●—, BHA: —■—, BAC: —◆—.

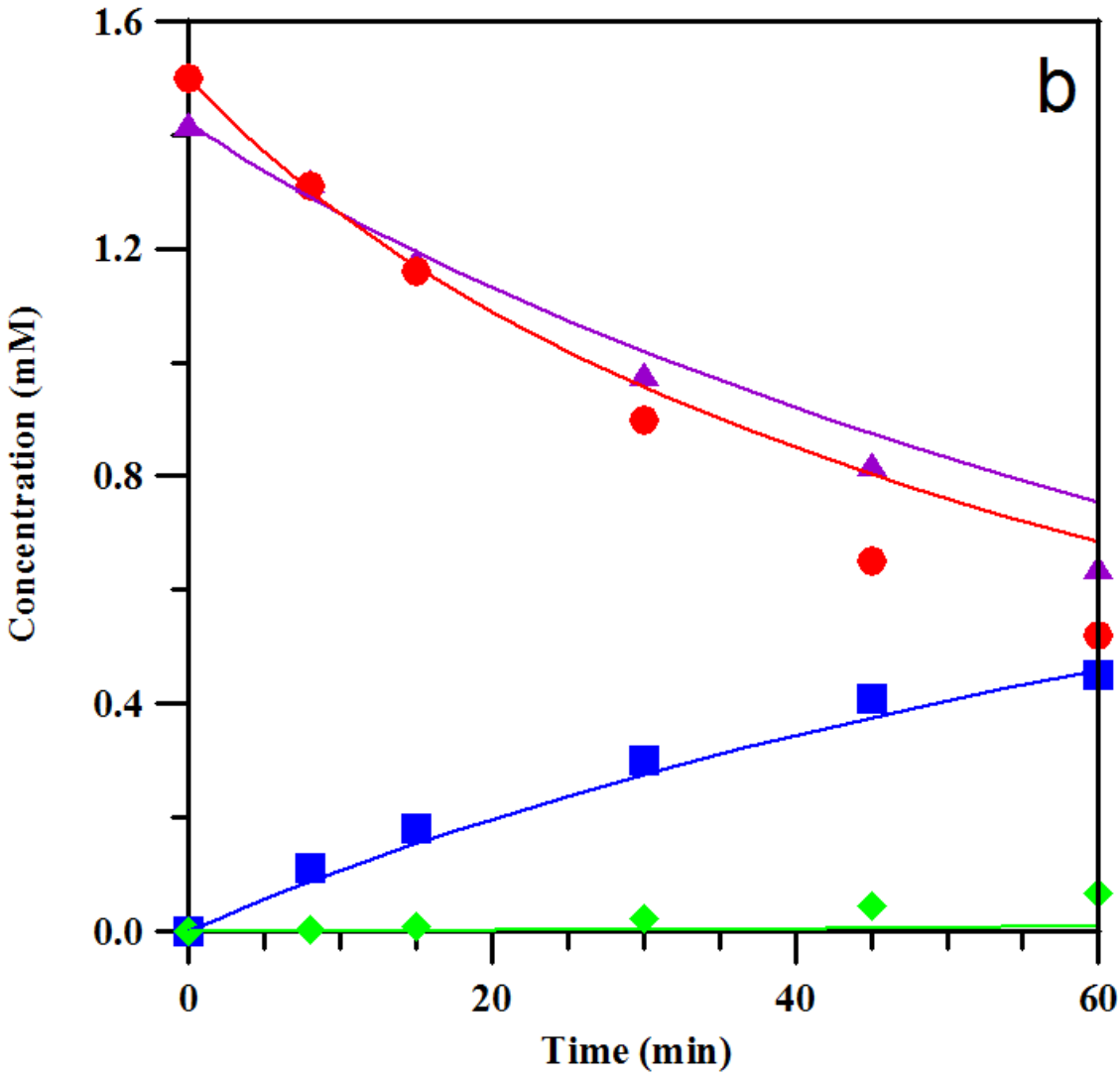

Fig. 46b Predicted (solid lines) and experimental (symbols) concentration-time profile for BA selective oxidation.

pH = 2.0. T = 25 °C. m_{TiO_2}=56.6 mg.

$[BA]_0$ = 1.42 mM, $[Cu(II)]_0$ = 1.50 mM, $[BC]_0$ = 0 mM

BA: —▲—,Cu(II): —●—, BHA: —■—, BAC: —◆—.

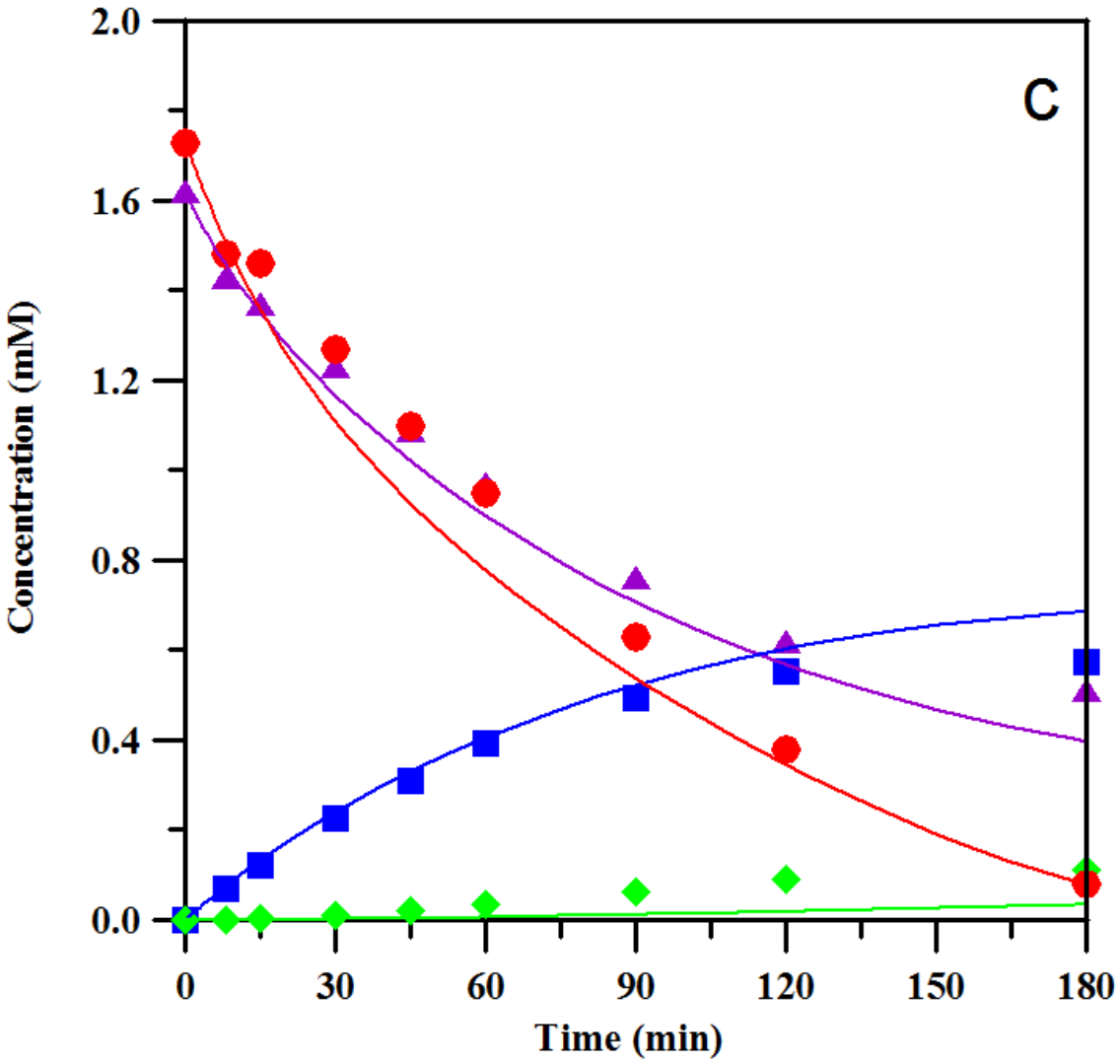

Fig. 46c Predicted (solid lines) and experimental (symbols) concentration-time profile for BA selective oxidation.

pH = 2.0. T = 25 °C. m_{TiO_2}=56.6 mg.

$[BA]_0$ = 1.62 mM, $[Cu(II)]_0$ = 1.73 mM, $[BC]_0$ = 10.86 mM

BA: —▲—,Cu(II): —●—, BHA: —■—, BAC: —◆—.

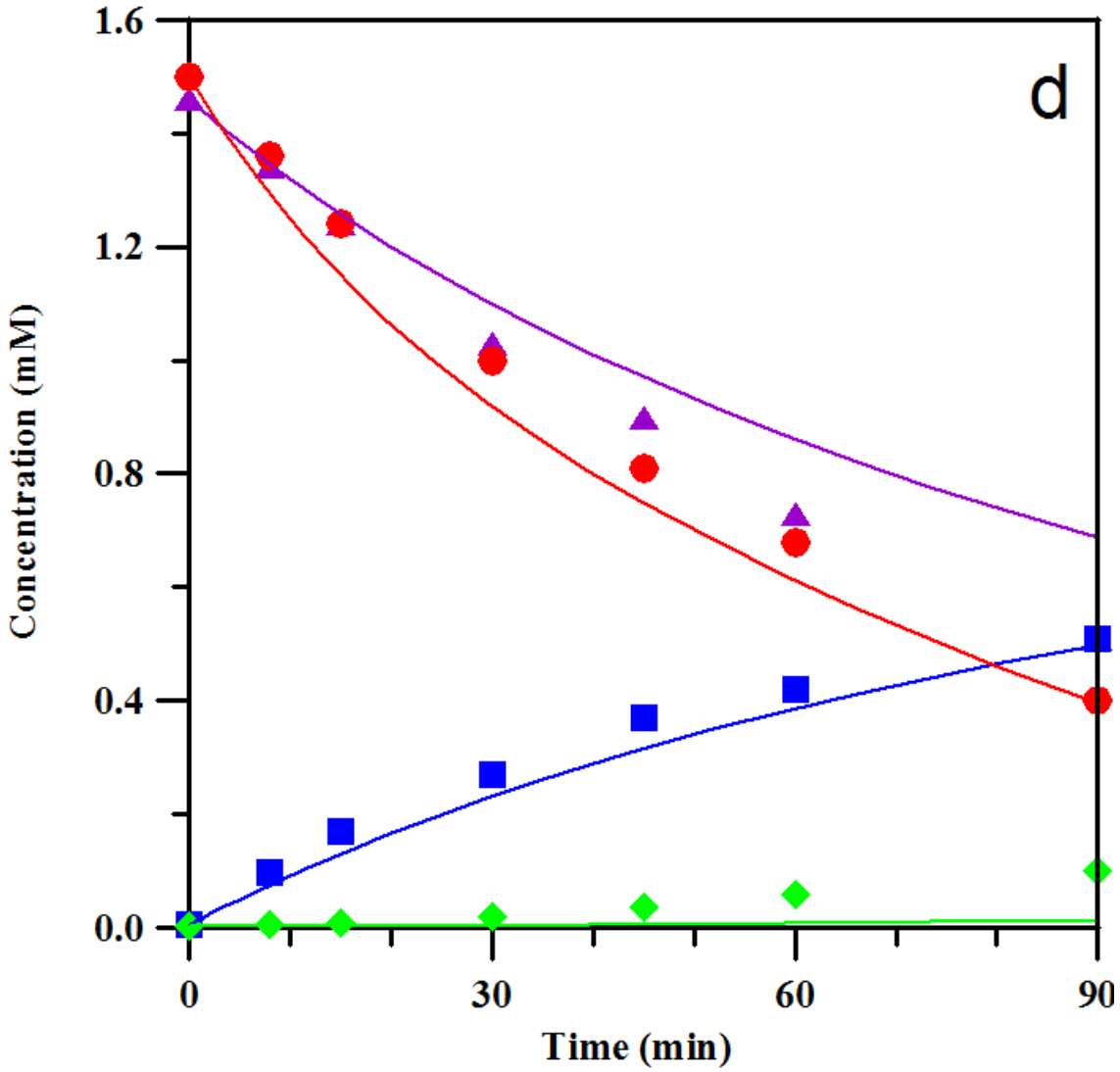

Fig. 46d Predicted (solid lines) and experimental (symbols) concentration-time profile for BA selective oxidation.

pH = 2.0. T = 25 °C. m_{TiO_2}=56.6 mg.

$[BA]_0$ = 1.46 mM, $[Cu(II)]_0$ = 1.50 mM, $[BC]_0$ = 10.75 mM

BA: —▲—,Cu(II): —●—, BHA: —■—, BAC: —◆—.

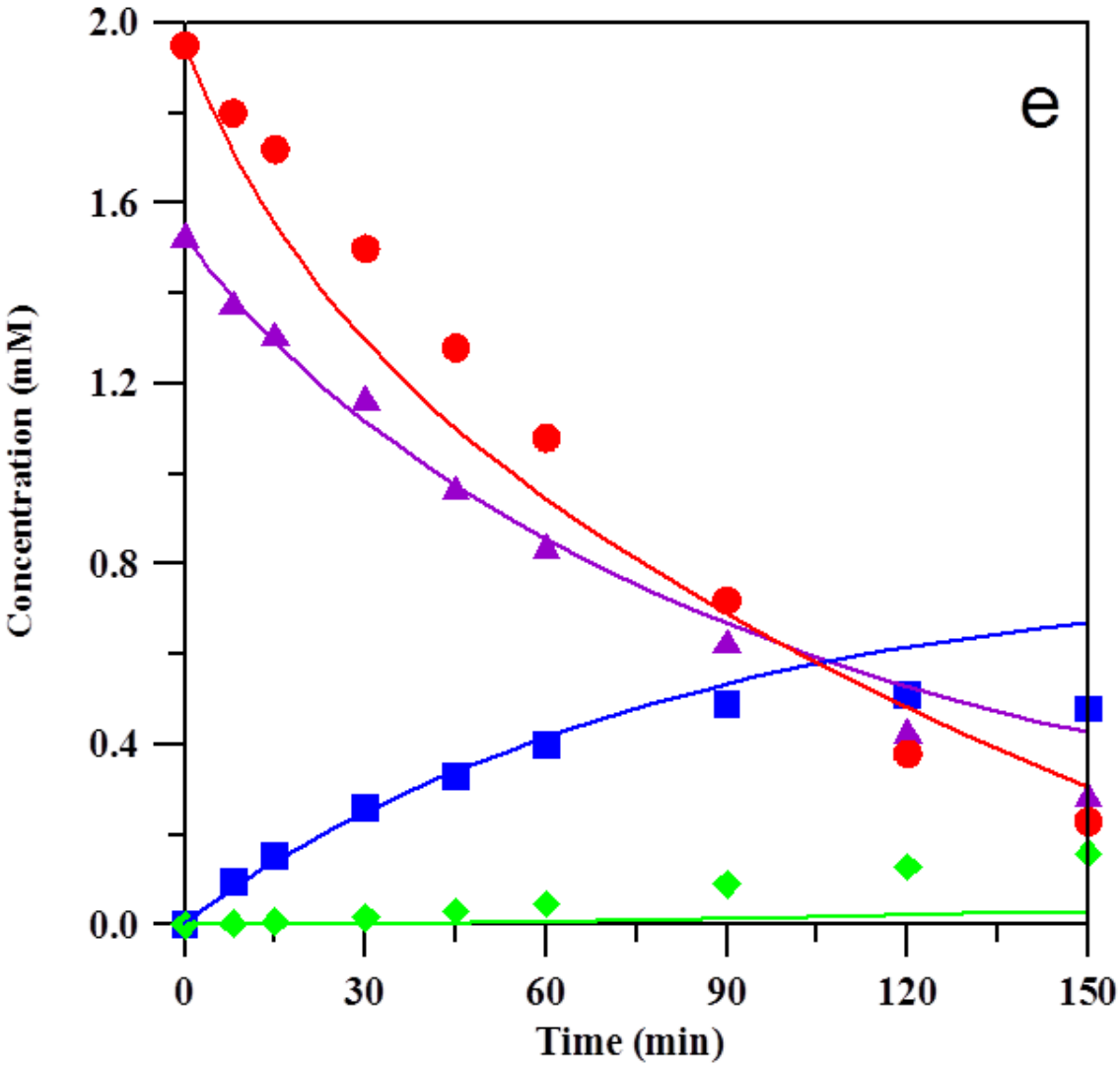

Fig. 46e Predicted (solid lines) and experimental (symbols) concentration-time profile for BA selective oxidation.

pH = 2.0. T = 25 °C. m_{TiO_2}=56.6 mg.

$[BA]_0$ = 1.53 mM, $[Cu(II)]_0$ = 1.95 mM, $[BC]_0$ = 10.98 mM

BA: —▲—,Cu(II): —●—, BHA: —■—, BAC: —◆—.

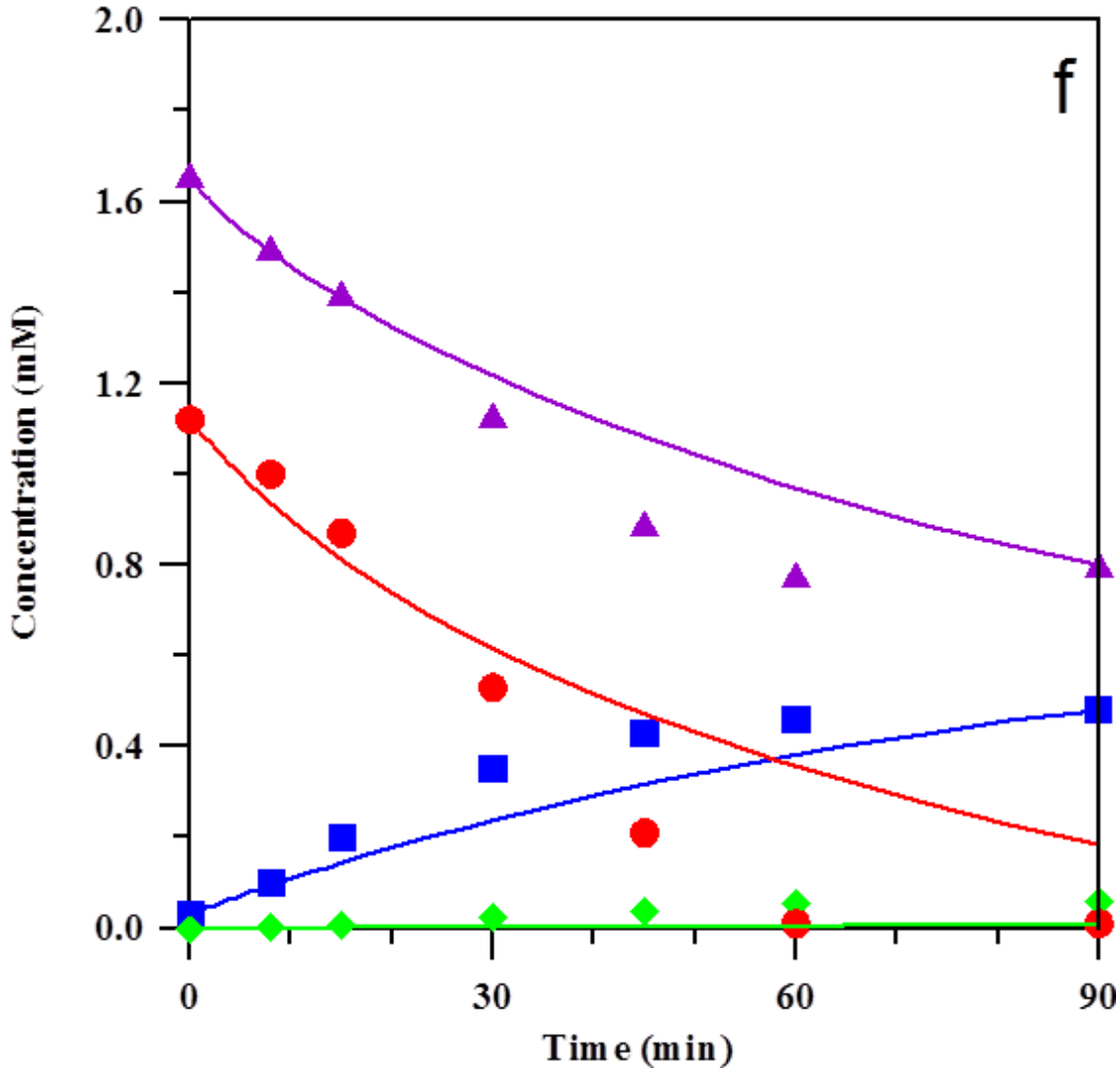

Fig. 46f Predicted (solid lines) and experimental (symbols) concentration-time profile for BA selective oxidation.

pH = 2.0. T = 25 °C. m_{TiO_2}=56.6 mg.

$[BA]_0$ = 1.66 mM, $[Cu(II)]_0$ = 1.12 mM, $[BC]_0$ = 10.56 mM

BA: —▲—,Cu(II): —●—, BHA: —■—, BAC: —◆—.

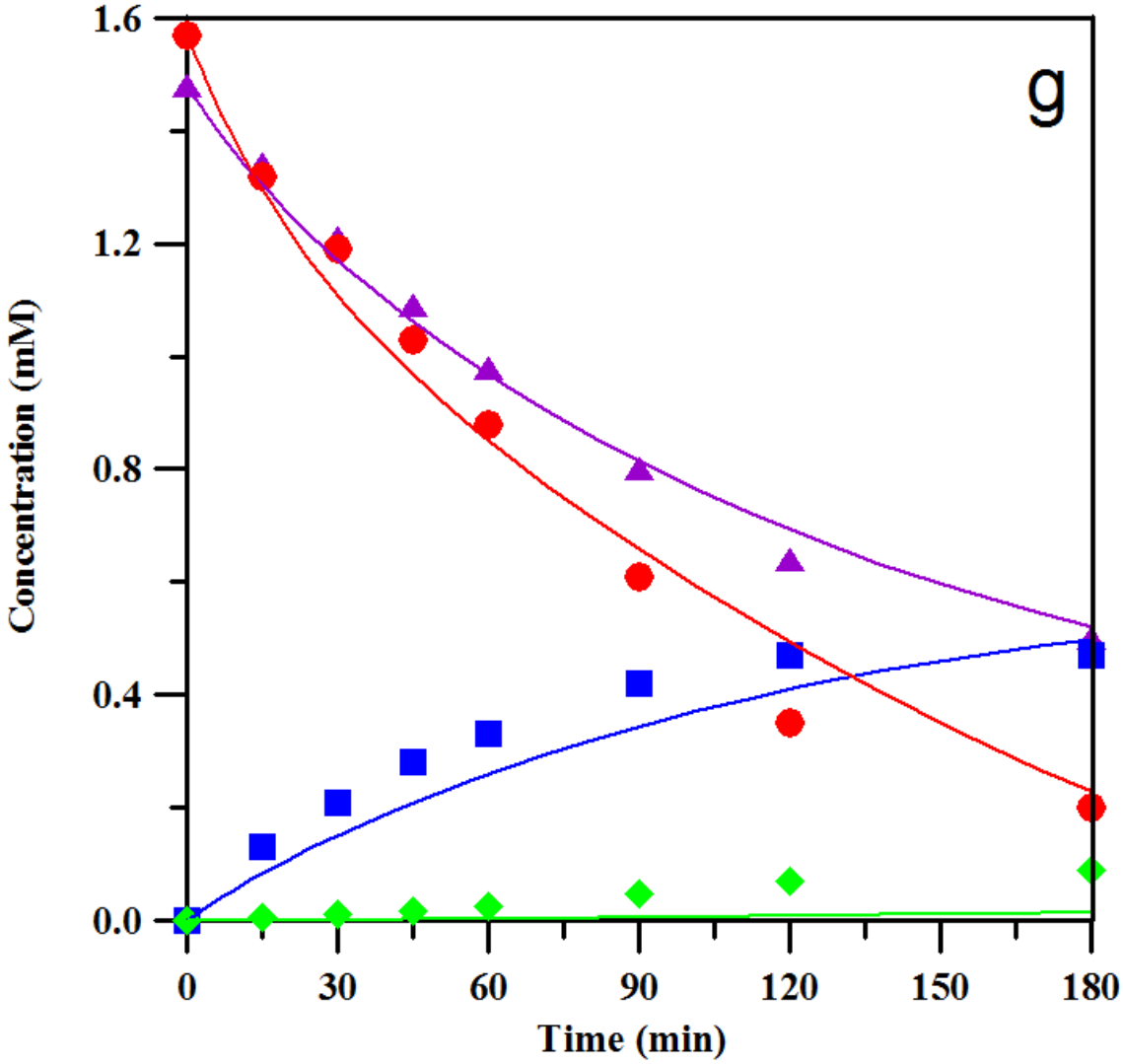

Fig. 46g Predicted (solid lines) and experimental (symbols) concentration-time profile for BA selective oxidation.

pH = 2.0. T = 25 °C. m_{TiO_2}=28.1 mg.

$[BA]_0$ = 1.48 mM, $[Cu(II)]_0$ = 1.57 mM, $[BC]_0$ = 10.79 mM

BA: —▲—,Cu(II): —●—, BHA: —■—, BAC: —◆—.

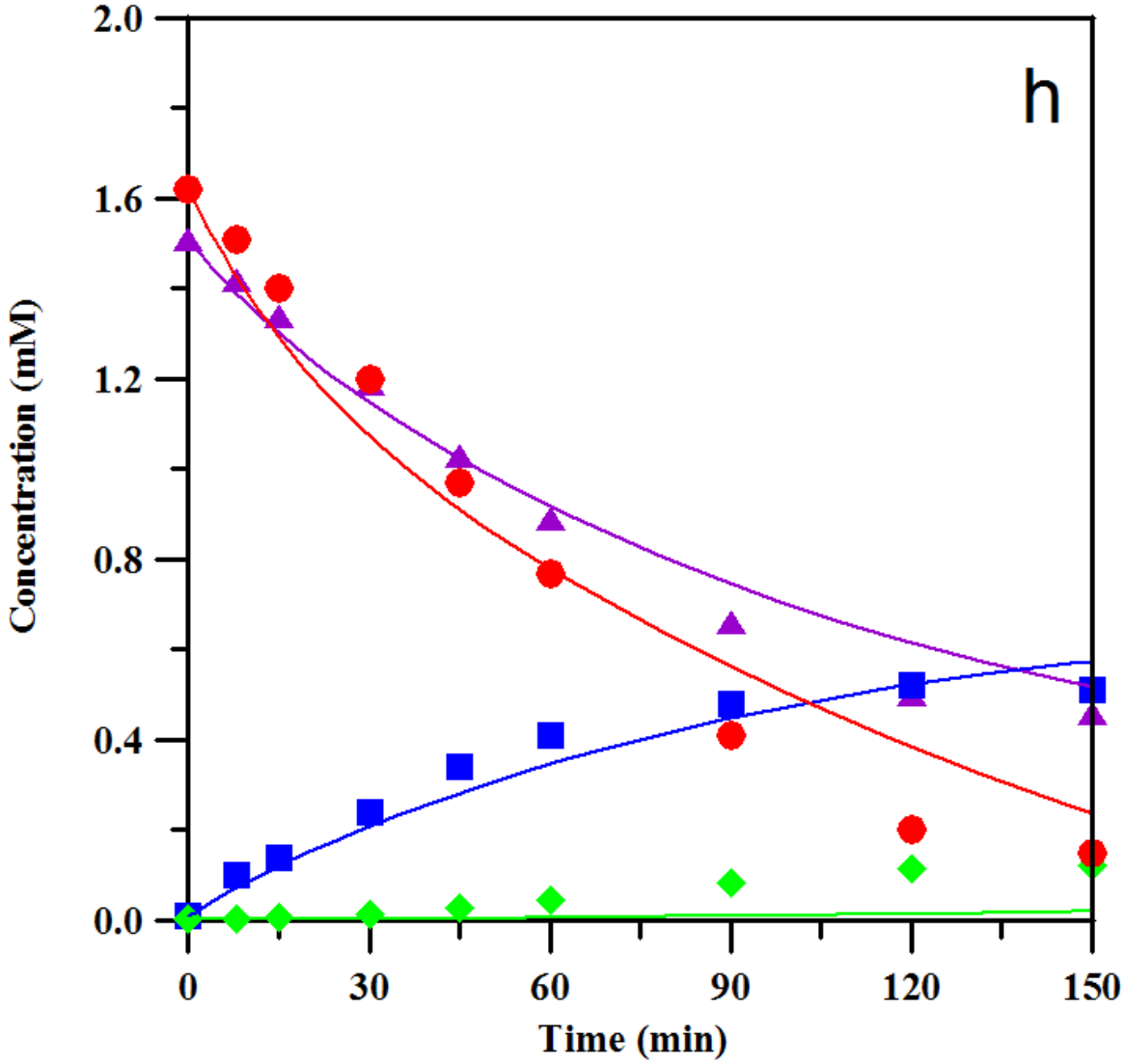

Fig. 46h Predicted (solid lines) and experimental (symbols) concentration-time profile for BA selective oxidation.

pH = 2.0. T = 25 °C. m_{TiO_2}=42.5 mg.

$[BA]_0$ = 1.51 mM, $[Cu(II)]_0$ = 1.62 mM, $[BC]_0$ = 10.81 mM

BA: —▲—,Cu(II): —●—, BHA: —■—, BAC: —◆—.

5.4 Summary

The TiO_2 photocatalytic selective oxidation of benzyl alcohol to benzaldehyde and benzaldehyde to benzoic acid in the presence of cupric ions in water, at pH = 2.0, under deareated conditions has been investigated aiming at clarifying the reaction mechanism.

A reaction mechanism with competitive adsorption has been proposed in which the aromatic substrates get adsorbed by TiO_2 surface and react with the positive holes. Whereas, Cu(II) ions are reduced to Cu(0) by the photogenerated electrons.

According to the proposed reaction scheme, a Langmuir–Hinshelwood kinetic model, not previously reported, has been proposed by writing a set of mass balance equations for the main species involved in the photocatalytic oxidation process.

The resulting mathematical model has been tested by using the data collected at different starting substrates concentrations and resulted capable to predict satisfactorily the concentrations of Cu(II) species and organic substrates during the selective photo-oxidation process.

The effect of SO_4^{2-} and $H_2PO_4^-$ species, which compete with benzyl alcohol for the reaction with positive holes on the catalyst and behave as scavengers towards surface HO radicals, has been included in the model.

The values of the rate constants of reactions of the holes with benzyl alcohol ($k_{BA/h}$), benzaldehyde ($k_{BHA/h}$), Cu(I) species ($k_{Cu(I)/h}$), and inorganic (SO_4^{2-} and $H_2PO_4^-$) anions ($k_{BC/h}$) have been estimated by a proper optimizing procedure. The following values ($M^{-1} \cdot s^{-1}$) have been respectively found: $k_{BA/h} = 3.80 \cdot 10^5 \pm 3.25 \cdot 10^3$, $k_{BHA/h} = 3.00 \cdot 10^4 \pm 3.15 \cdot 10^3$, $k_{Cu(I)/h} = 4.65 \cdot 10^3 \pm 9.52 \cdot 10^2$, and $k_{BC/h} = 1.47 \cdot 10^6 \pm 4.33 \cdot 10^5$.

The optimized value for the adsorption equilibrium constant for the pseudo-component BC ($K_{BC} = 95.3 \pm 24.3\ M^{-1}$) is close to that reported in the literature for the adsorption of sulfate ions on pure anatase TiO_2.

In conclusion, the developed model validates the main reactions previously considered on a qualitative approach and may be used for the performance prediction of a TiO_2-photocatalitic oxidation process of aromatic alcohols in water and in presence of cupric ions.

6 EFFECT OF THE STRUCTURE OF THE ORGANIC SUBSTRATE

In the present chapter, the investigations of the capability of TiO_2/Cu(II)/hv system to promote a selective TiO_2 photo-oxidation of some substituted benzyl alcohols in water, in absence of oxygen, is reported. In particular, the effect of the chemical structure of the substrates has been studied on the selectivity for partial oxidation to the corresponding substituted benzaldehyde. The choice of the species under examination has been based on some reports indicating an effect of ring substituents on the selectivity to the desired products during TiO_2-photoxidation[49,75]. With this aim, attention has been focused on TiO_2 photo-oxidation of benzyl alcohol, hydroxybenzyl alcohols (ortho (2HBA), meta (3HBA) and para (4HBA) isomers), 4-nitrobenzyl alcohol (4NBA), and methoxybenzyl alcohols (ortho (2MBA) and para (4MBA) isomers) into the corresponding aldehydes and acids, adopting the same optimal experimental condition found as in the fourth chapter: pH = 2.0 (with H_3PO_4), TiO_2 (Aldrich pure anatase) load = 200 mg/L. Cu(II) ions have been introduced in the reactive solution as cupric sulfate pentahydrate ($CuSO_4 \cdot 5H_2O$). In these studies, the batch anular glass reactor, described in the third chapter (figure 29), has been used.

6.1 Oxidation of hydroxybenzyl alcohols (HBAs)

The photocatalytic oxidation of hydroxybenzyl alcohols to the corresponding aldehydes proceeded with lower conversions and selectivities than those obtained with aqueous solutions containing benzyl alcohol (BA) as substrate (figure 47a and b) under the same operating conditions. From figures 47a and b, it is clear that the photoreactivity of the investigated alcohols follows the sequence: BA > 3HBA > 2HBA ≈ 4HBA. The profiles of the concentration of cupric ions and hydroxybenzoic acids during the photocatalytic oxidation of the different substrates are shown in figures 48a and b. It is immediately evident from these diagrams that the reactivity for the photoreduction Cu(II) ions (figure 48a) follows the same sequence reported for alcohol consumption (figure 47a).

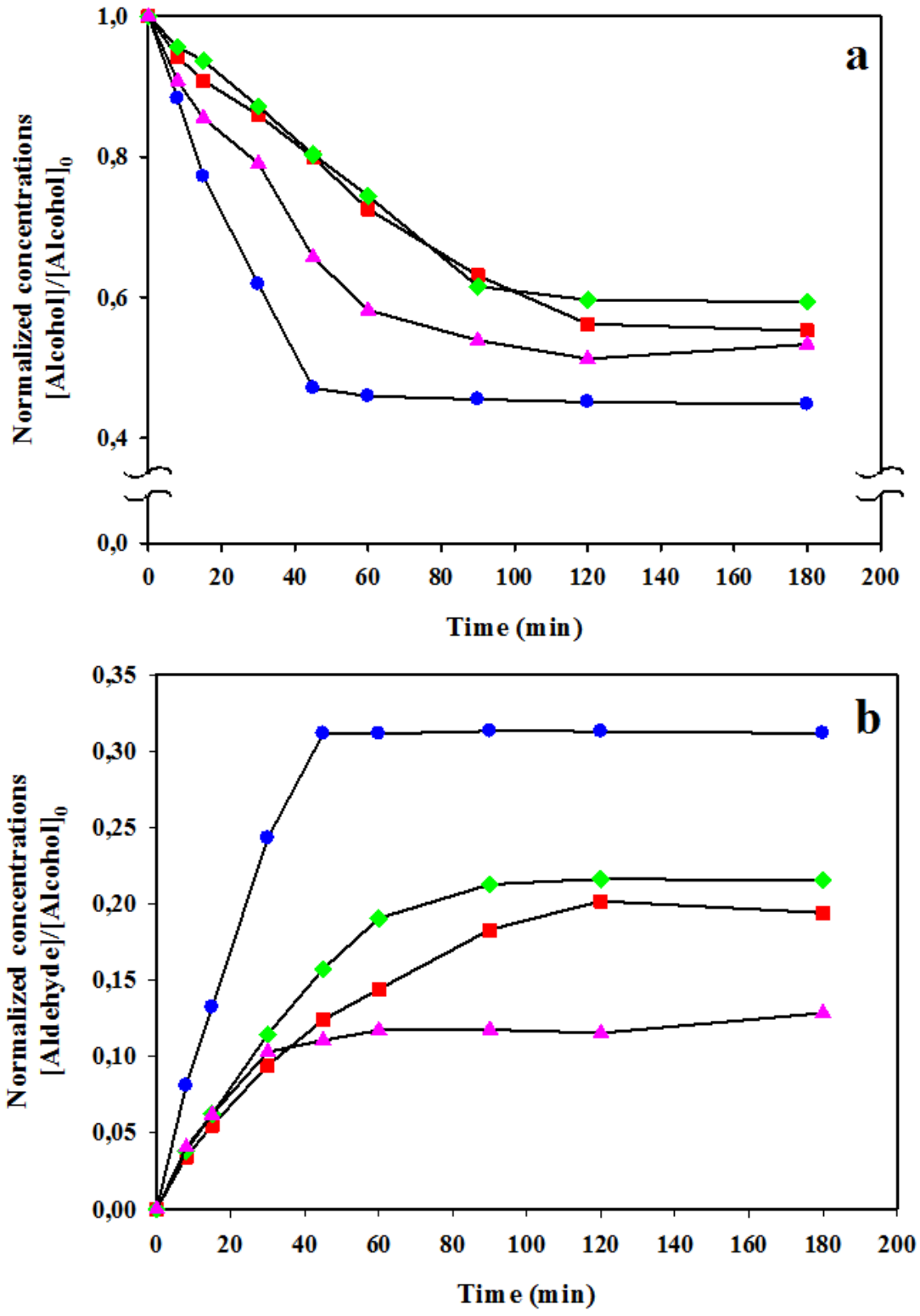

Fig. 47 Benzyl and Hydroxybenzyl alcohol photo-oxidation: conversion of Benzyl and Hydroxybenzyl alcohols (a) production of Benzaldehyde and Hydroxybenzaldehydes (b). $[Cu(II)]_0$ = 0.50 mM. $[Alcohol]_0$ = 0.50 mM. pH = 2.0. T = 25 °C. TiO_2 (Aldrich, pure anatase) = 200 mg/L.

● BA-BHA. ■ 2HBA-2HBHA. ▲ 3HBA-3HBHA. ◆ 4HBA-4HBHA.

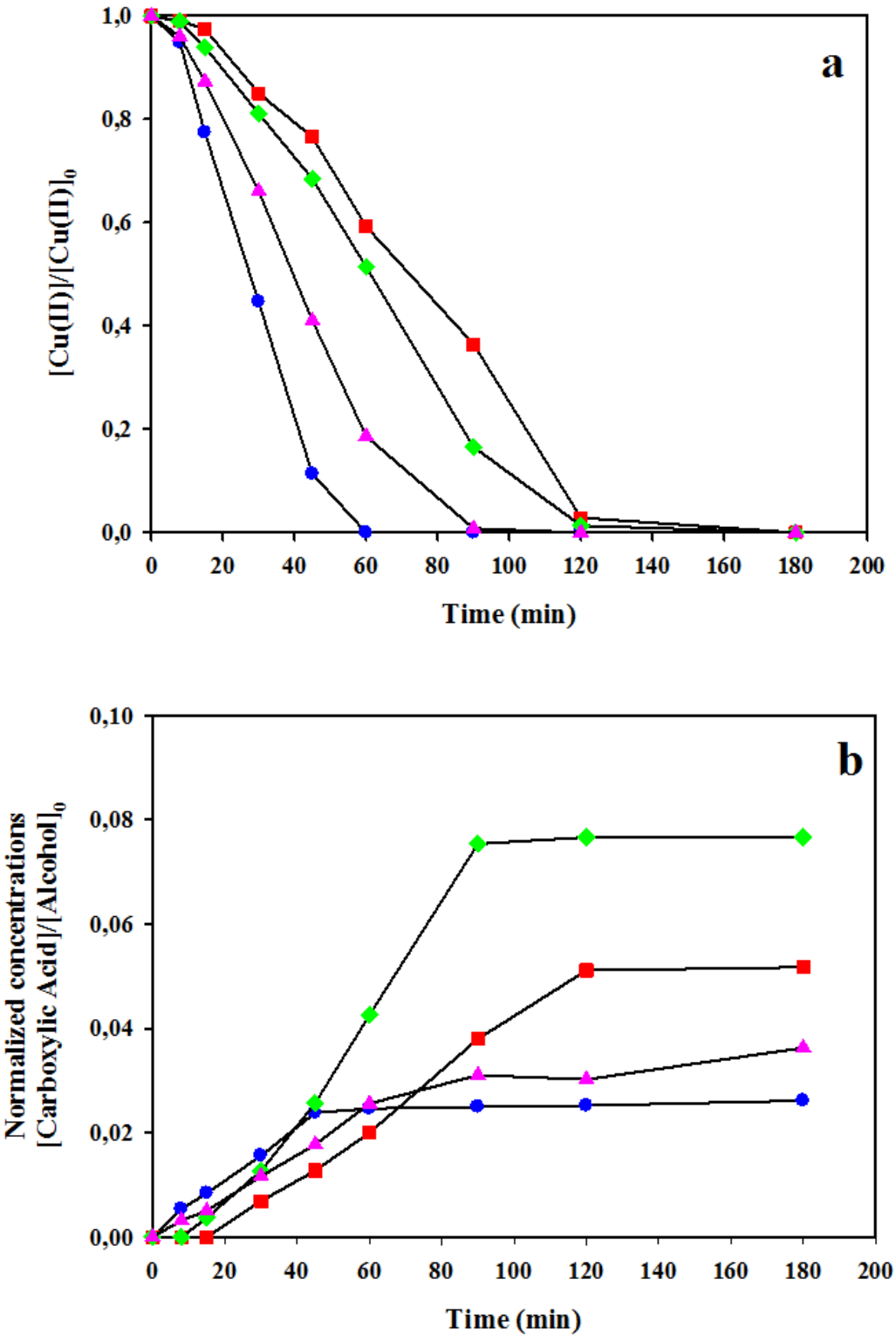

Fig. 48 Benzyl and Hydroxybenzyl alcohol photo-oxidation: Cu(II) reduction (a) production of Benzoic and Hydroxybenzoic acids (b).

$[Cu(II)]_0$ = 0.50 mM. $[Alcohol]_0$ = 0.50 mM. pH = 2.0. T = 25 °C.

TiO_2 (Aldrich, pure anatase) = 200 mg/L.

● Cu(II)-BAC. ■ Cu(II)-2HBAC. ▲ Cu(II)-3HBAC. ◆ Cu(II)-4HBAC.

When Cu(II) species was completely reduced into Cu(0), i.e. at 60 min for BzA, 90 min for 3HBzA, and 120 min for 2HBzA and 4HBzA, no further consumption of alcohols (figure 47a) nor production of both aldehydes and benzoic acid derivatives was observed (figure 47b and 48b).

In particular, when all cupric ions have been reduced to Cu(0), the oxidation stopped and conversions percentages of 55.5 % of BA, 48.2 % of 3HBA, 42.1% of 4HBA and 44.1% of 2HBA have been recorded.

The oxidation yields to the corresponding aldehydes, estimated at reaction times where complete reduction of cupric ions into Cu(0) has been observed, equal to 31.3% (BHA), 21.6% 4-hydroxybenzaldehyde (4HBHA), 11.5% 3-hydroxybenzaldehyde (3HBHA) and 20.2% 2-hydroxybenzaldehyde (2HBHA) have been found (figure 47b). The results, reported in figure 48b, indicate that the investigated system is capable of partially converting the aldehydes to the corresponding carboxylic acids. The oxidation yields to hydroxybenzoic acids are higher for all hydroxybenzyl alcohols (2HBA, 3HBA and 4HBA) than that of BA to benzoic acid (BAC).

A possible explanation of the observed trend in the oxidation reactivity can be given on the basis of some indications reported in the literature[95]. It has been demonstrated that benzoquinone is present in the reacting medium during hydroquinone photodegradation promoted by TiO_2. In particular, benzoquinone is reported to form, as a result of hydroquinone oxidation by the positive holes h^+_{VB}, and to reduce to the latter by the photo-generated electrons (e^-_{CB}), as reported in figure 49:

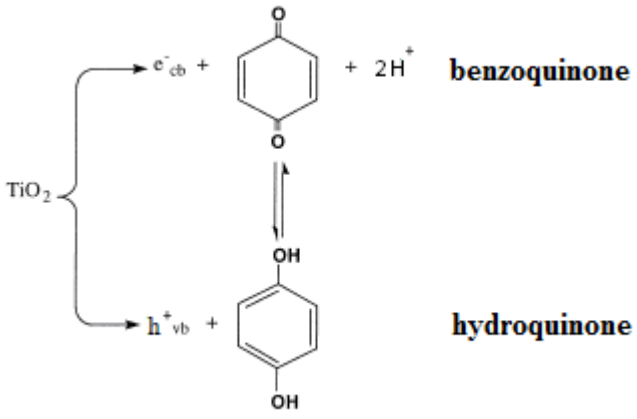

Fig. 49 Keto-enolic oxy-reductive tautomerism of hydroquinone

This effect, well-known as the keto-enolic oxy-reductive tautomerism of hydroquinone, reduces the concentration of the substrate in the reacting solution and considerably diminishes the rate of its degradation. The delay in the selective TiO_2 photo-oxidation of 2HBA, 3HBA, and 4HBA with respect to BA can then be ascribed to the possibility of establishing, at least for two of the hydroxyl alcohols studied, a keto-enolic oxy-reductive tautomeric equilibrium with the formation of quinone methide species, by analogy to that reported for hydroquinone.

Quinone methides are widely occurring reactive intermediates in the chemistry of phenols and are generated by processes of photoinduced electron transfer involving transient phenolic species.

In detail, for 2HBzA and 4HBzA, a similar reactivity has been recorded. The oxidation of both ortho and para hydroxybenzyl alcohols by two photogenerated h^+_{VB} gives quinone methide species, which react with two photogenerated e^-_{CB} to regenerate the phenolic forms, as reported in figure 50:

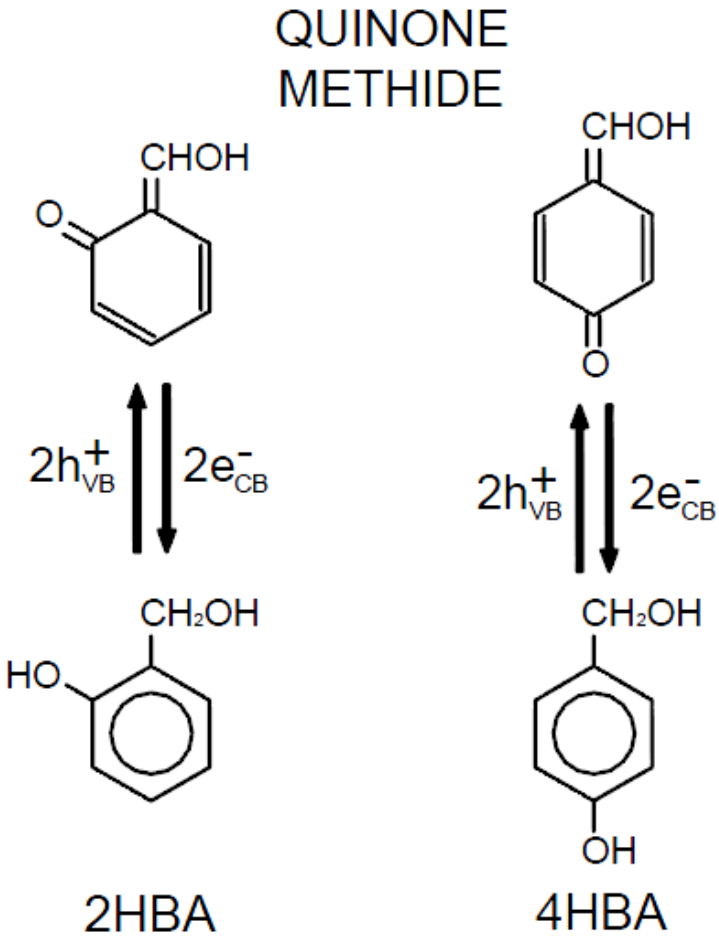

Fig. 50 Keto-enolic oxy-reductive tautomeric equilibrium with the formation of quinone methide species from 2HBA and 4HBA.

Since for 3HBA, a higher reactivity than that of 2HBA and 4HBA but lower than that of BA was observed, a slightly different explanation can be found. In this case, a consideration of structure indicates that its oxidation involves only one photogenerated hole with the formation of aromatic radical species which, capturing one electron from the conducting band of TiO_2, gives rise to the equilibrium shown in figure 51.

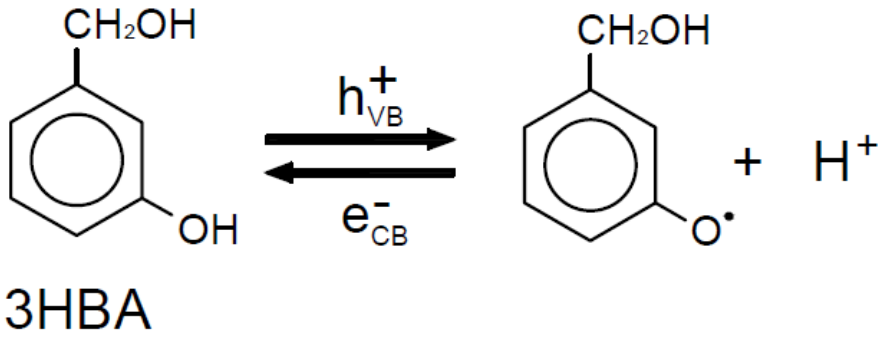

Fig. 51

Since no quinonic form can be written for the radical species at the right side of the last reaction, it can be concluded that its stability is lower than that of the quinone methide of 4HBA and 2HBA.

Therefore, it can be expected that in the case of the last two species, when they undergo photocatalytic oxidation, the fraction present in the solution as free alcohol is lower than in the case of 3HBzA, thus showing reactivity lower than that recorded for the latter. On the other hand, the reactivities of all three substrates (2HBA, 3HBA and 4HBA) are always lower than that of BzA since it can neither be involved in a keto-enolic oxy-reductive tautomeric equilibrium nor in one similar to that reported for 3HBzA. The observed lower photoreactivity of hydroxybenzyl alcohols with respect to benzyl alcohols results in the presence of a higher residual Cu(II) concentration, at each reaction time (Fig. 48a), and in a more competitive oxidation reaction of hydroxybenzyl aldehydes to hydroxybenzoic acids (positive holes being for both alcohols and aldehydes the oxidant).

6.2 Oxidation of methoxybenzyl alcohols (MBAs)

In figure 52, the concentration profiles for the consumption of BA, 2MBA, and 4MBA are compared, whereas figure 53 shows the concentration profiles of corresponding aldehydes (BAD, 2MBAD and 4MBAD) and benzoic acids (BAC, 2MBAC and 4MBAC) generated by their oxidation. A slightly more marked reaction rate (only for 4MBA) and conversion degrees (for both methoxybenzyl alcohol isomers) have been recorded relative to benzyl alcohol.

Similar results have been previously observed for 4MBA only[48] and ascribed to the presence of methoxy group on the aromatic ring, an electron-donor substituent favoring the abstraction of an electron in the OH group by a positive hole. Nevertheless, the higher consumption of 2MBA and 4MBA does not result in higher yields to the corresponding aldehydes (2MBHA and 4MBHA) than BHA. Whereas, further oxidation of the last species forms the related acid derivatives, i.e. 2MBAC and 4MBAC, in concentrations equal or higher than that of BAC produced by the BAD photo-oxidation. In particular, for 2MBHA (solid green squares in figure 53), after 60 min treatment, its concentration rapidly decreases.

Separate experiments (figure 54) demonstrated that this species undergoes a direct photolysis (only UV), not resulting in the production of 2MBAC, which explains its partial degradation during the selective oxidation of 2MBA. On the other hand, no evidence of consumption for direct photolysis has been recorded for 4MBHA (data not shown). Whereas, a more pronounced conversion is obtained for the latter than for BHA to the carboxylic acids (figure 54). This is probably due to the electron-donating effect of the methoxy group on the aromatic ring which favours the reaction with the positive holes.

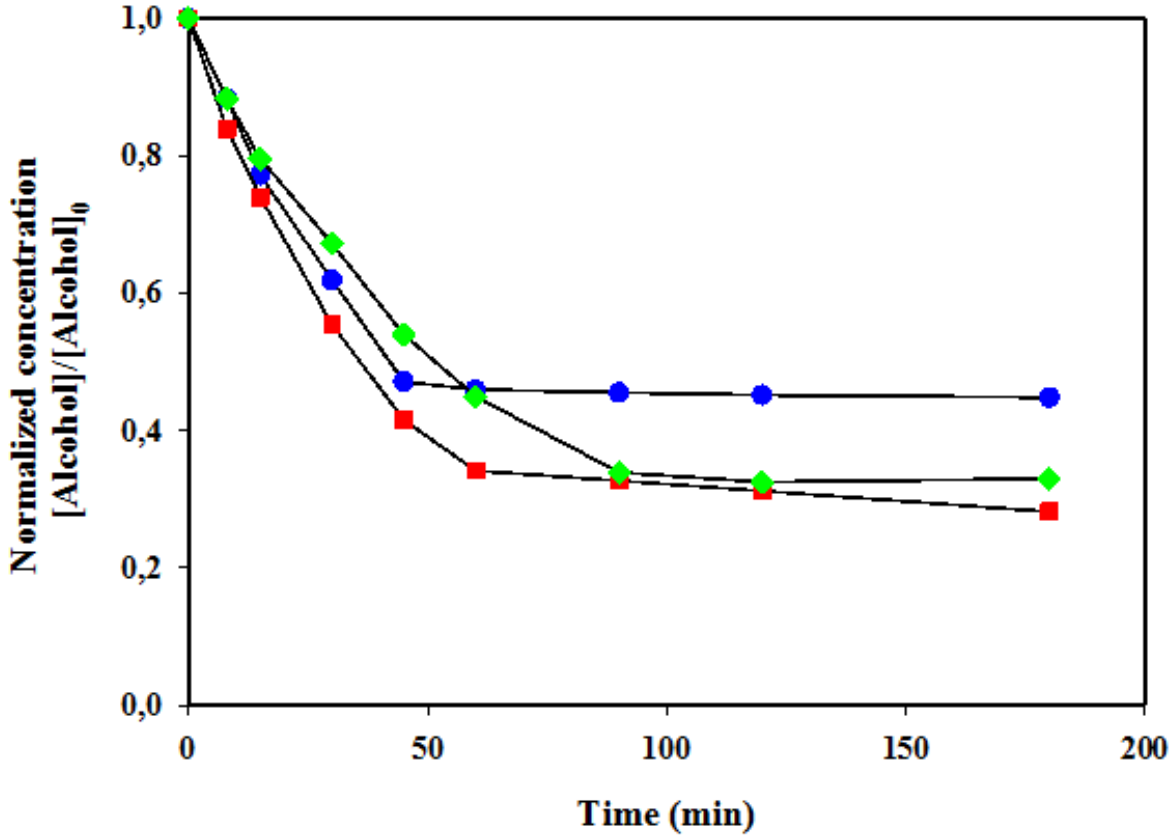

Fig. 52 Photo-oxidation of Benzyl and Methoxy benzyl alcohols: Benzyl and Methoxybenzyl alcohol conversion.

$[Cu(II)]_0$ = 0.50 mM. $[Alcohol]_0$ = 0.50 mM. pH = 2.0. T = 25 °C.

TiO_2 (Aldrich, pure anatase) = 200 mg/L.

● BA, ♦ 2MBA, ■ 4MBA

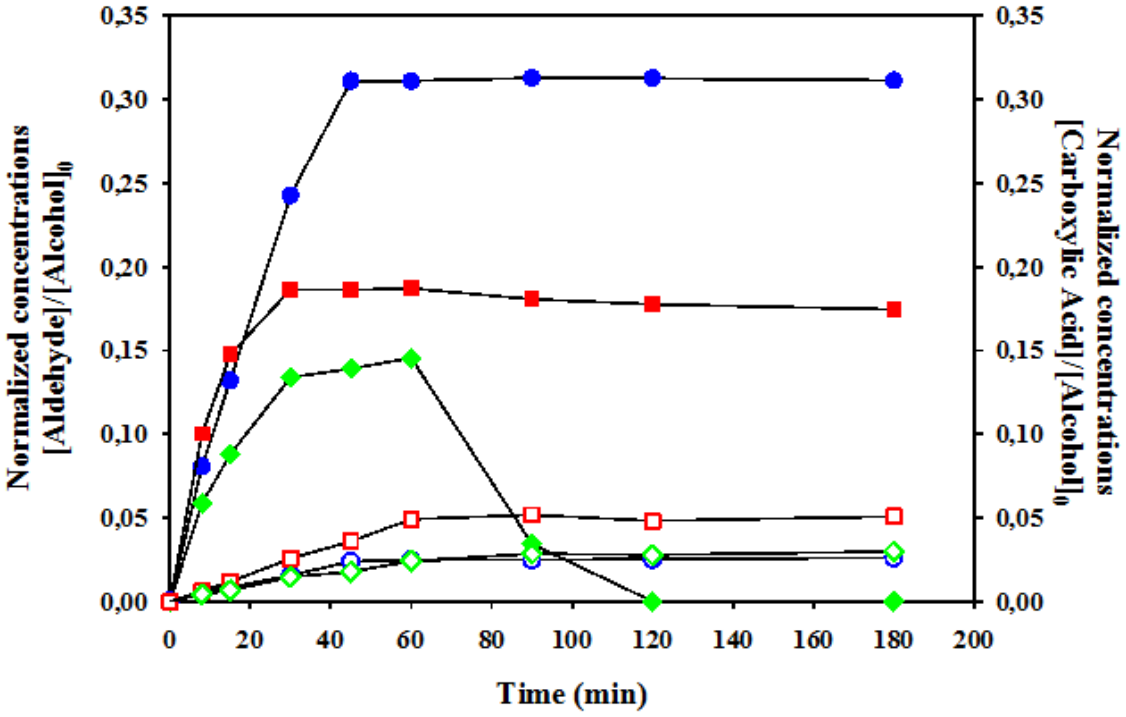

Fig. 53 Photo-oxidation of Benzyl and Methoxy benzyl alcohols: Benzaldehyde and Methoxybenzaldehydes yeld (full symbols) and Benzoic and Methoxybenzoic acids production (empty symbols).

$[Cu(II)]_0$ = 0.50 mM. $[Alcohol]_0$ = 0.50 mM. pH = 2.0. T = 25 °C.

TiO_2 (Aldrich, pure anatase) = 200 mg/L.

●,○: BHA, BAC. ◆,◇: 2MBHA, 2MBAC. ■,□: 4MBHA, 4MBAC.

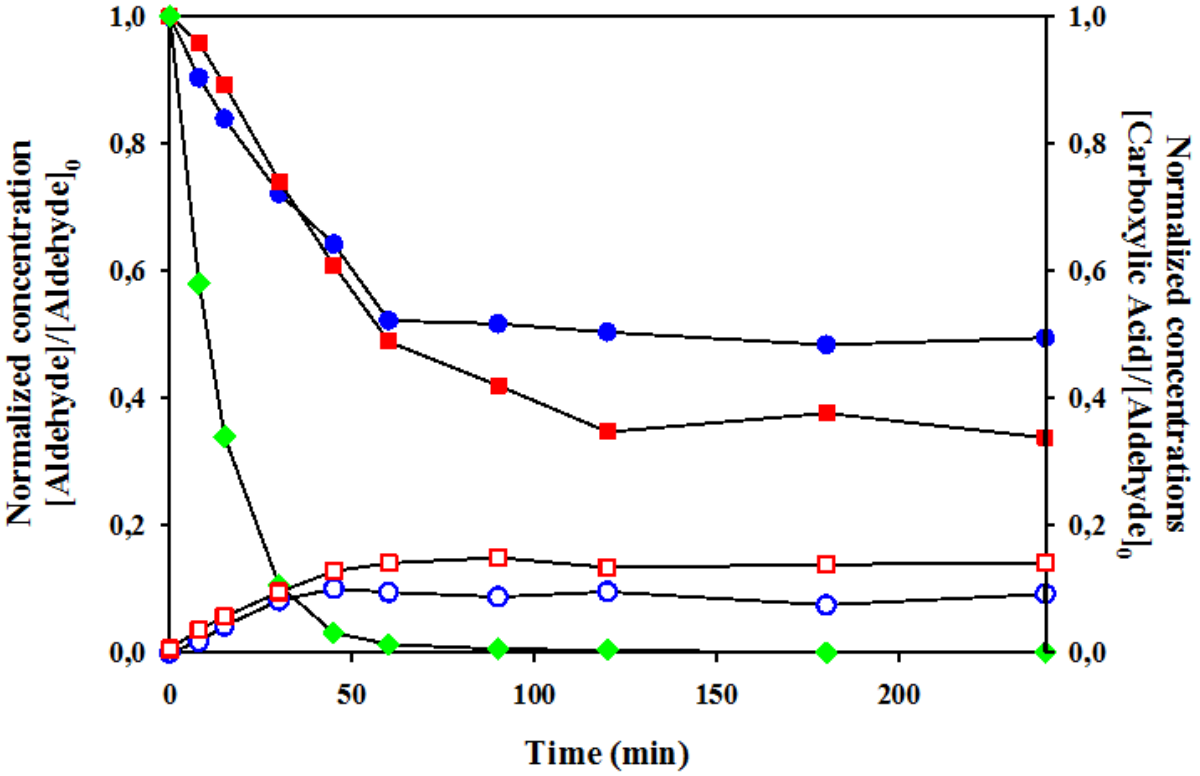

Fig. 54 Photo-oxidation of methoxybenzyl aldehydes under deaerated conditions: aldehydes decay (full symbols) and carboxylic acids (empty symbols) production.

Direct solar photolysis (without TiO_2 and Cu(II) and with $[2MBHA]_0$ = 0.50 mM):

◆ 2MBHA

Photo-oxidation by TiO_2/Cu((II)/hν system:

$[Cu(II)]_0$ = 0.50 mM. $[BHA]_0$ = $[BHA]_0$ = 0.50 mM. pH = 2.0. T = 25 °C.

TiO_2 (Aldrich, pure anatase) = 200 mg/L.

●,○: BHA, BAC. ■,□: 2MBHA, 2MBAC.

6.3 Oxidation of 4-nitrobenzyl alcohol (4NBA)

The concentration profiles for the oxidation of 4NBA (full symbols) and the production of 4 nitrobenzaldehyde (4NBHA) (empty symbols) with TiO_2/Cu(II)/hv and TiO_2/hv systems are shown in figure 55.

A rather different behavior of 4NBA substrate has been shown when compared with that of benzyl alcohol (figure 55, crosses). The disappearance of 4NBA proceeded along different pathways, one of which did not require, for its activation, the presence in the reacting solution of Cu(II) and contributing significantly to conversion of the substrate with a low selectivity to 4NBHA.

Although the reaction rate of 4NBA with TiO_2/Cu((II)/solar hν system seems comparable with the reactivity of BA, a detrimental influence due to the electron-withdrawing effect of nitro ($-NO_2$) group present on the aromatic ring[46] cannot be ruled out since it was clear that the rate of disappearance of 4NBA was strongly sustained by its photodecay in the presence of the sole TiO_2/solar hν.

A low selectivity of 5.2%, for a 50% conversion of the substrate, has been observed in the case of the oxidation of 4NBA into 4NBHA by the system TiO_2/Cu((II)/solar hν. This result is in agreement with those previously reported (3.3–5.3%) by others[46] and can be easily ascribed to the relevance to the disappearance of 4NBA of its photodecay in the presence of only TiO_2 without oxygen (figure 55, red solid squares), which showed negligible selectivity to the corresponding aldehyde (figure 55, red open squares).

Moreover, as reported in figure 56, 4NBHA, which is the desired product, is efficiently photoconverted, with clear production of 4-nitrobenzoic acid (empty symbols), by direct solar photolysis (hv) or TiO_2/hv system, thus indicating the absence of any further relevant effect due to the presence of Cu(II) in the reacting system (solid diamonds).

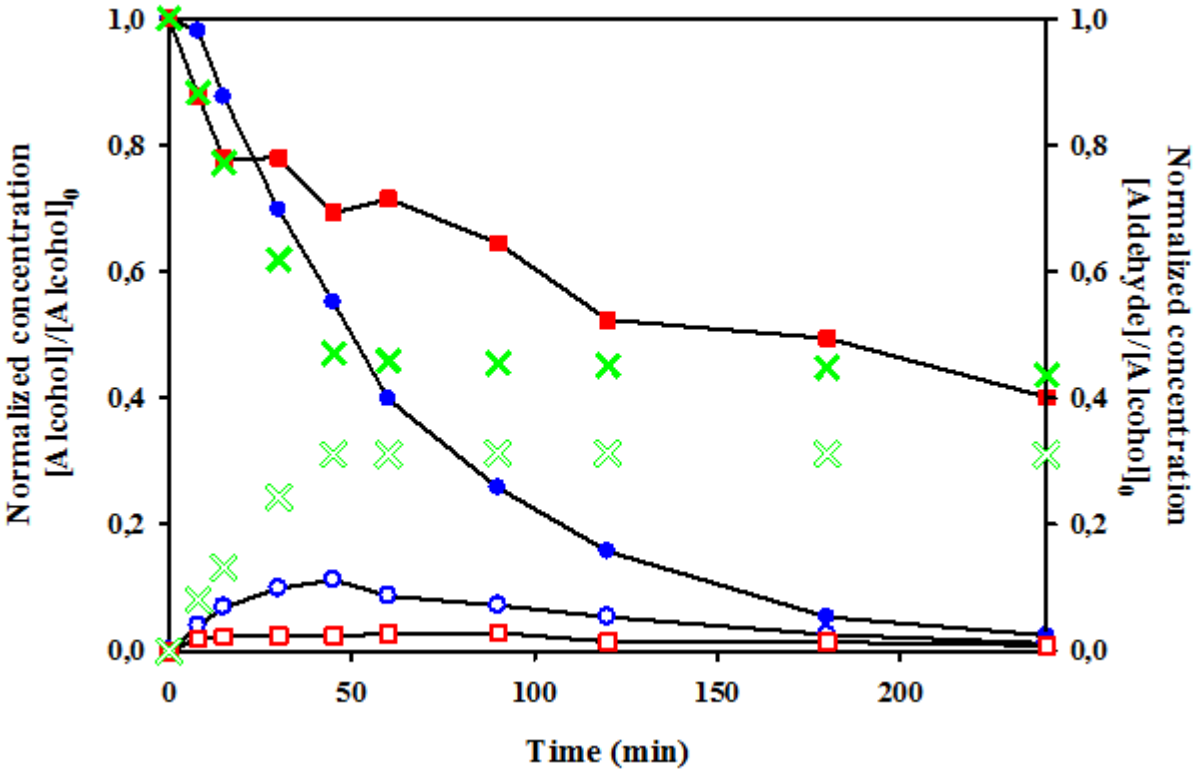

Fig. 55 4-Nitrobenzyl alcohol (4NBA), benzyl alcohol (BA) consumption and 4-nitrobenzaldehyde (4NBHA), benzaldehyde (BHA) formation under deaerated conditions.

TiO_2/Cu(II)/hv system: $[4NBA]_0 = [BzA]_0 = 0.50$ mM. $[Cu(II)]_0 = 0.50$ mM. pH = 2.0. T = 25 °C. TiO_2 (Aldrich, pure anatase) = 200 mg/L.

●, 4NBA; ○, 4NBHA

✖, BA; ⊠, BHA

TiO_2/hv system: $[4NBA]_0 = 0.50$ mM. pH = 2.0. T = 25 °C. TiO_2 (Aldrich, pure anatase) = 200 mg/L.

■, 4NBA; □, 4NBHA

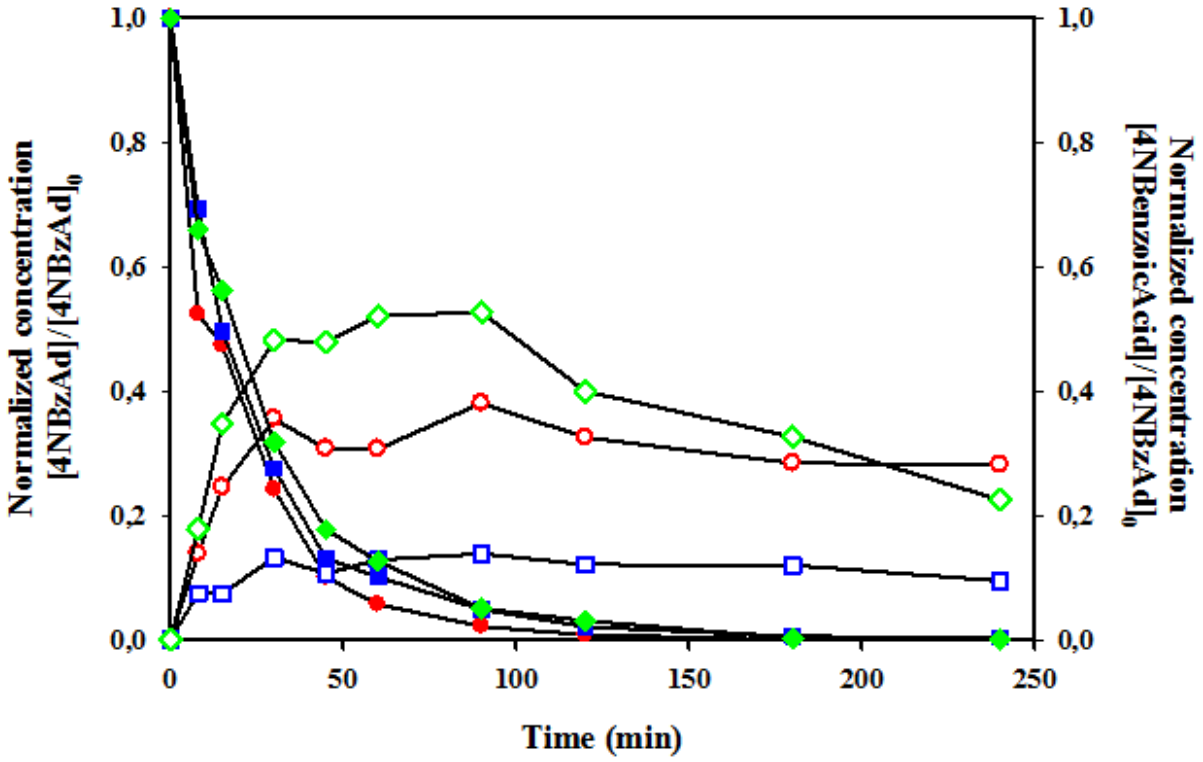

Fig.56 4-Nitrobenzaldehyde (4NBHA) consumption (full symbols) and 4-nitrobenzoic acid (4NBAC) formation (empty symbols) under deaerated conditions.

$[4NBHA]_0$ = 0.50 mM. pH = 2.0; T = 25 °C.

●○: direct solar photolysis;

■□: TiO_2/hv. TiO_2 (Aldrich, pure anatase) = 200 mg/L.

◆◇: TiO_2/Cu(II)/hv. TiO_2 (Aldrich, pure anatase) = 200 mg/L. $[Cu(II)]_0$ = 0.5 mM

On the basis of the previous results and following literature suggestions, the TiO_2 catalytic photo-transformation of 4NBA and 4NBHA with or without Cu(II) can be ascribed to different kinetic contributions (figure 57). First of all, 4NBA can be photoreduced to 4-nitrosobenzyl alcohol (4NsBA) and successively to 4-aminobenzyl alcohol (4ABA) by a transfer of photoinduced electrons (e^-_{CB}) from the TiO_2 surface to 4NBA and 4NsBA. Several Authors have shown that the photoinduced reduction of nitroaromatics by TiO_2 catalyst, under aerated or deaerated conditions, in organic solvents or in acidic aqueous suspension but in the presence of a 'hole scavenger', may be used as an alternative route for fine chemicals production[99-102]. For the system investigated, analytical efforts indicated the presence of small amounts of 4ABA in the reacting solution (data not shown).

Moreover, the irradiation of 4NBA in aqueous media can involve an intramolecular oxidation-reduction (photoredox reaction) in which the nitro group is reduced into nitroso group and concurrently the alcoholic group is oxidized to aldehydic group to give p-nitrosobenzaldehyde (4NsBHA) as the major product[103]. In addition to the photoredox reaction, the same group of Authors, reported that the photolysis of 4NBzA produces a significant amount of azoxyaldehyde (AZOAD), whose presence gives a yellow color to the solution[103] as observed in the present investigation after the photolytic treatment with TiO_2/hv. Since Cu(II) competes with 4NBA and 4NsBA for the reactions with the photogenerated electron, the addition of cupric ions to the reacting solution (TiO_2/Cu((II)/hv) increases the selectivity to 4NBHA , as shown in figure 55. The latter, once formed, reacts (figure 56) following different photoreactive pathways, as shown in the scheme reported in figure 57.

For direct photolysis, without TiO_2 catalyst and Cu(II), 4NBHA is partially converted to 4-nitrobenzoic acid (4NBAC). These results are in agreement with those previously collected by others[104–105] who reported the photo-isomerization of 4NBHA into p-nitrosobenzoic acid (4NsBAC) in water and indicated it as a photoredox reaction. The last one, for direct photolysis, leads, in part, to the formation of 4NBAC.

In presence of TiO_2, 4NsBAC can also be selectively oxidized to 4NBAC, by reacting with the positive hole, as reported by others[106]. On the other hand, the 4NBAC, by reacting with the photogenerated electron, can be reduced to 4NsBAC. For this reason, when TiO_2 is present in reacting solution, the addition of Cu(II) ions results into an increase of selectivity from 4NBHA to 4NBAC due to the fact that Cu(II) competes with 4NBAC for the reaction with the photogenerated electrons.

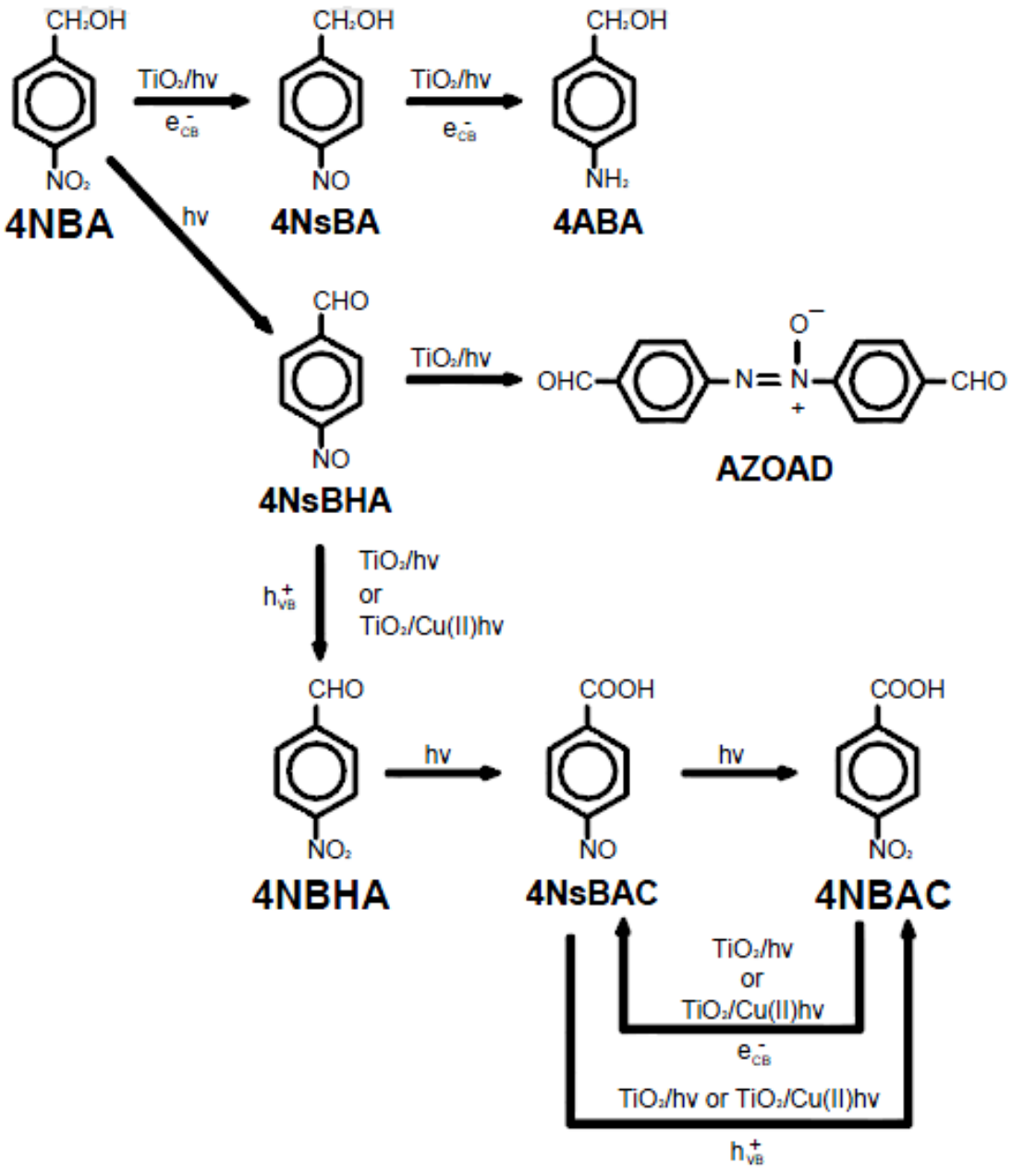

Fig. 57 4NBzA and 4NBzAD phototransformation pathways.

6.4 Summary

In the present work, the possibility of selective oxidation of hydroxybenzyl alcohols (ortho, meta and para isomers), 4-nitrobenzyl alcohol, and methoxybenzyl alcohols (ortho and para isomers) to the corresponding aldehydes in aqueous solution, at room temperature, under acidic (pH = 2.0) and deaerated conditions, has been evaluated using the photocatalytic system TiO_2/Cu(II)/hv system. For each run, at the end of the process, the complete reduction of Cu(II) into Cu(0) has been observed. The presence of a hydroxy, methoxy, or nitro group in the alcohol molecule markedly affects the maximum yield (table 8) of the partial oxidation of the selected substrate. In particular, both electron donating or withdrawing effects of the substituent groups have a detrimental effect on the selectivity of the process with respect to that observed for the unsubstituted benzyl alcohol. A partial conversion of aldehydes into the corresponding benzoic acid derivatives has also been observed. Different reactivities and selectivities to desired products have been registered during the experiments, according to the positions of the substituent group investigated on the aromatic ring. However, the selectivity values, recorded during the present investigation, indicate that the proposed system is a poor tool to achieve selective conversion of the substituted alcohols investigated into the corresponding aldehydes in aqueous solution.

The highest yields in aldehyde among the corresponding alcohol conversions and selectivity values are reported below in table 8, for each substituted benzyl alcohol studied:

	Time (min)	Yield in Aldehyde (%)	Alcohol Conversion (%)	Selectivity (%)
BA	60	31	54	57
2HBA	120	20	44	45
3HBA	90	12	46	26
4HBA	120	22	40	55
2MBA	60	15	55	27
4MBA	30	19	45	42
4NBA	45	11	45	24

Tab.8 Comparison of yield, conversion and selectivity values obtained from the selective oxidation of substituted and unsubstituted benzyl alcohol with TiO_2/Cu(II)/hv system.

7 SCALE UP AND PRECIPITATE CHARACTERIZATION

In the present chapter, the possibility to adopt the TiO_2/Cu(II)/hv system, by direct use of the solar radiation daily arriving on the earth surface, for the selective oxidation of benzyl alcohol to benzaldehyde in water has been taken in consideration. The effect of the solar radiation ($300< \lambda <800$ nm) on the system behaviour has been studied, using the solar photocatalytic pilot plant described in the experimental section (figure 31), at different operating conditions, changing the:

- TiO_2 photocatalyst type;
- Cu(II) initial concentration;
- irradiance of solar radiation.

TiO_2 load and pH values have been fixed (TiO_2 load = 200 mg/L and pH = 2.0) according to those adopted in previous chapters of this thesis and in other studies[107]. H_3PO_4 and $CuSO_4$ have been selected to adjust the pH and used as source of Cu(II) ions respectively.

7.1 Effect of TiO_2 type

The results obtained during different experimental runs of solar photo-oxidation of benzyl alcohol, with two different typologies of commercial TiO_2 samples, at the same load (200 mg/L), are shown in figures 58a and 58b and have been reported in function of the accumulate energy (Q_n).

The runs have been carried out in two consecutive days. At the end of first day, when the reactor has been covered, the UV-irradiances (wavelength 300-400 nm) and temperatures decreased (see figs 58a and 58b). During the runs, measured UV-irradiances approximately ranged between 40 and 50 W/m^2 approximately (fig. 58b, continuous lines).

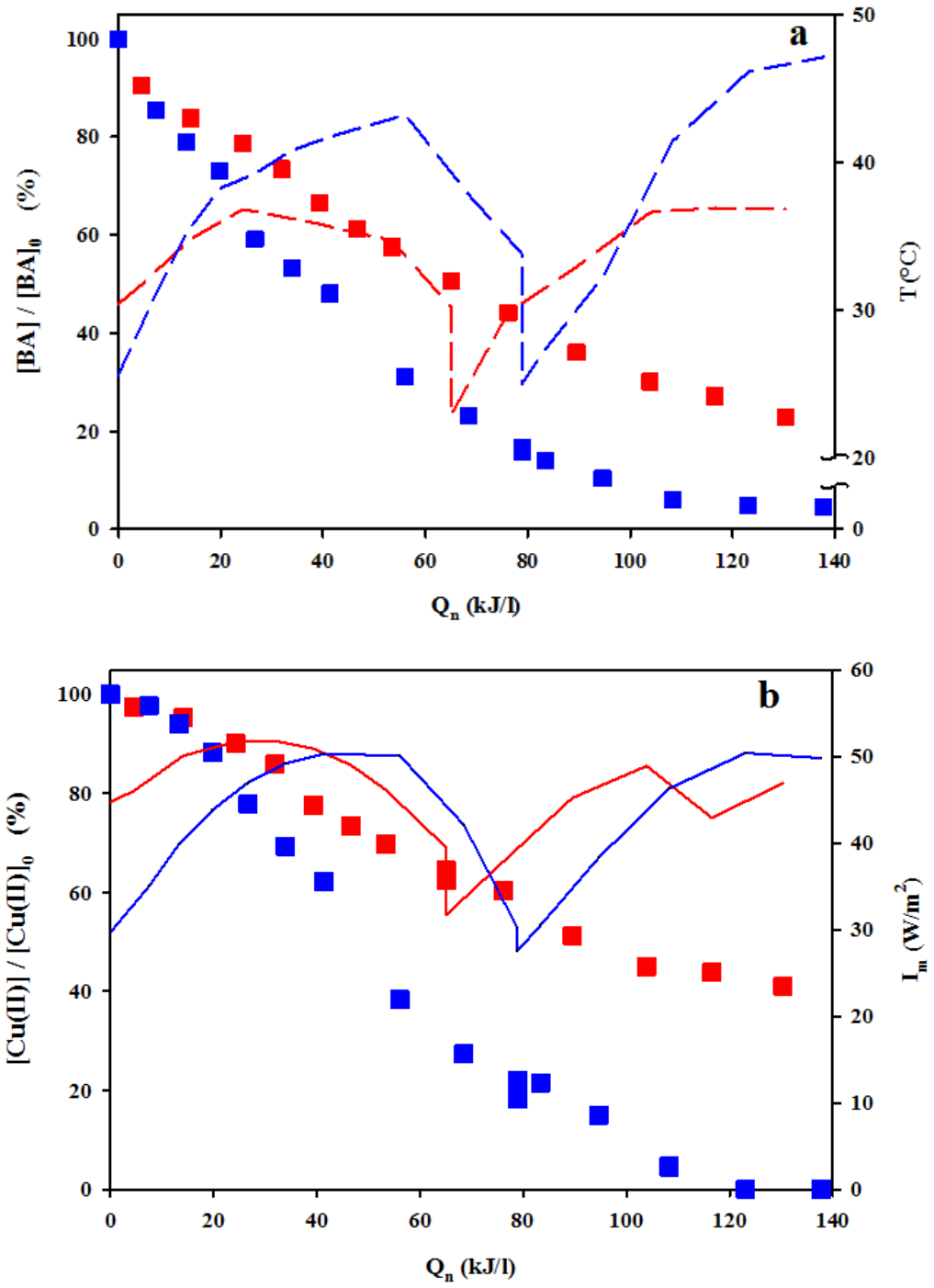

Fig. 58 Effect of TiO_2 type: BA solar photoxidation (squares) and temperatures profiles (dashed lines) (a); Cu(II) solar photoreduction (squares) and UV-irradiance (continuous lines) (b).

$[BA]_o$ = 1.5 mM. $[Cu(II)]_o$ = 1.5 mM. Initial TiO_2 load = 200 mg/L. pH=2.

56a: (■, - - -) Aldrich TiO_2, (■, - - -) P25 Degussa TiO_2.

56b: (■, ——) Aldrich TiO_2, (■, ——) P25 Degussa TiO_2.

As shown in the diagrams, the reactivity of the system is higher when TiO_2 P25 by Degussa is used instead of the TiO_2 Aldrich catalyst. In particular, in presence of P25 Degussa sample (blue symbols), for a Q_n value of 123 kJ/L, the BA concentration approached zero (figure 58a) and Cu(II) ions were totally reduced (figure 58b). Whereas, if Aldrich TiO_2 sample is used (red symbols), about 27% of initial benzyl alcohol and Cu(II) ions were still present in the solution.

The higher reactivity observed for the system in presence of P25 Degussa TiO_2 is in disagreement with the earlier results, reported in the fourth chapter in figures 33 and 35, that show a similar reactivity when P25 Degussa and Aldrich TiO_2 catalysts are used in presence of UV radiation emitted by a laboratory thermostated lamp.

This discrepancy may probably be due to the different emission spectra characterizing the lamp and the sun as well as different light absorption characteristics, in the range of 300-800 nm, of the two used catalysts.

Moreover, the different reactivities, recorded in the solar experiments, could be also attributed to the differences between the averages of the measured temperatures: 38.6 °C and 34.3 °C for runs carried out in presence of Degussa P25 (blue dashed lines) and Aldrich TiO_2 (red dashed lines) catalysts respectively (figure 58a).

As shown in figure 59, the BA solar photocatalytic oxidation resulted in the production of BHA (diamonds), for Aldrich (red symbols) and P25 Degussa (blue symbols) TiO_2 catalysts, and BAC, an undesired product that derives from the reaction between the positive photogenerated holes on the TiO_2 surface and benzaldehyde. BAC yields are also reported in the same figure (triangles). According to previous results, the highest BHA production rates were obtained in presence of P25 Degussa TiO_2. Moreover, for this catalyst, the maximum BAC production rate was reached at the highest yields of BHA.

However, for accumulated energy values higher than 80 kJ/L, when the unconverted BA concentration was less than 20% of its initial concentration (figure 58a, blue squares), a decrease in BHA yield with respect of initial BA amount, from 53.3% to 45.5%, has been observed using P25 Degussa TiO_2 samples. This result can be explained by considering a competition between the BA and BHA molecules in the reaction with the photogenerated positive holes on the TiO_2 surface.

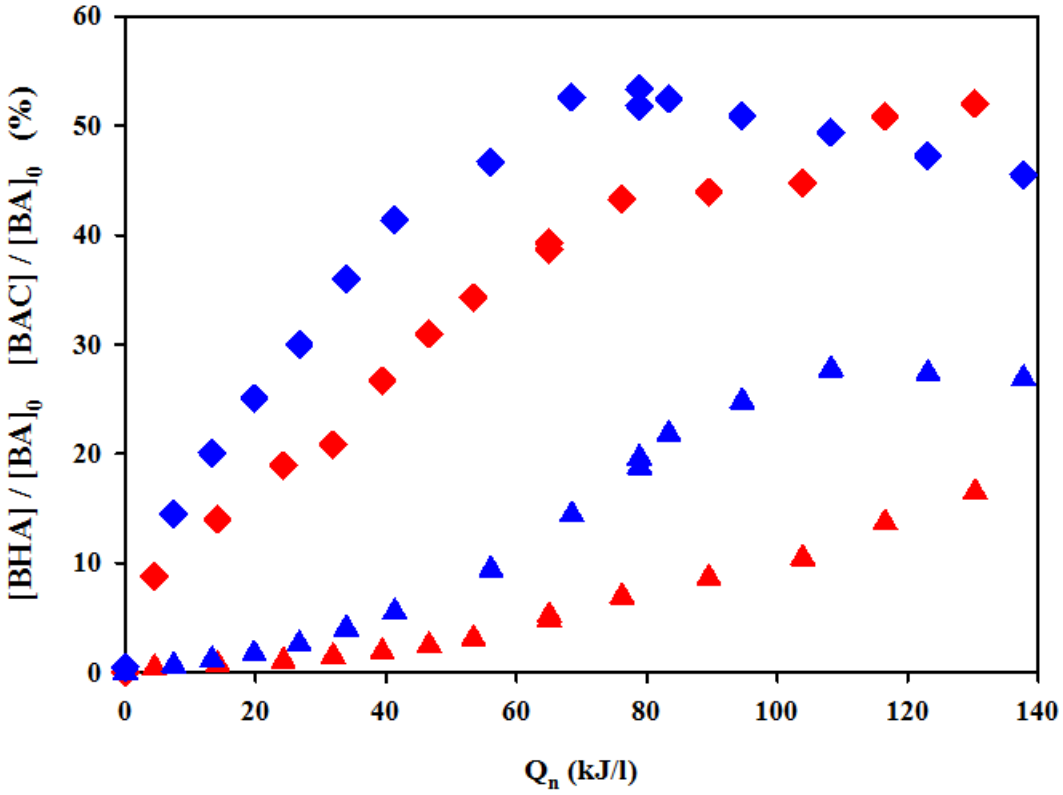

Fig. 59 Effect of TiO_2 type on the BHA and BAC production.

$[BA]_o$ = 1.5 mM. $[Cu(II)]_o$ = 1.5 mM. Initial TiO_2 load = 200 mg/L. pH=2.0.

Aldrich TiO_2: ◆ BHA, ▲ BAC.

P25 Degussa TiO_2: ◆ BHA, ▲ BAC.

The BHA selectivity, with respect to BA consumption, has been calculated and reported in figure 60 for both TiO_2 types. As shown in the diagram, it seems that the use of Aldrich TiO_2 sample renders the system more selective, reaching, for Q_n values of 130 kJ/L, BHA selectivity values close to 70% (in presence of P25 Degussa, only a value of 50% has been obtained at the same Q_n).

The highest selectivity achieved in presence of Aldrich TiO_2 sample is correlated to the lower degree of conversion (figure 58a, red squares) when compared with the test in which Degussa P25 is used (figure 58a, blue squares).

TOC measurements collected during the runs are also reported in figure 60, in terms of mineralization degrees (dashed lines). The trends are very similar, with a degree of mineralization at the end of the experimental runs of 9% and 7% in presence of P25 Degussa and Aldrich TiO_2 respectively.

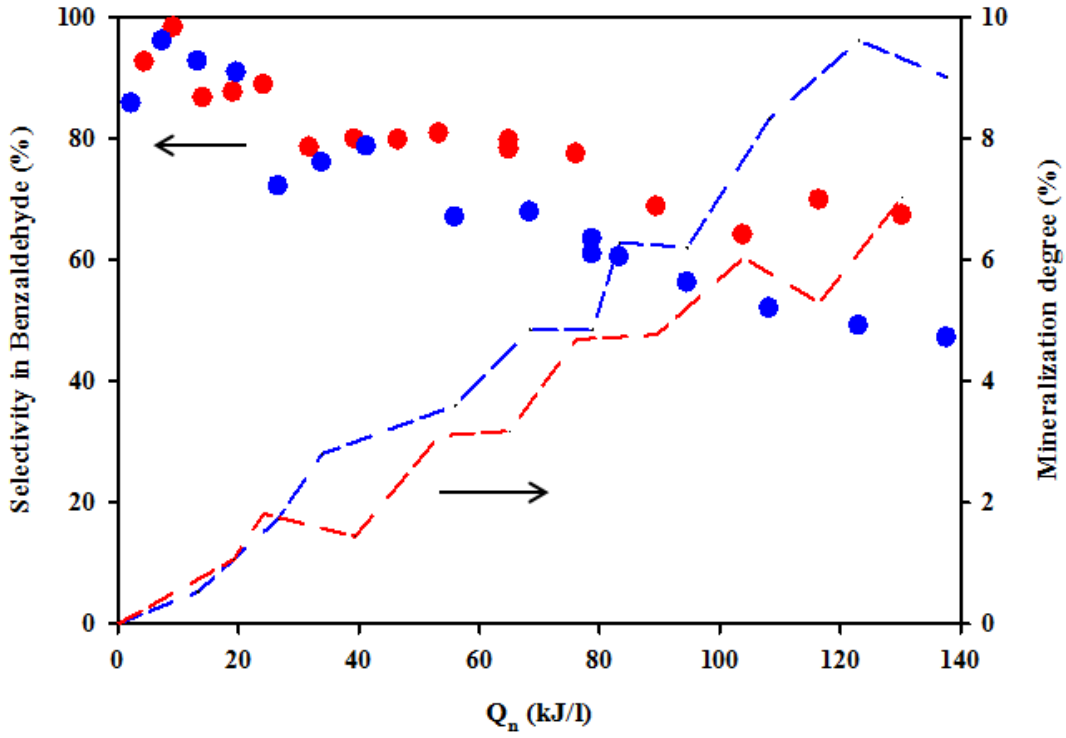

Fig. 60 Effect of TiO_2 type on the BHA selectivity (full cyrcles) and mineralization degree (dashed lines).

$[BA]_0$ = 1.5 mM. $[Cu(II)]_0$ = 1.5 mM. Initial TiO_2 load = 200 mg/L. pH=2.0.

Aldrich TiO_2: (●) BHA selectivity, (---) mineralization degree.

P25 Degussa TiO_2: (●) BHA selectivity, (---) mineralization degree.

7.2 Effect of cupric ions concentration

To evaluate the effect of the initial concentration of Cu(II) ions, some experimental runs of solar photoxidation of benzyl alcohol have been carried out with Aldrich TiO_2 at the load of 200 mg/l and pH = 2.0, varying the $CuSO_4$ starting concentration (0.5 mM, 1.0 mM and 1.5 mM).

As shown in figures 61a and 61b, the temperatures and UV-irradiances profiles (solid and dashed lines) are so similar to be considered equals for the three runs.

With Cu(II) and BA starting concentrations of 0.5 mM and 1.5 mM respectively, the BA oxidation stopped for Q_n values close to 35 kJ/l where a complete reduction of cupric ions has been observed (green triangles).

The highest Cu(II) initial concentration (1.5 mM) resulted into a decrease of the system reactivity and BA conversion (fig. 61a, blue circles) and, at the same time, the Cu(II) reduction rates decrease. According to the results reported in figure 39 of the fourth chapter and reactions r_{22} and r_{24}, shown in the fifth chapter, the observed results are due to a partial catalyst deactivation by the adsorbed sulphate ions which may block the TiO_2 active sites (s*). In addition, they are due to an inhibition of BA photo-oxidation rates because these ions are in competition with BA molecules in the reaction with the positive holes.

In fact, since Cu(II) species have been added to the reactive solution as cupric sulphate, increasing the initial concentration of Cu(II) ions results into an increase of sulphate concentration and, consequently, into a decrease of system reactivity.

In figure 62, the experimental concentration profiles of BHA and BAC (full and empty symbols) that are in agreement with BA concentration trends shown in figure 61a are reported. In particular, the best result found, in term of yield, has been of 43% for BHA, starting with $[Cu(II)]_0$ = 1.0 mM, for a accumulated energy value of 67 kJ/L. For all the runs, the selectivity was always higher than 67% and the mineralization degrees were lower than 4.5% (data not shown).

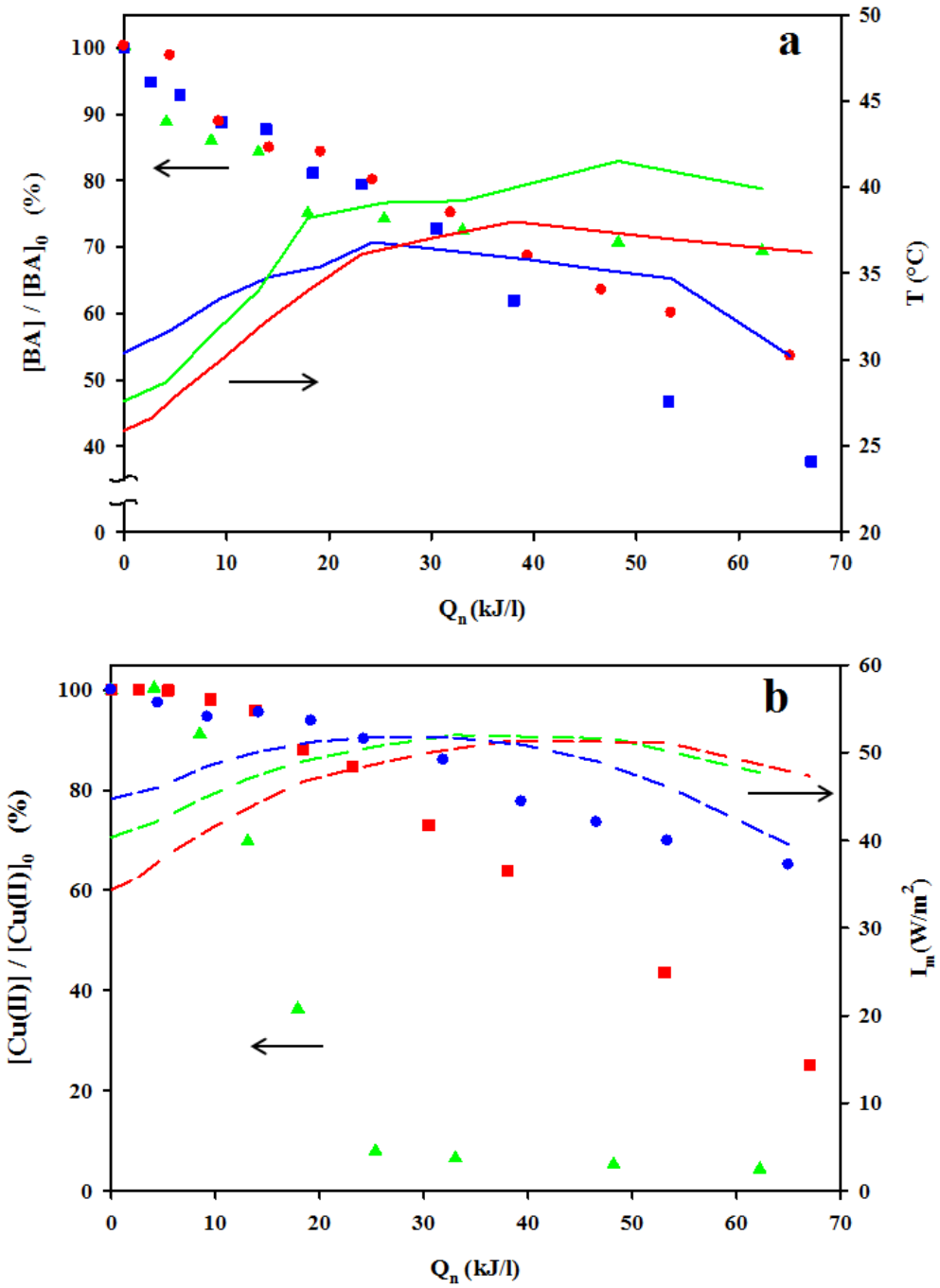

Fig. 61 Effect of initial Cu(II) concentration on the BA and Cu(II) concentration profiles: BA solar photoxidation and temperatures profiles (6a); Cu(II) solar photoreduction and UV-irradiances profiles (6b).

$[BA]_0$ = 1.5 mM. Initial TiO_2 (Aldrich) load = 200 mg/L. pH = 2.0.

56a: (▲,—) $[Cu(II)]_0$ = 0.5 mM, (■,—) $[Cu(II)]_0$ = 1.0 mM, (●,—) $[Cu(II)]_0$ = 1.0 mM,

56b: (▲,---) $[Cu(II)]_0$ = 0.5 mM, (■,---) $[Cu(II)]_0$ = 1.0 mM, (●,---) $[Cu(II)]_0$ = 1.0 mM,

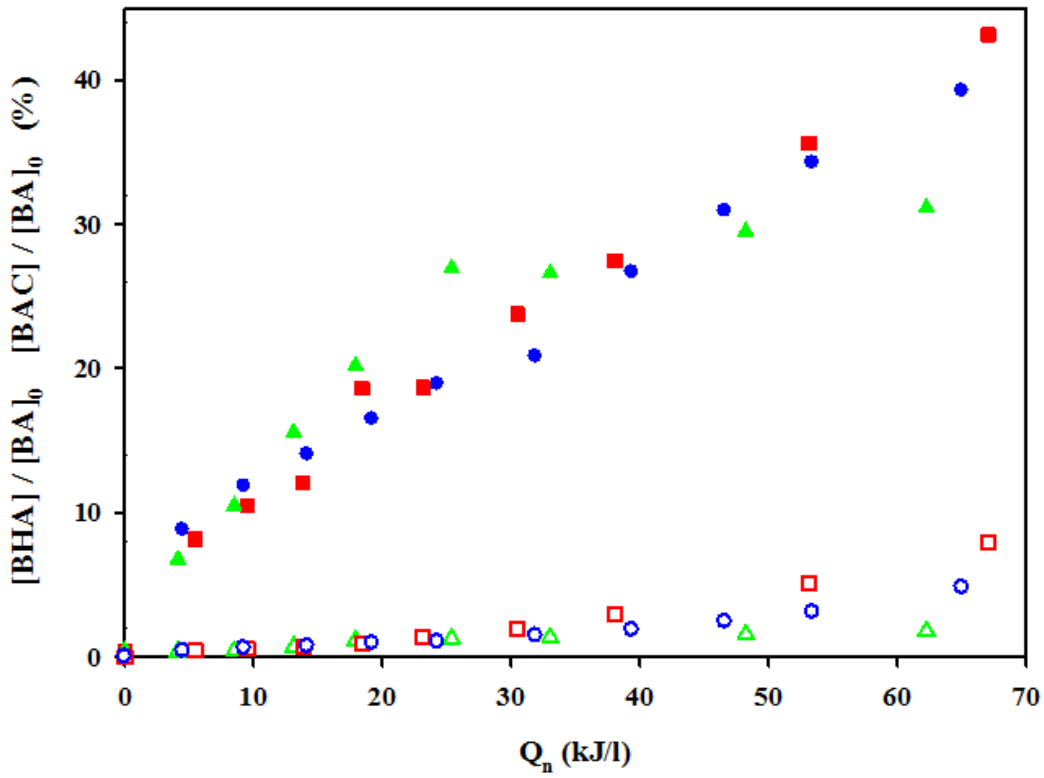

Fig. 62 Effect of initial Cu(II) concentration on the BHA and BAC concentration profiles:

BHA (full symbols) and BAC (empty symbols) productions.

$[BA]_0$ = 1.5 mM. Initial TiO_2 (Aldrich) load = 200 mg/L. pH = 2.0.

(▲,△) $[Cu(II)]_0$ = 0.5 mM, (■,□) $[Cu(II)]_0$ = 1.0 mM, (●,○) $[Cu(II)]_0$ = 1.5 mM.

7.3 Effect of irradiance and temperature

As previously shown in figures 58b and 61b, the Cu(II) concentrations are characterized by a s-shaped profile and, in particular, when the solar UV radiations and reactor temperatures reached the top, a marked increase of Cu(II) reduction rate has been observed. With the aim to better assess the relationship between the changes of both irradiances and temperatures during a solar run and the s-shaped of cupric ions concentration profile, a set of three laboratory photolytic experiments, with Cu(II) initial concentration equal to 0.5 mM, have been carried out at three different irradiances, kept constant during a single run and under controlled solution temperature (T=35 °C). For this purpose, the solar box apparatus, described in the experimental section (figure 30), has been used. Since the internal diameters of CPC solar reactor tubes and the solar box vials are 31 mm and 24 mm respectively, the TiO_2 load that maximizes the adsorption of UV radiation emitted by solar lamp is higher than that used for solar experiments carried out in CPC reactor.

The optimum TiO_2 concentration (c_{cat}), for which the optical thickness equals that of CPC reactor configuration (τ=9.12) can be easily calculated as suggested by others[107-108]:

$$c_{cat} = \frac{\tau}{(\sigma + k) \cdot d} = 258 \text{ mg/L}$$

where σ is the scattering coefficient ($1.295 \cdot 10^3$ m^2/kg), k is the catalyst specific mass absorption ($1.75 \cdot 10^2$ m^2/kg) and d the internal tube diameter (24 mm).

As shown in figure 63, by increasing the UV irradiance from 39.5 W/m^2 to 59.7 W/m^2, the Cu(II) photoreduction rate increases.

A parallel increase of BA oxidation rate has also been observed (data not shown). The results collected during these runs indicate that, under controlled temperature and irradiance, no S-shaped concentration profile has been recorded.

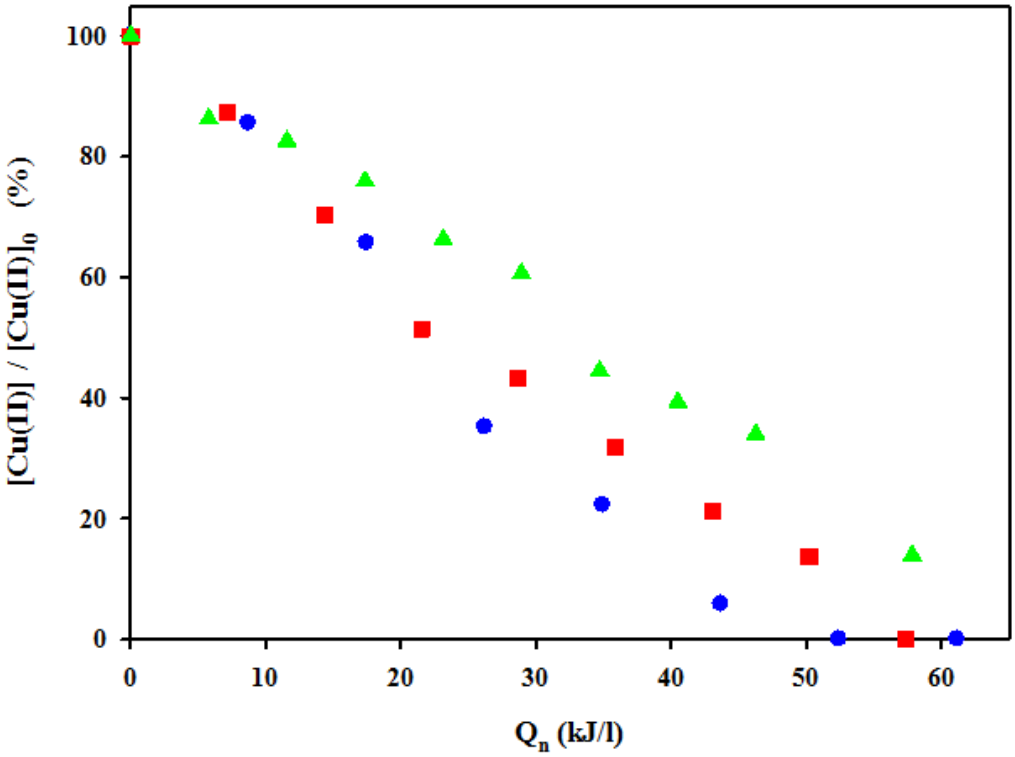

Fig. 63 Effect of irradiance on the Cu(II) concentration profiles.

$[BA]_0$ = 1.5 mM. $[Cu(II)]_0$ = 0.5 mM. Initial TiO_2 (Aldrich) load = 258 mg/L.

pH = 2.0 and T = 35 °C.

UV Irradiance (solar box): ▲ 39.5 W/m^2, ■ 49.0 W/m^2 , ● 59.7 W/m^2.

7.4 Figure-of-merit: collector area per mass

To estimate the operating costs of sole natural radiation, the figure-of-merit concept, proposed by others[109], has been used. For solar-energy-driven systems, the figure-of-merit allows the assessment of the solar technology efficiency used for the investigated process. In fact, even if there is no cost for solar radiation, there could be a non-marginal capital cost for the collector. Being the capital cost of a solar collector generally proportional to its area, a figure-of-merit, based on the solar collector area, is appropriate.

For the adopted experimental batch conditions, the appropriate figure-of-merit is the collector area per mass (A_{CM}), defined as the collector area required to reduce a unit mass of substrate in the reacting system in 1 hour (t_o) for an incident solar irradiance of 1000 W m^{-2} (E_S^o):

$$A_{CM} = \frac{1000 \cdot A_r \cdot t \cdot \overline{E_s}}{M \cdot V_t \cdot t_0 \cdot \overline{E_s^0} \cdot (c_i - c_f)}$$

where A_r (3.19 m^2) is the real collector area, M is the molar mass of the substrate (108.14 g/mol), V_t (39 L) is the volume of treated solution, $\overline{E_S}$ (814.6 W/m^2) is the average direct solar irradiance over the reaction time t (4.83 h), c_i and c_f are respectively the initial and final substrate concentrations (mol/l), E_S^o is the standardized irradiance (1000 W/m^2, based on the AM1.5 standard solar spectrum on a horizontal surface)[110], and t_0 is the reference time (1 h).

On the basis of the previous formula, an average value of $A_{CM} = 3.08 \cdot 10^3$ m^2 per kilogram of benzyl alcohol consumed per hour has been thus calculated for the collector area per mass (200 mg/L of Aldrich TiO_2, pH=2.0, $[Cu(II)]_0$ = 1.0 mM, and $[BA]_0$ = 1.5 mM).

7.5 Copper reuse and analyses of precipitated solid

The possibility to reuse the reduced copper, as catalyst, has been tested by carrying out an experimental run, by using the CPC solar reactor, consisting in three cycles of BA photo-oxidation. When all Cu(II) species has been totally reduced into precipitate copper, its reoxidation has been carried out, in dark conditions, under air bubbling in the recirculation tank for 30 minutes. At the end of the first cycle, the reactive solution has been re-purged with nitrogen gas, for other 30 minutes, to remove the dissolved oxygen and a new photocatalytic cycle has been started. The experimental results, reported in figure 64, pointed out that it's possible, for each cycle, to reoxidize completely the precipitate copper to cupric species (empty blue diamonds).

During the first two cycles of BA solar photo-oxidation, no particular changes have been observed on the reactivity of the system. Whereas, during the third cycle, a decrease of both BA consumption and BHA production rates have been observed. This behavior could be explained by considering that the solution composition changes during the experimental run. In particular, at the beginning of the 3rd cycle, BA conversion and BHA yield have been 43% and 33% respectively thus favoring competition kinetics between BA and BHA, both adsorbed on TiO_2 surface, towards the reaction with the photogenerated holes.

The BHA selectivities of the process for the three photocatalytic cycles are reported in figure 65. As shown in the diagram, the highest selectivities (up to 100%) have been obtained in the first cycle, whereas lower selectivities have been observed during the second (close to 75%) and the third cycle (close to 40%) thus supporting the idea that, increasing the reaction time, there is an intervention of undesired oxidation reactions of BHA once produced.

After each photocatalytic cycle under anoxic conditions, the solid has been separated from the solution, stored under inert atmosphere and submitted to SEM, EDS, XRD, and XPS analysis in order to better investigate the distribution of copper deposited on the solid and its oxidation states.

The images and the results obtained from SEM and EDS analysis are reported in Appendix 2. In particular, from the EDS investigations, Ti/Cu atom ratios, for the solids, have been found to be 97.8/2.2, 96.5/3.5 and 85.2/14.8 (w/w) for the samples withdrawn at the end of the first, second and third cycle respectively.

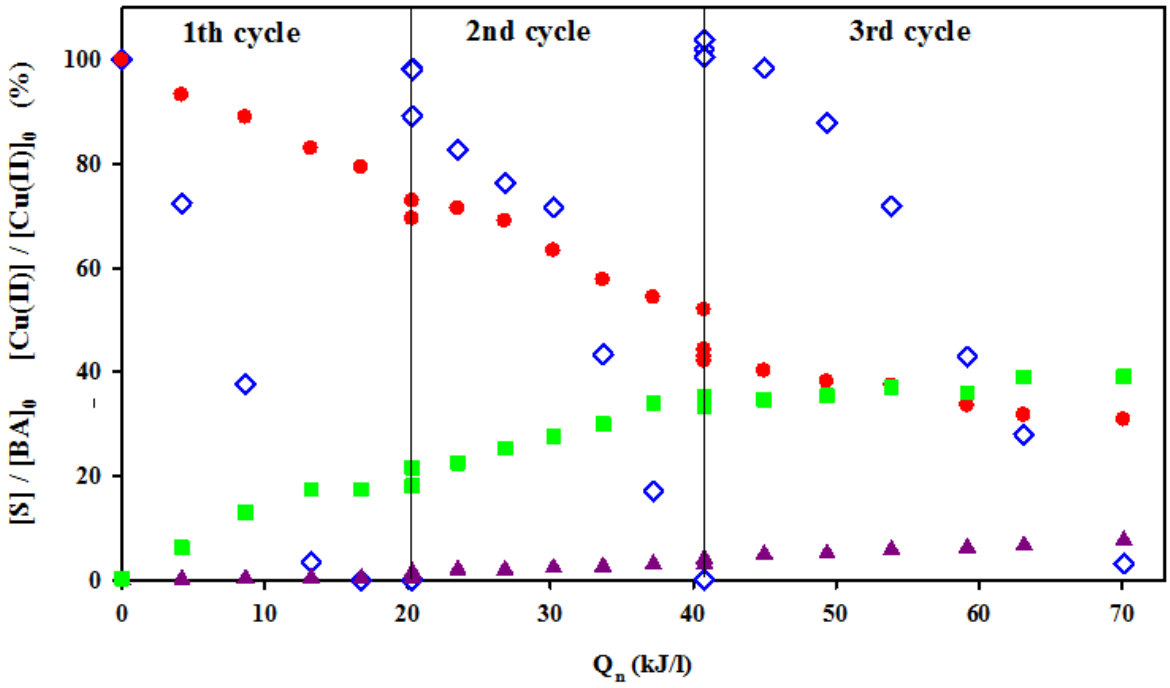

Fig. 64 Copper reuse: Normalized concentration profiles for Cu(II), BA, BHA and BAC. $[BA]_0$ = 2.5 mM. $[Cu(II)]_0$ = 0.5 mM. Initial TiO_2 (Aldrich) load = 200 mg/L. pH = 2.0. ◇ Cu(II), ● BA, ■ BHA, ▲ BAC.

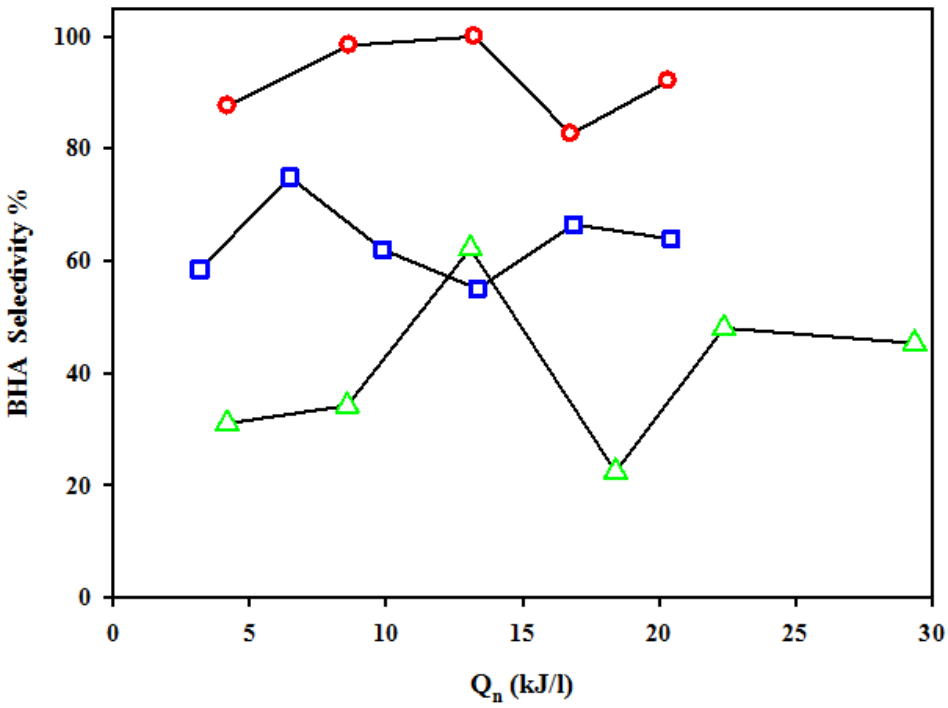

Fig. 65 Copper reuse: BHA selectivities during the three cycles.

$[BA]_0$ = 1.5 mM. $[Cu(II)]_0$ = 0.5 mM. Initial TiO_2 (Aldrich) load = 200 mg/L. pH = 2.0.

○ 1th cycle, □ 2nd cycle, △ 3rd cycle.

The results from EDS analysis support the idea that reduced Cu species, formed during the photo-oxidative runs and accumulated on TiO_2 surface, increase from the first cycle to third one up to 17.4% by weight. The increase of Cu amount on TiO_2 is probably due to the deposition of a part of photocatalyst powders, during the experimental run, in the recirculation tank and/or along the hydraulic connections of the plant, thus decreasing its active load available in the solar photo reactor. Consequently, a reduction of BA consumption and BHA production rates, really observed, occurred, in particular during the third cycle.

A typical XPS spectra for the solid samples, reported in figure 66, show different peaks. The peaks at 932.8 eV and 952.6 eV indicate the predominant presence of copper reduced species (+1/0) as previously reported by others[55, 65, 111]. Whereas, the existence of peaks at 935.4 eV and 955.2 eV can be attributed to the presence of cupric species[65], such as CuO, probably an artifact produced during the preparation of the sample before the XPS analysis.

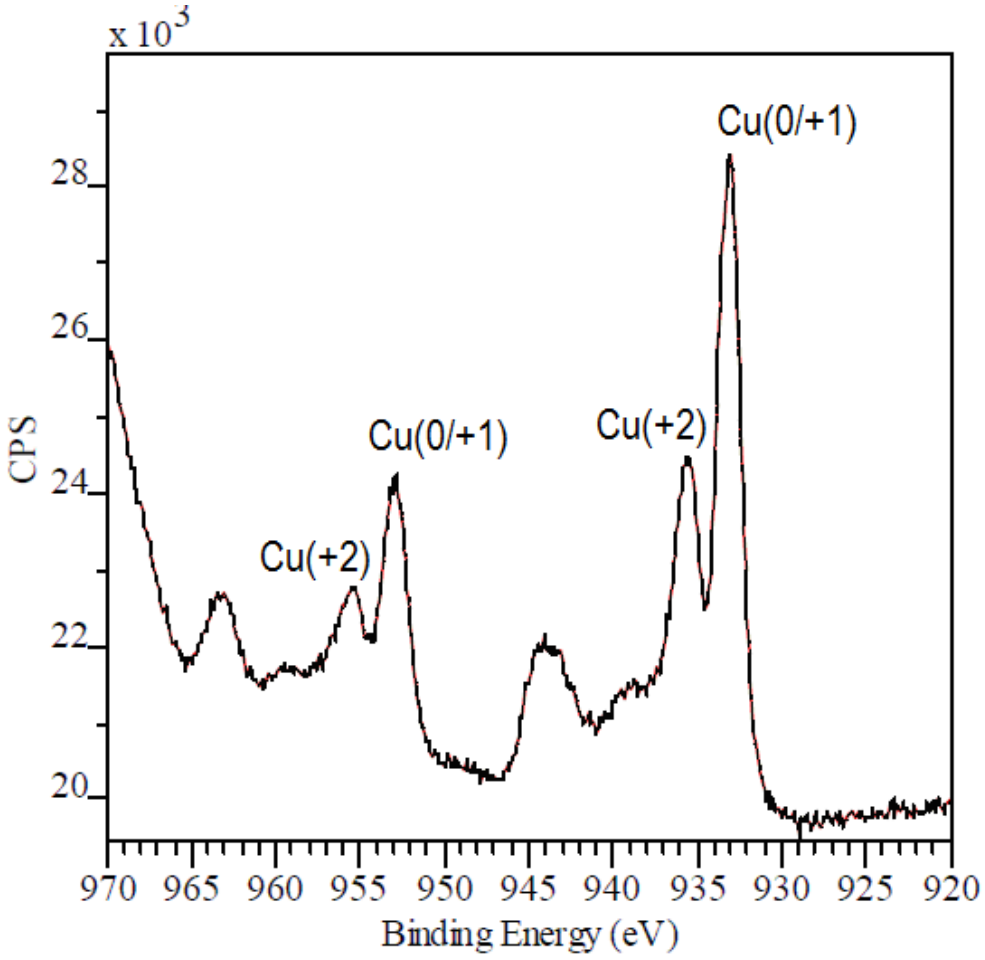

Fig. 66 XPS spectra for the solid sample after the photocatalytic oxidation run.

Unfortunately, no results have been obtained from XRD analysis. This is because the amount of Cu reduced species accumulated on the TiO_2 surface (max 17.4%) is below XRD detection limit that is about 50% (w/w), as reported earlier. For this reason in figure 65, where the results of XRD analysis have been reported, only the peaks relative to anatase appear.

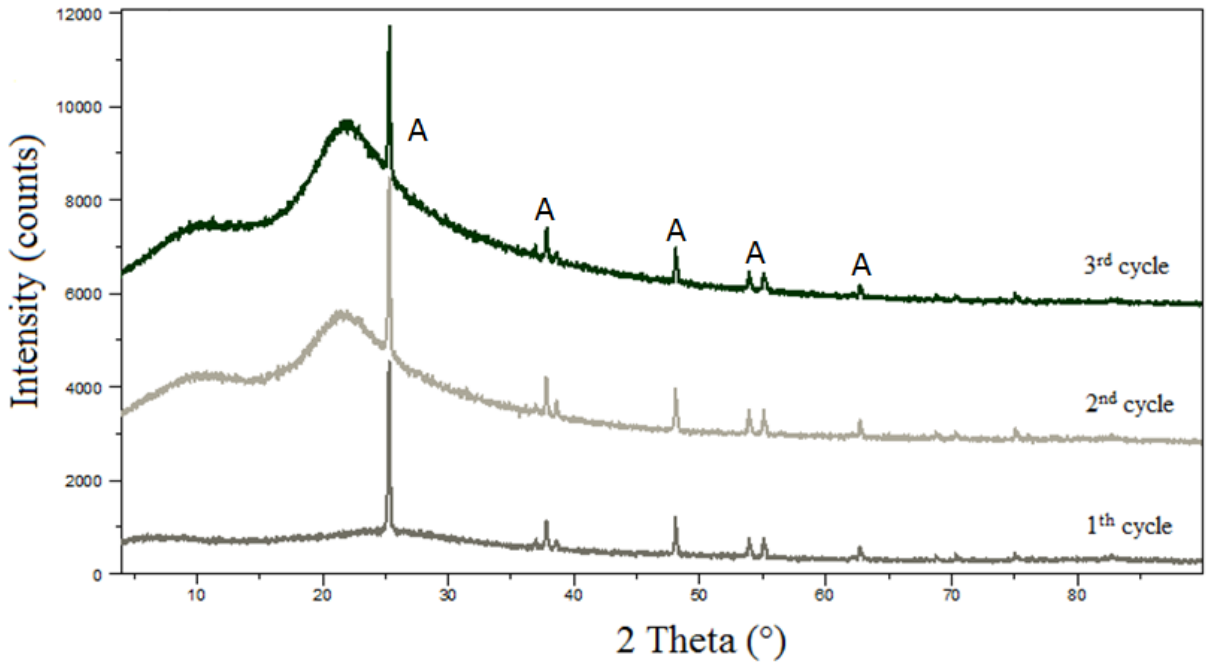

Fig. 67 XRD analysis.

Therefore, it is possible to hypothesize that the oxidation of precipitate copper begins with the reaction between metallic copper and oxygen, as reported below:

$$Cu(0) + O_2 \rightarrow Cu(I) + O_2^{\bullet -}$$
$$Cu(I) + O_2 \rightarrow Cu(II) + O_2^{\bullet -}$$

The superoxide radical, in presence of H^+, is in equilibrium with the hydroperoxide radical:

$$O_2^{\bullet -} + H^+ \leftrightarrow HO_2^{\bullet}$$

The hydroperoxide radical can terminate, leading to the formation of hydrogen peroxide, or can react with the cuprous ions reducing them to cupric ions [112-113]:

$$2HO_2^{\bullet} \rightarrow H_2O_2 + O_2$$
$$HO_2^{\bullet} + Cu(II) \rightarrow Cu(I) + H^+ + O_2$$

The Cu(I) ions can contribute to the production of $HO^{\bullet}$ radicals in the bulk from the Fenton-like reaction[113]:

$$Cu(I) + H_2O_2 \rightarrow Cu(II) + HO^{\bullet} + HO^-$$

The $HO^{\bullet}$ radicals, generated in the last reaction, can oxidize Cu(I) ions to Cu(II) or can attack the organic substances present in the solution (BA, BHA, and BAC) leading to the formation of undesired by-products:

$$Cu(I) + HO^{\bullet} \rightarrow Cu(II) + HO^-$$
$$S + HO^{\bullet} \rightarrow \text{by-products}$$

Since the reoxidation of Cu(0), in water and in presence of O_2, leads to the formation of $HO^{\bullet}$ radical, it is better to reoxidize the precipitated copper once it is separated from the solution containing the organic substances.

7.6 Summary

The possibility to convert benzyl alcohol into benzaldehyde by photocatalytic oxidation in aqueous solution under natural solar radiation has been demonstrated at pilot plant scale. The oxidation rates have been strongly influenced by the initial cupric ions concentration, incident solar irradiance, and temperatures. The best result found, in terms of yield, is of 53.3% for benzaldehyde with respect to the initial benzyl alcohol concentration (63.4 % of selectivity) for an accumulated energy value (Q_n) of 78.9 kJ/L (reaction time of 385 min) and operating with an average temperature of 38.6 °C.

EPS investigations, carried out on the solids withdrawn during different photocatalytic cycles, confirm the existence of both Cu reduced (0/+1) and oxidized species, the latter probably produced during the sample preparation before the analysis.

The results also indicate that cupric species can be easily regenerated and reused with air or oxygen in dark conditions.

A figure-of-merit (A_{CM}) has been calculated to be equal to $3.08 \cdot 10^3$ m^2 per kilogram of benzyl alcohol converted and per hour.

8 CONCLUSIONS

The possibility to produce benzaldehyde through a selective oxidation od benzyl in aqueous solution, under acidic conditions, using the photocatalytic system TiO_2/Cu(II)/hv has been studied, in laboratory-scale and pilot plant reactors, at varying operating condition.

Four samples of TiO_2 characterized by different crystallographic forms and specific surface areas have been used during some laboratory-scale experiments. The best result found has been a yield of 35% of benzaldehyde, with respect of the initial benzyl alcohol, in presence of pure anatase. Benzaldehyde has been also partially converted to benzoic acid. The presence of undesired by-products, such as 2-hydroxy-benzyl alcohol, 4-hydroxy-benzyl alcohol, 2-hydroxy-benzaldehyde and 4-hydroxy-benzaldehyde, has been demonstrated and indicated an active production of surface HO radicals.

The sulphate and dihydrogenphosphate anions resulted to exert a negative effect on the photo-oxidation rates of benzyl alcohol and to behave as scavengers towards surface HO radicals. A decrease of benzyl alcohol oxidation and benzaldehyde formation rates has been observed by increasing the pH from 2.0 to 4.0. Moreover, an increase of irradiance corresponds to an increase of reactivity of the system.

A reaction mechanism with competitive adsorption has been proposed in which the aromatic substrates (benzyl alcohol, benzaldehyde and benzoic acid) adsorb on TiO_2 surface and react with the positive holes whereas Cu(II) ions are reduced to Cu(0) by the photogenerated electrons. The competition of SO_4^{2-} and $H_2PO_4^-$ species with aromatic substances, for the adsorption on TiO_2 surface and for the reaction with positive holes on the catalyst, and the behavior of these ions as scavengers towards surface HO radicals have been included in reaction mechanism.

The resulting mathematical model, not firstly reported, has been tested, by using the data collected at different starting concentrations of substrates and catalyst, and results capable to predict satisfactorily the concentrations of Cu(II) species, organic substrates and intermediates during the selective photo-oxidation process, thus validating the main reactions considered in the kinetic scheme. Moreover, the values of eight parameters, unknown *"a priori"*, have been estimated by a proper optimizing procedure.

The presence of a hydroxy, methoxy or nitro group on the aromatic ring of the alcohol molecule markedly affects the yield of the partial oxidation of the substrate investigated in the sense that both the electron donating or withdrawing effects of the substituent have a detrimental effect on the selectivity of the process with respect to that observed for unsubstituted benzyl alcohol.

The results obtained with the system TiO_2/Cu(II)/hv, by using the solar radiation daily arriving on the earth surface in a pilot-plant reactor, are in accordance with the ones collected by using the laboratory scale reactor. In particular, the best result found, in terms of yield, has been of 53.3% for benzaldehyde with respect to the initial benzyl alcohol concentration (63.4 % of selectivity) for an accumulated energy value (Q_n) of 78.9 kJ/L (reaction time of 6.42 h) and operating with an average temperature of 38.6 °C.

From the experiments conducted in the pilot-plant reactor, a collector area per mass of 3080 m^2 has been obtained. This number indicates that a collector area of 3080 m^2 is enough to oxidize 1 kg/h of benzyl alcohol for an incident solar irradiance of 1000 W m^{-2}.

The results also indicated that cupric species can be easily regenerated and reused with air or oxygen in dark conditions.

EPS investigations, carried out on the solids, withdrawn during different photocatalytic cycles carried out with the pilot-plant, confirmed the existence of both Cu reduced (0/+1) and oxidized species, the latter probably produced during the sample preparation before the analysis.

APPENDIX 1

Benzyl Alcohol

CAS number: 100-51-6

Molecular Weight: 108.14 g/mol

Boiling Point: 205 °C

Solubility in water: 40 g/L

Purchased from: Sigma Aldrich

Purity: ≥99% (w/w)

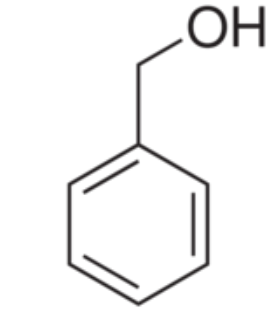

Benzaldehyde

CAS number: 100-52-7

Molecular Weight: 106.12 g/mol

Boiling Point: 178.1 °C

Solubility in water: 3 g/L

Purchased from: J.T. Baker

Purity: ≥95% (w/w)

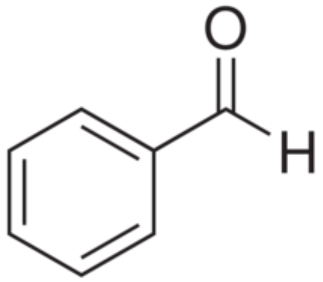

Benzoic Acid

CAS number: 65-85-0

Molecular Weight: 122.12 g/mol

Melting Point: 122.41 °C

Solubility in water: 2.9 g/L

Purchased from: Sigma Aldrich

Purity: ≥99.5% (w/w)

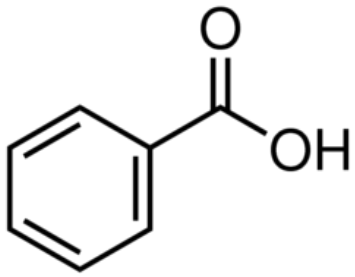

2-Hydroxybenzyl Alcohol

CAS number: 90-01-7

Molecular Weight: 124.14 g/mol

Melting Point: 83-87 °C

Solubility in water: 6.9 g/L

Purchased from: Sigma Aldrich

Purity: 99.0% (w/w)

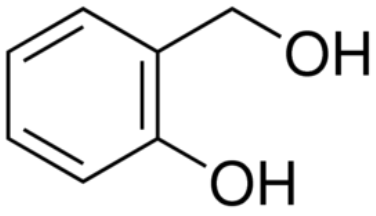

3-Hydroxybenzyl Alcohol CAS number: 620-24-6 Molecular Weight: 124.14 g/mol Melting Point: 69-72 °C Solubility in water: soluble Purchased from: Sigma Aldrich Purity: 99.0% (w/w)	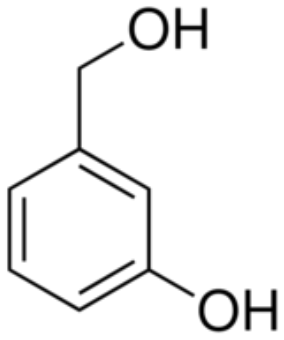
4-Hydroxybenzyl Alcohol CAS number: 623-05-2 Molecular Weight: 124.14 g/mol Melting Point: 114-122 °C Solubility in water: Purchased from: Sigma Aldrich Purity: ≥98.0% (w/w)	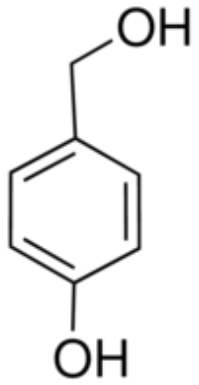
2-Hydroxybenzaldehyde CAS number: 90-02-8 Molecular Weight: 122.12 g/mol Melting Point: 196-197 °C Solubility in water: slightly soluble Purchased from: Sigma Aldrich Purity: ≥98.0% (w/w)	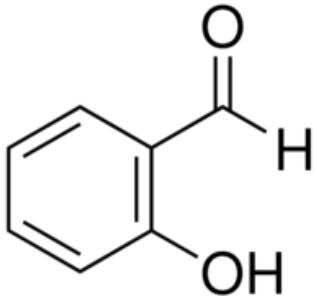
3-Hydroxybenzaldehyde CAS number: 100-83-4 Molecular Weight: 122.12 g/mol Melting Point: 100-103 °C Solubility in water: soluble Purchased from: Sigma Aldrich Purity: 97.0% (w/w)	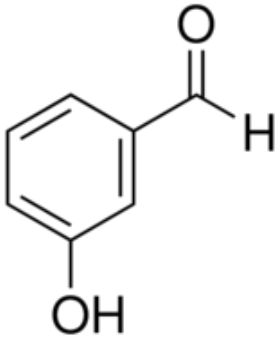

4-Hydroxybenzaldehyde CAS number: 123-08-0 Molecular Weight: 122.12 g/mol Melting Point: 112-116 °C Solubility in water: 1.3 g/L Purchased from: Sigma Aldrich Purity: 98% (w/w)	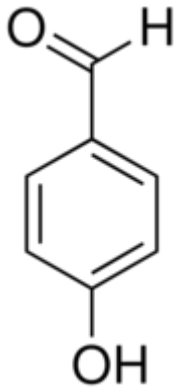
2-Hydroxybenzoic Acid CAS number: 69-72-7 Molecular Weight: 138.12 g/mol Melting Point: 159 °C Solubility in water: 2.3 g/L Purchased from: Sigma Aldrich Purity: ≥99.0% (w/w)	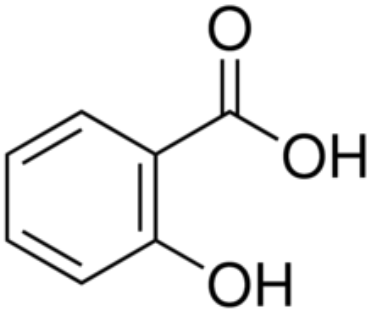
3-Hydroxybenzoic Acid CAS number: 99-06-9 Molecular Weight: 138.12 g/mol Melting Point: 201 °C Solubility in water: slightly soluble Purchased from: Sigma Aldrich Purity: 99.0% (w/w)	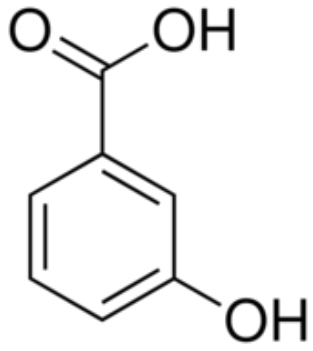
4-Hydroxybenzoic Acid CAS number: 99-96-7 Molecular Weight: 138.12 g/mol Melting Point: 214-217 °C Solubility in water: 6 g/L Purchased from: Sigma Aldrich Purity: 99.0% (w/w)	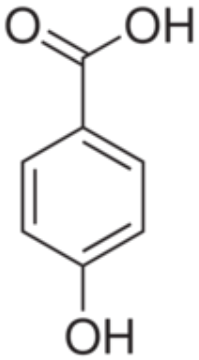

2-Methoxybenzyl Alcohol CAS number: 612-16-8 Molecular Weight: 138.16 g/mol Boiling Point: 248-250 °C Solubility in water: slightly soluble Purchased from: Sigma Aldrich Purity: 99.0% (w/w)	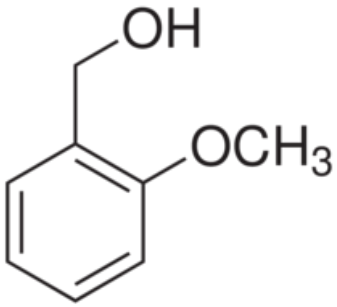
2-Methoxybenzaldehyde CAS number: 135-02-4 Molecular Weight: 136.16 g/mol Boiling Point: 238 °C Solubility in water: slightly soluble Purchased from: Sigma Aldrich Purity: 98% (w/w)	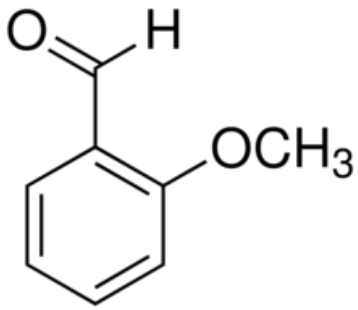
2-Methoxybenzoic Acid CAS number: 579-75-9 Molecular Weight: 152.15 g/mol Melting Point: 98-100 °C Solubility in water: very soluble Purchased from: Sigma Aldrich Purity: 99% (w/w)	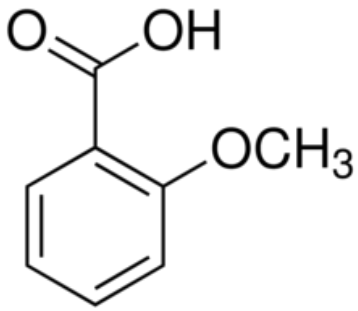
4-Methoxybenzyl Alcohol CAS number: 105-13-5 Molecular Weight: 138.16 g/mol Melting Point: 22-25 °C Solubility in water: slightly soluble Purchased from: Sigma Aldrich Purity: 98.0% (w/w)	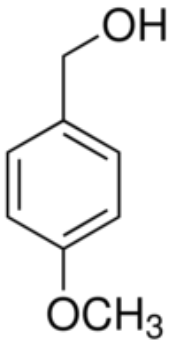

4-Methoxybenzaldehyde

CAS number: 123-11-5

Molecular Weight: 136.15 g/mol

Boiling Point: 248 °C

Solubility in water: 2 g/L

Purchased from: Sigma Aldrich

Purity: 98.0% (w/w)

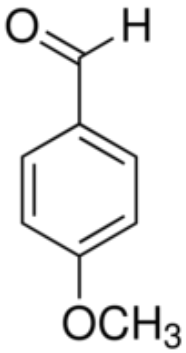

4-Methoxybenzoic Acid

CAS number:

Molecular Weight: g/mol

Melting Point: 182-185 °C

Solubility in water: 0.53 g/L (37 °C)

Purchased from: Sigma Aldrich

Purity: 99 % (w/w)

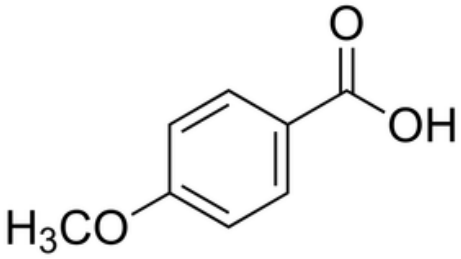

4-Nitrobenzyl Alcohol

CAS number: 619-73-8

Molecular Weight: 153.14g/mol

Melting Point: 92-97°C

Solubility in water: 2 g/L

Purchased from: Sigma Aldrich

Purity: 99% (w/w)

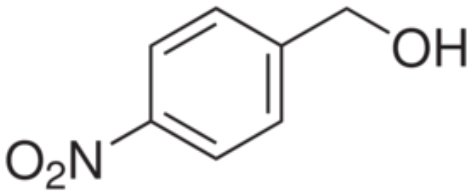

4-Nitrobenzaldehyde

CAS number: 55-16-18

Molecular Weight: 151.12 g/mol

Melting Point: 103-106°C

Solubility in water: slightly soluble

Purchased from: Sigma Aldrich

Purity: 98% (w/w)

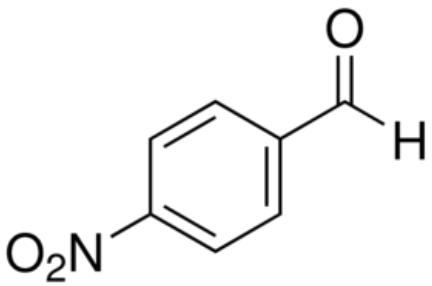

4-Nitrobenzoic Acid

CAS number: 62-23-7

Molecular Weight: 167.12 g/mol

Melting Point: 237-240 °C

Solubility in water: 0.42 g/L

Purchased from: Sigma Aldrich

Purity: 98% (w/w)

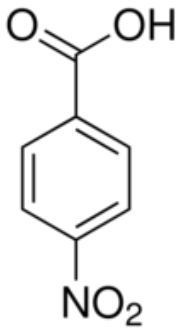

APPENDIX 2

SEM and EDX Analysis

SEM and EDX Spectrum details 1th Cycle

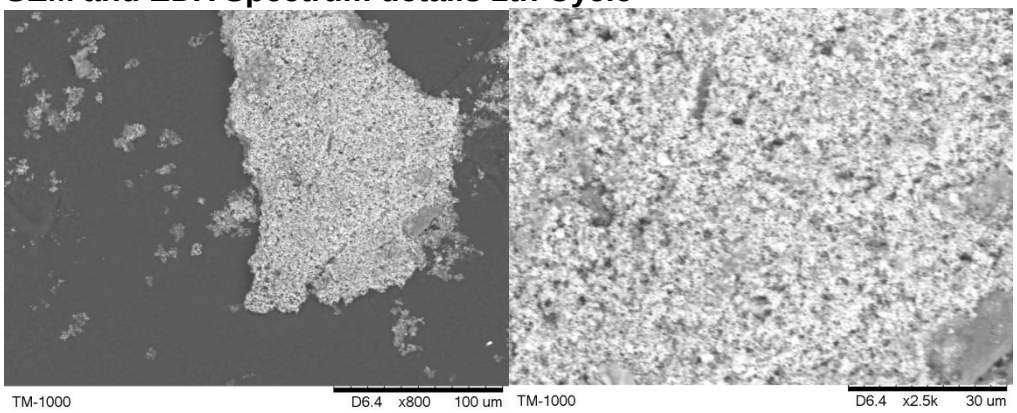

Acquisition conditions

Acquisition time (s)	90.0
Process time	3
Accelerating voltage (kV)	15.0

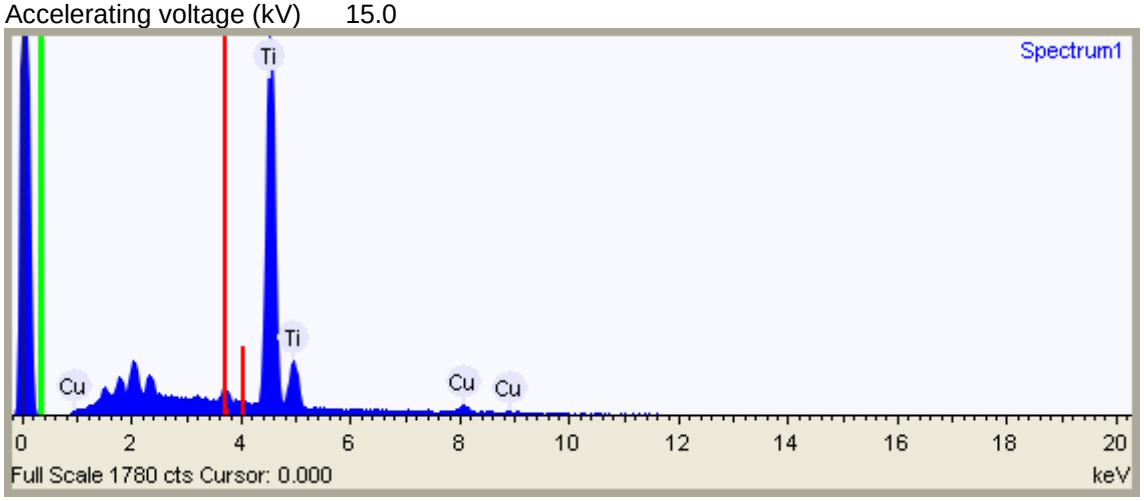

Summary results

Element	Weight %
Titanium	97.8
Copper	2.2

SEM and EDX Spectrum details 2th Cycle

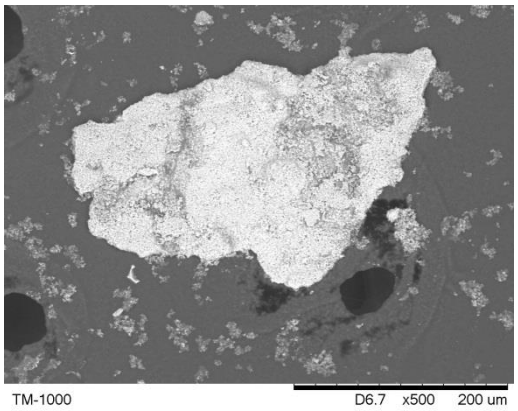

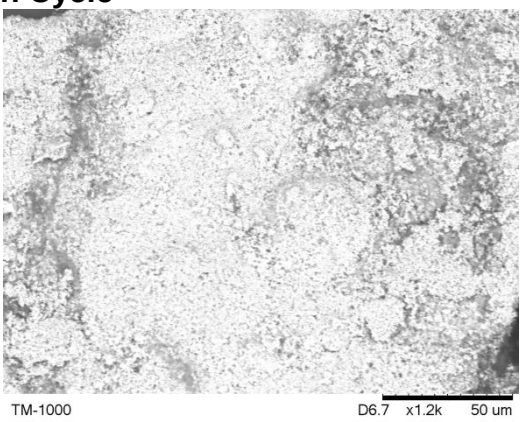

Acquisition conditions

Acquisition time (s)	90.0
Process time	3
Accelerating voltage (kV)	15.0

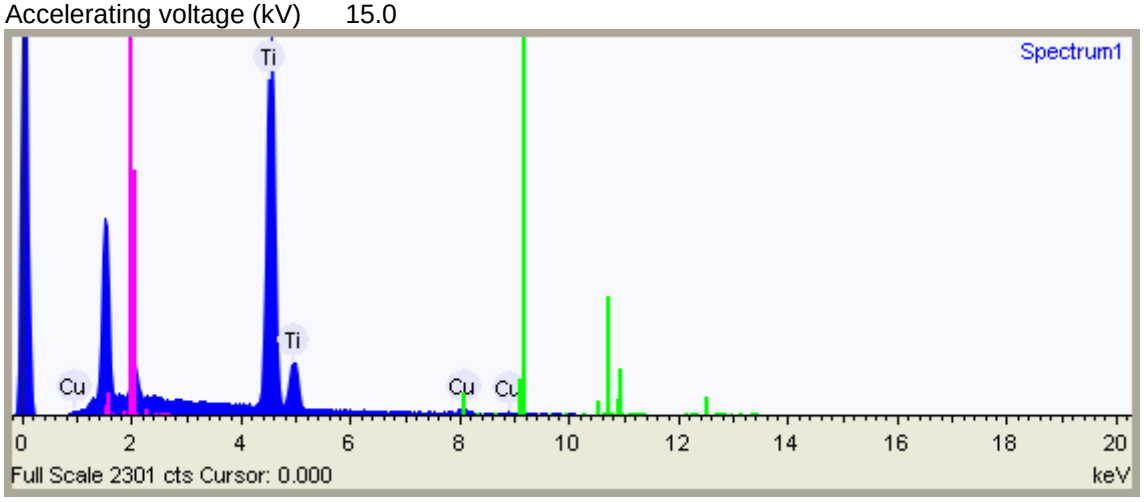

Summary results

Element	Weight %
Titanium	96.5
Copper	3.5

SEM and EDX Spectrum details 3th Cycle

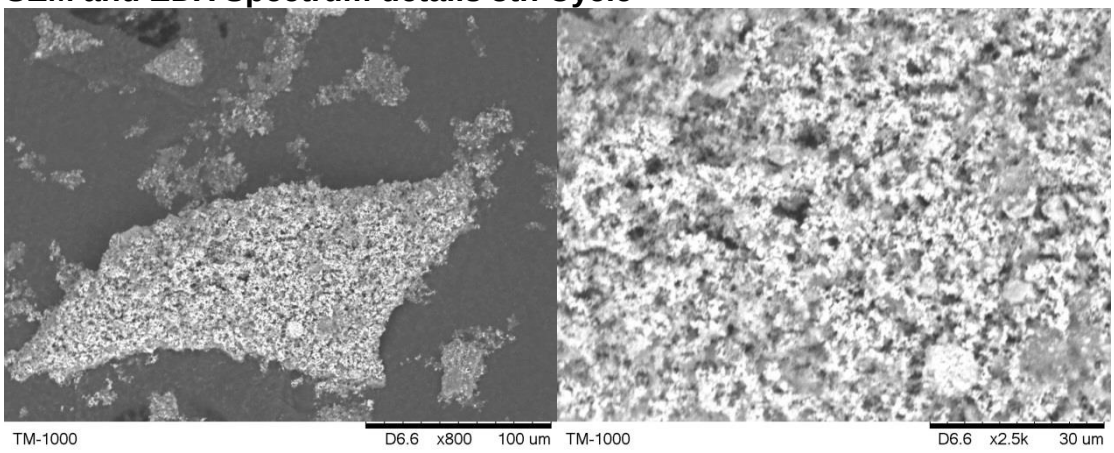

Acquisition conditions

Acquisition time (s)	90.0
Process time	3
Accelerating voltage (kV)	15.0

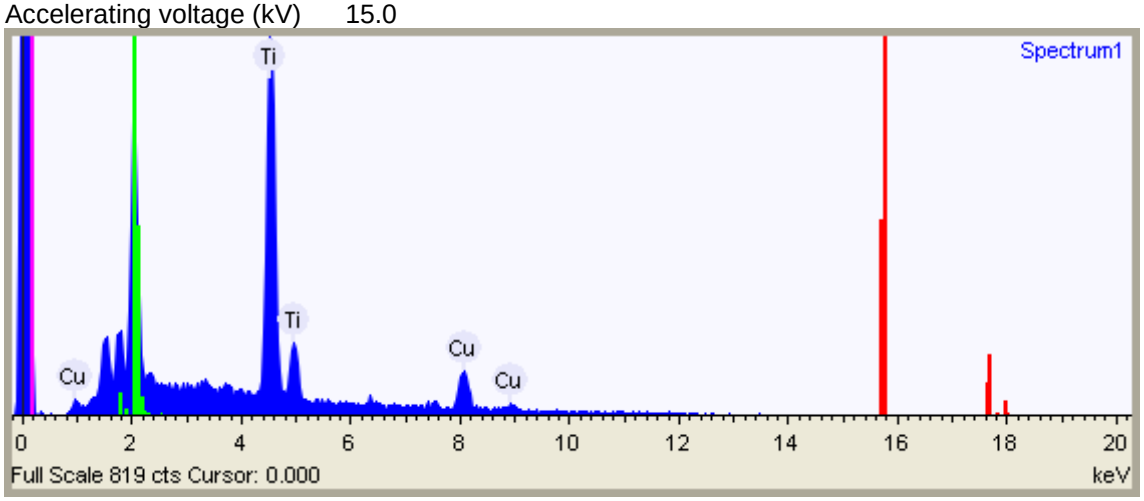

Summary results

Element	Weight %
Titanium	85.2
Copper	14.8

REFERENCES

[1] M. Musawir, P.N. Davey, G. Kelly I.V. and Kozhevnikov, "*Highly efficient liquid-phase oxidation of primary alcohols to aldehydes with oxygen catalysed by Ru-Co oxide*", Chem. Commun., 2003, 12, 1414-1415.

[2] S.Y. Sun, W.G. Jiang and Y.P. Zhao, *"Characterization of the aroma-active compounds in five sweet cherry cultivars grown in Yantai (China)"*, Flavour Fragr. J., 2010, 25, 206-213

[3] E. Aprea, F. Biasioli, S. Carlin, I. Endrizzi and F. Gasperi, *"Investigation of volatile compounds in two raspberry cultivars by two hadspace techniques: solid-phase microextractions/gas chromatography-mass spectrometry (SPME/GC-MS) and proton-transfer reaction-mass spectrometry (PTR-MS)"*, J. Agric. Food Chem., 2009, 57, 4011-4018.

[4] M. D. Sharp, N.A. Kocaoglu-Vurma, V. Langford, L.E. Rodriguez-Saona and W.J. Harper, *"Rapid Discrimination and characterization of vanilla bean extracts by attenuated total reflection infrared spectroscopy and selected ion flow tube mass spectrometry"*, Journal of Food Science, 2012, 77, 284-292.

[5] D.I Enache, J.K. Edwards, P. Landon, B. Solsona-Espriu, A.F. Carley, A.A. Herzing, M. Watanabe, C.J. Kiely, D.W. Knight and G.J. Hutchings, "*Solvent-free oxidation of primary carbon-hydrogen bonds in toluene using Au-Pd alloy nanoparticles*", Science, 2006, 311, 362–365.

[6] G. Ten Brink, I.W.C.E. Arends and R.A. Sheldon, "*Green catalytic oxidation of alcohols in water*", Science, 2000, 287, 1636–1639.

[7] C. Kohlpaintner, M. Schulte, J. Falbe, P. Lappe, J. Weber, "*Aldehydes, aliphatic and araliphatic"*, Ulmann's Encyclopedia of Industrial Chemistry, 6th Edition, 2003.

[8] B.M. Choudary, M. Lakshmi Kantam and P. Lakshmi Santhi, "*New and ecofriendly options for the production of speciality and fine chemicals*", Catalysis Today, 2000, 57, 17–32.

[9] G.-J. ten Brink, I.W.C.E. Arends, R. A. Sheldon, "*Green, catalytic oxidation of alcohols in water*", Science, 2000, 287, 1636 – 1639.

[10] M.A. Gonzalez, S. Garry Howell and S. K. Sikdar, "*Photocatalytic Selective Oxidation of Hydrocarbons in the Aqueous Phase*", Journal of Catalysis, 1999, 183, 159–162.

[11] K.H. Funken, G. Leudtke, J. Ortner, K.J. Riffelmann, "*Solar photochemical production of ε-caprolactam using highly concentrated sunlight"*, Jounal of Information Recording, 2000, 25(1-2), 3-14.

[12] K.H. Funken, F.G. Muller, J. Ortner, K.J. Riffelmann, C. Sattler, "*Solar collector versus lamp – A comparision of the energy demand of industrial photochemical processes as exemplified by the production of ε-caprolactam"*, Energy, 1999, 24, 681-687.

[13] M. Oelgemöller, N. Healy, L. de Oliveira, C. Jung and J. Mattay, *"Green photochemistry: solar-chemical synthesis of Juglone with medium concentrated sunlight"*, Green Chem., 2006, 8, 831-834.

[14] M. Oelgemöller, C. Jung, J. Ortner, J. Mattay and E. Zimmermann, *"Green photochemistry: solar photooxygenations with medium concentrated sunlight"*, Green Chem., 2005, 7, 35-38.

[15] D.J. Crouse, M.M. Wheeler, M. Goemann, P.S. Tobin, S.K. Basu, M. S. Wheeler, *"Oxidation of 1,5-naphthalenediol and its methyl ether: preparation of juglone methyl ether monoacetal"*, J. Org. Chem.,*1982*, 46, 1814-1817.

[16] C. Grundmann, *"A new synthesis of juglone",* Synthesis, 1977, 644.

[17] O. Suchard, R. Kane, B.J. Roe, E. Zimmermann, C. Jung, P.A. Waske, J. Mattay, M. Oelgemöller, *"Photooxygenations of 1-naphthols: an environmentally friendly access to 1,4-naphthoquinones"*, Tetrahedron, 2006, 63, 1467-1473.

[18] M. Oelgemöller, C. Jung, J. Mattay, *"Green photochemistry: Production of fine chemicals with sunlight"*, Pure Appl. Chem., 2007, 79, 1939–1947.

[19] J. Ortner, D. Faust, K.-H. Funken, T. Lindner, J. Schulat, C.G. Stojanoff, P. Fröning, *"New developments using holographic concentration in solar photochemical reactors"*, Phys. IV, 1999, 9, Pr3-379.

[20] J. Blanco, S. Malato, P. Fernández, A. Vidal, A. Morales, P. Trincado, J.C. Oliveira, C. Minero, M. Musci, C. Casalle, M. Brunotte, S. Tratzky, N. Dischinger, K-H. Funken, C. Sattler, M. Vincent, M. Collares-Pereira, J.F. Mendes, C.M. Rangel, *"Compound parabolic concentrator technology development to commercial solar detoxification applications"*, Solar Energy, 2000, 67, 317-330.

[21] S. Malato, P. Fernandez-Ibanez, M.I. Maldonado, J. Blanco, W. Gernjak, *"Decontamination and disinfection of water by solar photocatalysis: recent overview and trends*", Catal. Today, 2009, 147, 1–59.

[22] J. Blanco, S. Malato, P. Fernández-Ibañez, D. Alarcón, W. Gernjak, M.I. Maldonado *"Review of feasible solar energy applications to water processes"*, Renewable and Sustainable Energy Reviews, 2009, 13, 1437–1445.

[23] Z. Cheng-Wu, O. Zmora, R. Kopel, A. Richmond, *"An industrial-sizze flat plate glass reactor for mass production of Nannochloropsis sp. (Eustigmatophyceae)"*, Acuaculture, 2001, 195, 35-49

[24] J.W.F. Zijffers, M. Janssen, J. Tramper, R.H. Wijffels, *"Design process of an Area-Efficient photobioreactor"*, Mar. Biotechnol., 2008, 10, 404-415.

[25] M.R. Tredici and R. Materassi, *"From open ponds to vertical alveolar panels: the Italian experience in the development of reactors for the mass cultivation of phototrophic microorganisms"*, Journal of Applied Phycology, 1992, 4, 221-231.

[26] J. Muschaweck, W. Spirkl, A. Timinger, N. Benz, M. Dörfler, M. Gut and E. Kose, *"Optimized reflectors for non-tracking solar collectors with tubular absorbers"*, Solar Energy, 2000, 68, 151-159.

[27] D. S. Ollis, H. Al-Ekabi, *"Photocatalitic purification of water and air"*, Elsevier Amsterdam, 1993.

[28] R. Rajeshwar, *"Photoelectrochemistry and the environment"*, Journal of Applied Electrochemistry. 1995, 25(12), 1067-1082.

[29] K. Kabra, R. Chaudhary, R.L. Sawhney, *"Treatment of hazardous organic and inorganic compounds through aqueous-phase photocatalysis: a review"*, Ind. Eng. Chem. Res., 2004, 43, 7683–7696.

[30] J.M. Herrmann, *"Heterogeneous photocatalysis: state of the art and present applications"*, Topics Catal., 2005, 34 (1–4), 49–65.

[31] J.M. Herrmann, M. Lacroix, *"Environmental photocatalysis in action for green chemistry"*, Kinet. Catal., 2006, 51 (6), 793–800.

[32] A. Maldotti, A. Molinari, R. Amadelli, *"Photocatalysis with organized systems for the oxofunctionalization of hydrocarbons by O_2"*, Chem. Rev., 2002, 102, 3811– 3836.

[33] D. Tsukamoto, M. Ikeda, Y. Shiraishi, T. Hara, N. Ichikuni, S. Tanaka, T. Hirai, *"Selective photocatalytic oxidation of alcohols to aldehydes in water by TiO_2 partially coated with WO_3"*, Chem. Euro. J., 2011, 17, 9816–9824.

[34] S. Higashimoto, N. Suetsugu, M. Azuma, H. Ohue, Y. Sakata, *"Efficient and selective oxidation of benzylic alcohol by O_2 into corresponding aldehydes on a TiO_2 photocatalyst under visible light irradiation: effect of phenyl-ring substitution on the photocatalytic activity"*, J. Catal., 2010, 274, 76–83.

[35] J. Matos, A. Garcia, T. Cordero, J.M. Chovelon, C. Ferronato, *"Eco-friendly TiO2–AC photocatalyst for the selective photooxidation of 4-chlorophenol"*, Catal. Lett., 2009, 130, 568–574.

[36] M. Zhang, Q.Wang, C. Chen, L. Zhang, W. Ma, J. Zhao, "*Oxygen atom Transfer in the photocatalytic oxidation of alcohols by TiO_2: oxigen isotope studies"*, Angew. Chem, Int. Ed, 2009, 48, 6081-6084.

[37] S. Higashimoto, N. Kitao, N. Yohida, T. Sakura, M. Azuma, H. Ohue and Y. Sakata, "*Selective photocatalytic oxidation of benzyl alcohol and its derivatives into corresponding aldehydes by molecular oxygen on titanium dioxide under visible light irradiation"*, J. Catal., 2009, 266, 279-285.

[38] S. Farhadi, M. Afshari, M. Malesi, Z. Babazadeh, "*Photocatalytic oxidation of primary and secondary benzylic alcohols to carbonyl compounds catalyzed by $H_3PW_{12}O_{40}/SiO_2$ under O_2 atmosphere"*, Tetrahedron Letters, 2005, 46, 8483–8486.

[39] S. Farhadi, M. Zaidi, *"Polyoxometalate–zirconia (POM/ZrO_2) nanocomposite prepared by sol–gel process: A green and recyclable photocatalyst for efficient and selective aerobic oxidation of alcohols into aldehydes and ketones",* Applied Catalysis A: General, 2009, 354, 119–12.

[40] Noritaka Mizuno and Makoto Misono, "*Heterogeneous catalysis*", Chem. Rev, 1998, 98(1), 199-218

[41] Y. Guo, C.Hu, *"Heterogeneous photocatalysis by solid polyoxometalates"*, Journal of Molecular Catalysis A: Chemical, 2007, 262, 136-148.

[42] A. Hiskia, A. Mylonas and E. Papaconstantinou, *"Comparision of the photoredox properties of polyoxometallates and semiconducting particles"*, Chem. Soc. Rev, 2001, 30, 62-69.

[43] M. Poliakoff and P.Licence, *"Green chemistry"*, Nature, 2007, 450 (6).

[44] G. Palmisano, S. Yurdakal, V. Augugliaro, V. Loddo and L. Palmisano, *"Photocatalytic Sselective oxidation of 4-Methoxybenzyl Alcohol to Aldehyde in aqueous suspension of home-prepared titanium dioxide catalyst"*, Adv. Synth. Catal. 2007, 349, 964 – 970.

[45] V. Loddo, S. Yurdakal, G. Palmisano, G. E. Imoberdorf, H. A. Irazoqui, O. M. Alfano, V. Augugliaro, H. Berber and L. Palmisano, *"Selective photocatalytic oxidation of 4-Methoxybenzyl Alcohol to p-Anisaldehyde in organic-free water in a continuous annular fixed bed reactor"*, International Journal of Chemical Reactor Engineering, 2007, 5, A57.

[46] S. Yurdakal, G. Palmisano, V. Loddo, V. Augugliaro and L. Palmisano, *"Nanostructured rutile TiO_2 for selective photocatalytic oxidation of aromatic alcohols to aldehydes in water"*, J. Am. Chem. Ssoc., 2008, 130, 1568-1569.

[47] M. Addamo, V. Augugliaro, M. Bellardita, A. Di Paola, V. Loddo, G. Palmisano, L. Palmisano and S. Yurdakal, *"Environmentally friendly photocatalytic oxidation of aromatic alcohol to aldehyde in aqueous suspension of brookite TiO_2"*, Catal. Lett., 2008, 126, 58–62.

[48] V. Augugliaro, T. Caronna, V. Loddo, G. Marcì, G. Palmisano, L. Palmisano and S. Yurdakal, *"Oxidation of aromatic alcohols in irradiated aqueous suspensions of commercial and home-prepared rutile TiO_2: a selectivity study"*, Chem. Eur. J. 2008, 14, 4640 – 4646.

[49] S. Yurdakal, G. Palmisano, V. Loddo, O. Alagoz, V. Augugliaro and L. Palmisano, *"Selective photocatalytic oxidation of 4-substituted aromatic alcohols in water with rutile TiO_2 prepared at room temperature"*, Green Chem., 2009, 11, 510–516.

[50] D. Chen, A.K. Ray, *"Removal of toxic metal ions from wastewater by semiconductor photocatalysis"*, Chemical Engineering Science 2001, 56, 1561-1570.

[51] S.G. Botta, D.J. Rodriguez, A.G. Leyva, A.I. Litter, *"Features of the transformation of Hg(II) by heterogeneous photocatalysis over TiO_2"*, Catalysis Today, 2002, 76, 247-258.

[52] L. Murrini, G. Leyva, M.I.Litter, *"Photocatalytic removal of Pb(II) over TiO_2 and Pt-TiO_2 powders"*, Catalysis Today, 2007, 129, 127-135.

[53] K. Kabra, R. Chaudhary, R.L. Sawhney, *"Effect of pH on solar photocatalytic reduction and deposition of Cu(II), Ni(II), Pb(II), and Zn(II): Speciation modelling and reaction kinetics"*, Journal of Hazardous Materials, 2007, 149, 680-685.

[54] K. Kabra, R. Chaudhary, R.L. Sawhney, *"Solar photocatalytic removal of Cu(II), Ni(II), Zn(II) and Pb(II): Speciation modelling of metal-citric acid complex"*, Journal of Hazardous Materials, 2008, 155, 424-432.

[55] M. Canterino, I. Di Somma, R. Marotta, R. Andreozzi, *"Investigaton of Cu(II) ions photoreduction in presence of titanium dioxide and formic acid"*, Water Research, 2008, 42, 4498-4506.

[56] N.S. Foster, R.D. Noble, C.A. Koval, *"Reversible photoreductive deposition and oxidative dissolution of copper ions in titanium dioxide aqueous suspensions"*, Environ. Sci. Technol., 1993, 27, 350-356.

[57] J.W.M. Jacobs, F.W.H. Kampers, J.M.G Rikken, C.W.T. Bulle-Lieuwma, D.C. Doningsberger, *"Copper photodeposition on TiO_2 studied with HrEM and EXAFS",* Journal of The Electrochemical Society,1989, 136, 2914-2023.

[58] M. Bideau, B. Claudel, L. Faure, M. Rachimoellah, *"Photooxidation of formic acid by oxygen in the presence of titanium dioxide and dissolved copper ions: oxygen transfer and reaction kinetics"*, Chemical Engineering Communications, 1990, 93, 167–179.

[59] S. Morishita, *"Photoelectrochemical deposition of copper on TiO_2 particles. Generation of copper patterns without photoresists"*, Chemistry Letters, 1992, 10, 1979-1982.

[60] S.W. Zou, C.W. How, J.P. Chen, *"Photocatalytic treatment of wastewater contaminated with organic waste and copper ions from the semiconductor industry"*, Ind. Eng. Chem. Res., 2007, 46(20), 6566–6571.

[61] H. Reiche, W.W. Dunn, A.J. Bard, *"Heterogeneous photocatalytic and photosynthetic deposition of copper on TiO_2 and WO_3 powders"*, Journal of Physical Chemistry, 1979, 83, 2248-2251.

[62] S. Xu, J. Ng, A.J. Du, J. Liu, D.D. Sun, *"Highly efficient TiO_2 nanotube photocatalyst for simultaneous hydrogen production and copper removal from water"*, International Journal of Hydrogen Energy, 2011, 36, 6538-6545.

[63] Friedrich Bruhne, Bayer AG, Krefeld-Uerdingen, Elaine Wright, *"Benzaldehyde"*, Ulmann's Encyclopedia of Industrial Chemistry, 6th Edition, 2003.

[64] H.J. Kuhn, S.E. Braslavsk, R. Schmidt, *"Chemical actinometry (IUPAC Technical Report)"*, Pure Appl. Chem., 2004, 76, 2105–2146.

[65] R.G. Zepp, M.M. Gumz, W.L. Miller, H. Gao, *"Photoreaction of valerophenone in aqueous solution"*, Journal of Physical Chemistry, A, 1998, 102(28), 5716–5723.

[66] M. Kositzi, I. Poulios, S. Malato, J. Cáceres, A. Campos, *"Solar photocatalytic treatment of synthetic municipal wastewater"*, Water Research, 2004, 38, 1147-1154.

[67] S. Malato, J. Blanco, C. Richter, M.I. Maldonado, *"Optimization of pre-industrial solar photocatalytic mineralization of commercial pesticides: application to pesticide container recycling"*, Appl. Cat. B: Environ., 2000, 25, 31–38.

[68] R. Long, Y. Dai, B. Huang, *"Structural and electronic properties of iodine-doped anatase and rutile TiO_2"*, Comput. Mater. Sci., 2009, 45, 223–228.

[69] H.A. Schwarz, R.W. Dodsonj, *"Equilibrium between hydroxyl radicals and thallium(II) and the oxidation potential of OH(aq)"*, J. Phys. Chem., 1984, 88, 3643–3647.

[70] M.I. Litter, *"Heterogeneous photocatalysis transition metal ions in photocatalytic systems"*, Appl. Catal. B: Environ., 1999, 23, 89–114.

[71] J. Ryu, W. Choi, *"Substrate-specific photocatalytic activities of TiO_2 and multiactivity test for water treatment application"*, Environ. Sci. Technol., 2008, 42, 294–300.

[72] S. Ahmed, M.G. Rasul, N. Martens Wayde, R. Brown, M.A. Hashib, *"Heterogeneous photocatalytic degradation of phenols in wastewater: a review on current status and developments"*, Desalination, 2010, 261, 3–18.

[73] D. Vione, C. Minero, V. Maurino, M.E. Carlotti, T. Picatonotto, E. Pelizzetti, *"Degradation of phenol and benzoic acid in the presence of a TiO2-based heterogeneous photocatalyst"*, Appl. Catal. B: Environ., 2005, 58, 79–88.

[74] C. Hu, T. Yuchao, L. Lanyu, H. Zhengping, W. Yizhong, T. Hongxiao, *"Effects of inorganic anions on photoactivity of various photocatalysts under different conditions"*, J. Chem. Technol. Biotechnol., 2004, 79, 247–252.

[75] O. Carp, C.L. Huisman, A. Reller, *"Photoinduced reactivity of titanium dioxide"*, Prog. Solid State Chem., 2004, 32, 33–177.

[76] M. Ziegmann, T. Doll, F.H. Frimmel, *"Matrix effects on the photocatalytical degradation of dichloroacetic acid and atrazine in water"*, Acta Hydrochim. Hydrobiol., 2006, 34, 146–154.

[77] M. Abdullah, G.K.C. Low, R.W. Matthews, "Effects of common inorganic anions on rates of photocatalytic oxidation of organic carbon over illuminated titanium dioxide", J. Phys. Chem., 1990, 94, 6820–6825.

[78] F.M. Menger, M. Ladika, *"Origin of rate accelerations in an enzyme model: the p-nitrophenyl ester syndrome"*, J. Am. Chem. Soc., 1987, 109, 3145–3146.

[79] Krýsa, J., Waldner, G., Měšťánková, H., Jirkovský J., Grabner G., *"Photocatalytic degradation of model organic pollutants on an immobilized particulate TiO_2 layer roles of adsorption processes and mechanistic complexity"*, Appl. Cat. B: Environ., 2006, 64, 290–301.

[80] J. Cunningham, S. Srijaranai, *"Sensitized photo-oxidations of dissolved alcohols in homogeneous and heterogeneous systems. Part 2. TiO_2-sensitized photodehydrogenations of benzyl alcohol"*, J. Photochem. Photobiol. A: Chem., 1991, 58, 361–371.

[81] R.W. Matthews, *"Photocatalytic oxidation of organic contaminants in water: an aid to environmental preservation"*, Pure Appl. Chem., 1992, 64 (9), 1285–1290.

[82] Y. Xu, C.H. Langford, *"Variation of Langmuir adsorption constant determined for TiO_2-photocatalyzed degradation of acetophenone under different light intensity"*, J. Photochem. Photobiol. A: Chem., 2000, 133, 67–71.

[83] F. Zhang, J. Zhaoa, T. Shen, H. Hidakab, E. Pelizzetti, N. Serpone, *"TiO_2-assisted photodegradation of dye pollutants II. Adsorption and degradation kinetics of eosin in TiO2 dispersions under visible light irradiation"*, Appl. Cat. B: Environ., 1998, 15, 147–156.

[84] A. Mills, P. Sawunyama, *"Photocatalytic degradation of 4-chlorophenol mediated by TiO2: a comparative study of the activity of laboratory made and commercial TiO_2 samples"*, J. Photochem. Photobiol. A: Chem., 1994, 84, 305–309.

[85] J. Cunningham, G. Al-Sayyed, *"Factors influencing efficiencies of TiO2-sensitised photodegradation. Part 1. Substituted benzoic acids: discrepancies with darkadsorption parameters"*, J. Chem. Soc., Faraday Trans., 1990, 86, 3935–3941.

[86] G.V. Buxton, C.L. Greestock, W.P. Helman, A.B. Ross, *"Critical review of rate constants for oxidation of hydrated electrons, hydrogen atoms and hydroxyl radicals (•OH/•O$^-$) in aqueous solutions"*, J. Phys. Chem. Ref. Data, 1988, 17, 513–886.

[87] I.V. Khudyakov, P.F. McGarry, N.J. Turro, *"A time-resolved electron spin resonance and laser flash spectroscopy investigation of the photolysis of benzaldehyde and benzoin in homogeneous solvents and micellar solution"*, J. Phys. Chem., 1993, 97, 13234–13242.

[88] G.R. De Mare, J.R. Fox, *"Heterogeneous photosensitization-IV. The structure and properties of benzaldehyde photopolymer"*, Euro. Polym. J., 1981, 17, 315–321.

[89] P.A. Connor, A.J. McQuillan, *"Phosphate adsorption onto TiO_2 from aqueous solutions: an in situ internal reflection infrared spectroscopic study"*, Langmuir, 1999, 15, 2916–2921.

[90] W.H. Glaze, Y. Lay, J.W. Kang, *"Advanced oxidation processes. A kinetic model for the oxidation of 1,2-dibromo-3-chloropropane in water by thecombination of hydrogen peroxide and UV radiation"*, Ind. Eng. Chem. Res.,1995, 34, 2314–2323.

[90] W.Z. Tang, *"In Physicochemical Treatment of Hazardous Wastes"*, CRC Press, Lewis Publishers, 2003 (chapter 7).

[91] M. Bideau, B. Claudel, M. Otterbein, *"Photocatalysis of formic acid oxidation by oxygen in aqueous media"*, J. Photochem., 1980, 14, 291 – 302.

[92] G.V. Reklaitis, A. Ravindran, K.M. Regsdell, *"Engineering Optimization"*, Wiley, New York, 1983.

[94] G. Horanyi, *"Investigation of the specific adsorption of sulfate ions on powdered TiO_2"*, J. Coll. Interf. Sci.,2003, 261, 580–583.

[95] A.G. Rincon, C. Pulgarin, A. Nevenka and P. Peringer, *"Interaction between E. coli inactivation and DBP-precursors-dihydroxybenzene isomersin the photocatalytic process of drinking-water disinfection with TiO_2"*, J. Photochem. Photobiol. Part A Chem, 2001, 139, 233–241.

[96] C. Percivalle, A. La Rosa, D. Verga, F. Doria, M. Mella, M. Palumbo, *"Quinone methide generation via photoinduced electron transfer"*, J. Org. Chem., 2011, 76, 3096–3106.

[97] P. Wan and K. Yates, *"Photoredox chemistry of m- and p-nitrobenzyl alcohols in aqueous solution. Observation of novel catalysis by the hydronium and hydroxide ions in these photoreactions"*, J. Org. Chem., 1983, 48, 136–138.

[98] Y. Chiang, A.J. Kresge and Y. Zhu, *"Reactive intermediates. Some chemistry of quinone methides"*, Pure Appl. Chem., 2000, 72, 2299–2308.

[99] S.O. Flores, O. Rios-Bernij, M.A. Valenzuela, I. Cordova, R. Gomez and R. Gutierrez, *"Photocatalytic reduction of nitrobenzene over titanium dioxide: by-product identification and possible pathways"*, Topics Catal., 2007, 44, 507–511.

[100] H. Kominami, S. Iwasaki, T. Maeda, K. Imamura, K. Hashimoto, Y. Kera, *"Photocatalytic reduction of nitrobenzene to aniline in an aqueous suspension of titanium(IV) oxide particles in the presence of oxalic acid as a hole scavenger and promotive effect of dioxygen in the system"*, Chem. Lett., 2009, 38, 410–411.

[101] G. Palmisano, E. Garcıa-Lopez, G. Marcì, V. Loddo, S. Yurdakal, V. Augugliaro, *"Advances in selective conversions by heterogeneous photocatalysis"*, Chem. Commun., 2010, 46, 7074–7089.

[102] K. Imamura, S. Iwasaki, T. Maeda, K. Hashimoto, B. Ohtani and H. Kominami, *"Photocatalytic reduction of nitrobenzenes to aminobenzenes in aqueous suspensions of titanium(IV) oxide in the presence of hole scavengers under deaerated and aerated conditions"*, Phys. Chem., 2011, 13, 5114–5119.

[103] P. Wan and K. Yates, *"Photoredox chemistry of nitrobenzyl alcohols in aqueous solution. Acid and base catalysis of reaction"*, Can. J. Chem., 1986, 64, 2076–2086.

[104] H. Gorner, *"Photoisomerization of p-nitrobenzaldehyde to pnitrosobenzoic acid in aqueous solution"*, J. Photochem. Photobiol. A: Chem., 1998, 112, 155–158.

[105] G.G. Wubbels, T.F. Kalhorn, D.E. Johnson and D. Campbell, *"Mechanism of the water-catalyzed photoisomerization of p-nitrobemaldehyde"*, J. Org. Chem., 1982, 47, 4664–4670.

[106] D. Vione, V. Maurino, C. Minero and E. Pelizzetti, *"Reactions induced in natural waters by irradiation of nitrate and nitrite ions"*, The Handbook of Environmental Chemistry, 2005, Vol. 2, Part M.P. Boule, D.W. Bahnemann, P.K.J. Robertson (Ed.), Springer, Berlin, 221–253.

[107] L. Prieto Rodriguez, S. Miralles Cuevas, I. Oller, A. Agüera, G. Li Puma, S. Malato, *"Treatment of emerging contaminants in wastewater treatment plants (WWTP) effluents by solar photocatalysis using low TiO_2 concentrations"*, Journal of Hazardous Materials, 2012, 211– 212, 131– 137.

[108] J. Colina Márquez, F, Machuca Martínez, G. Li Puma, *"Radiation adsorption and optimisation of solar photocatalytic reactors for environmental applications"*, Environ. Sci. Technol., 2010, 44, 5112–5120.

[109] J.R. Bolton, K.G. Bircher, W. Tumas, C.A. Tolman, *"Figures-of merit for the technical development and application of advanced oxidation technologies for both electric and solar driven systems"*, Pure Appl. Chem., 2001, 73(4), 627–637.

[110] R. Hulstrom, R. Bird, C. Riordan, *"Spectral solar irradiance data sets for selected terrestrial conditions"*, Solar Cells, 1985, 15, 365–391.

[111] C.C. Chusuei, M.A. Brookshier, D.W. Goodman, *"Correlation of relative X-ray photoelectron spectroscopy shake-up intensity with CuO particle size"*, Langmuir, 1999, 15, 2806-2808.

[112] I. Sirés, J.A. Garrido, R.M. Rodríguez, P.L. Cabot, F. Centellas, C. Arias, E. Brillas, *"Electrochemical degradation of paracetamol from water by catalytic action of* Fe^{2+}, Cu^{2+}, *and UVA light on electrogenerated hydrogen peroxide"*, J. Electrochem. Soc., 2006, 153, D1-D9.

[113] R. Salazar, E. Brillas, I. Sirés, *"Finding the best* Fe^{2+}/Cu^{2+} *combination for the solar photoelectro-Fenton treatment of simulated wastewater containing the industrial textile dye Disperse Blue 3"*, Applied Catalysis B: Environmental, 2012, 115– 116, 107– 116